University of Pretoria

Analysis of the vibration of flexible structures

by

Tatiana Monique Blecher

Submitted in fulfilment of the requirements for the degree

Magister Scientiae

in the Department of Mathematics and Applied Mathematics
Faculty of Natural and Agricultural Sciences

December 2022

Declaration of Authorship

I, the undersigned, declare that the dissertation entitled Analysis of the vibration of flexible structures, which I hereby submit for the degree Magister Scientiae at the University of Pretoria, is my own work and has not previously been submitted by me for a degree at this or any other tertiary institution.

Name: Tatiana Blecher

Date: December 2022

Summary

The main aim of this dissertation was to conduct a literature study on existence and convergence theory for second-order hyperbolic type problems, implementation of the finite element method to example problems, and so-called "locally linear" rod models.

The existence and convergence theory for second-order hyperbolic type problems from the articles of van Rensburg and van der Merwe (2002) and of Basson, Stapelberg and van Rensburg (2017) respectively, was introduced and analysed. This theory was derived by writing the problem in an abstract variational form, using bilinear forms. The existence theory was subsequently applied to the Timoshenko model with axial force and the multi-dimensional wave equation, by showing that the assumptions necessary for the theory were satisfied.

The finite element method (FEM) was applied to the two-dimensional wave equation on a rectangle with Dirichlet boundary conditions, with both rectangle and triangle elements. It was found in both cases that the approximations achieved by the method converge to the exact solution of the initial value problem. The mixed FEM was applied to the Timoshenko model with no axial force, to obtain approximations to be compared with the locally linear Timoshenko (LLT) model.

The derivation of the LLT model and its variational forms was presented as in the article of van Rensburg, du Toit and Labuschagne (2021). Further, the finite element algorithm derived in a currently unpublished work of du Toit, Labuschagne and van der Merwe (2022) was used to replicate some of the numerical results presented there. The results showed that

the approximations using this algorithm and those of the mixed finite element method for a cantilever rod were in agreement. Additionally, there is a critical value of initial compression, after which a compressed pinned-pinned beam exhibits buckled states. Finally, the results were extended by investigating the effects of a more slender rod on the outcomes of the algorithm.

The possibility of deriving a locally linear theory was investigated for the Rayleigh beam model, using the same ideas as for the LLT rod model, and the resulting model was compared to that of Hegarty and Taylor (2012).

In this dissertation, valuable comparisons between the articles on the existence and convergence theories mentioned above and the results of two earlier articles using the same abstract form, but with different types of damping, are made. Simple illustrations of the theory and examples of finite element implementation and convergence are presented. An additional contribution is the confirmation of some of the results of the work on the LLT model.

Contents

Chapter 1

Introduction

1.1 Vibration of flexible structures

Research on vibrations of flexible structures is ongoing in engineering and applied mathematics fields. Flexible structures in practice can be considered as systems of interconnected rod-like components. Mathematical models for these vibrating structures consist of systems of partial differential equations, which are often complex and require numerical methods to find approximations of solutions. Additionally, the derivation and analysis of both the models and appropriate numerical methods can be a challenge [LA12].

The study of deformations of thin beams is of great practical importance in engineering [DRS21]. Rod models, a subject of interest particularly in mechanics, lend themselves to several applications in engineering, such as modelling of cables and steel strings [LA12], or the study of fibres in synthetic braided ropes [VDD15]. In the book of Hodges [Hod06], the author mentioned applications of slender beam theory in aerospace engineering, in particular helicopter rotor blades. Moreover, in [TLK74], beam theory was used to study the dynamics of spacecraft antennae. The article [MPW19] provides an extensive list of examples and sources for applications of these models beyond mechanics, ranging from fibres in paper to filaments involved in cell division. In [WT99], a beam model was used to analyse the vibration

of railway tracks, and [ET14] used a beam model in the study of bending deformation in high-rise buildings.

The practical applications of mathematical models for flexible structures are a motivation to investigate existence and convergence theory of their solutions, as well as the implementation of numerical methods. The book of Evans [Eva97] has dedicated sections on Sobolev theory (see also Appendix A of this dissertation) and weak solutions, and provides some existence results for second-order elliptic, parabolic and hyperbolic equations. The authors in [HT12] proved existence of classical solutions for a nonlinear cantilevered beam model with forcing at the free end. The main focus of this dissertation was second-order hyperbolic type problems. In [VV02], theorems for the existence of solutions of the general linear second-order hyperbolic vibration model with general, weak and strong damping were proven. This work was extended in [VS19], where slightly different assumptions were made on the symmetry of bilinear forms.

The finite element method (FEM) is a well-known and widely used method to approximate solutions of various mathematical models. Convergence of finite element approximations of the general linear hyperbolic problem was investigated in [BV13] and later in [BSV17]. In the former article, error estimates for the semi-discrete and fully discrete problems for the general linear problem with weak damping were derived. In the latter article, these estimates were obtained for general damping. An example of FEM application to flexible structures is in [FL97], where a modified finite element method is used to study the flexible rod in a quick-return mechanism, where the length of the rod is time-dependent. More recently, a finite element formulation for a model for vibrating thin-walled beams was developed in [SPS+22].

In some applications, the standard FEM with linear basis functions may lead to poor numerical results due to "shear locking" [Sem94]. As the thickness of the beam decreases, it is possible that the approximations diverge when linear elements are used [Arn81]. An alternative method that still leads to reasonable numerical results is the mixed FEM, where shear stress is also considered as a dependent variable [Arn81], [FXX99], [Sem94].

This dissertation consists largely of a literature study on some mathematical models for flexible structures and structural components, and includes existence theory and finite element analysis of these models and their solutions. These models include beam models such as the Timoshenko theory, Euler-Bernoulli theory, as well as recently published work on a so-called locally linear Timoshenko rod. The multi-dimensional wave equation is also used to illustrate the application of some of the theory in this dissertation.

In the following sections of this introduction, the models used throughout this dissertation are introduced, and their variational forms are derived. In Chapter 2, the main existence results from [VV02] are introduced, and compared to those in [VS19]. The chapter is concluded by a section on application of the theory to practical examples. The following chapter features an in-depth study of the results and proofs of the convergence theory from [BSV17]. Chapter 4 is dedicated to the implementation and convergence analysis of the finite element method to example problems. This is followed by two chapters on locally linear models - one chapter presents the derivation and numerical analysis of the locally linear Timoshenko model of [VDL21] and [DLV22], while the second chapter is a brief investigation into the locally linear Rayleigh model, also studied in [HT12].

1.2 The Timoshenko beam theory

Linear beam models are of significant interest in many applications in engineering and mathematics. Simplified beam models have been used to simulate the oscillation of buildings under the influence of earthquakes and wind, in a number of recent publications ([CH15], [TGA17], [PTL19]). In general, structural components of vibrating structures can also be modelled using these types of models. We consider two such models: the Timoshenko beam model, which is considered to be fairly realistic [ZVV04], and the Euler-Bernoulli beam model (see Section 1.3). In both models, it is assumed that cross sections remain undeformed after beam deformation, but shear deformation is taken into account only in the Timoshenko model, while it is ignored for the Euler-Bernoulli model [VV06], [NSH17], [SNH15], [II92].

The Euler-Bernoulli beam model can be derived from the Timoshenko theory, and this will be illustrated in Section 1.3.

1.2.1 The original Timoshenko model

The Timoshenko beam model is useful in many applications, and will serve as an example application of the calculations and analyses done in this dissertation.

Consider the original Timoshenko beam model. The derivation of the model can be found for example in [Tim37, p.337-338] and [Inm94, p.337-338]. The model comprises of two partial differential equations for the deflection of the beam, w, and the angle of rotation of a cross section, ϕ.

The equations of motion are

$$\rho A \partial_t^2 w = \partial_x V + P, \tag{1.2.1}$$

$$\rho I \partial_t^2 \phi = V + \partial_x M, \tag{1.2.2}$$

with constitutive equations

$$M = EI \partial_x \phi, \tag{1.2.3}$$

$$V = AG\kappa^2(\partial_x w - \phi). \tag{1.2.4}$$

In these equations, ρ is the density, A the area of a cross section, I is the area moment of inertia, M the moment, and V and P are the shear force and load respectively. Further, κ^2 is the shear correction factor, and E and G are elastic constants (see [Inm94, pp.337-338] for more details).

The partial differential equations for the model can be derived by substituting the constitutive equations into the equations of motion, and are as follows:

$$\rho A \partial_t^2 w = \partial_x \left(AG\kappa^2 \left(\partial_x w - \phi \right) \right) + P \text{ and}$$

$$\rho I \partial_t^2 \phi = AG\kappa^2 \left(\partial_x w - \phi \right) + \partial_x \left(EI \partial_x \phi \right).$$

Remark 1.2.1. For the Timoshenko model, the assumption is that $\partial_x w$ and ϕ are small [LVV09]. As a result, the theory is only applicable for small deformations and rotations.

It is useful to consider the model in dimensionless form. To this end, denote the length of the beam by ℓ. Let

$$\tau = \frac{t}{T},\ \xi = \frac{x}{\ell},\ w^*(\xi,\tau) = \frac{w(x,t)}{\ell} \text{ and } \phi^*(x,t) = \phi(x,t),$$

where the parameter T is chosen appropriately, and is given in Equation (1.2.5) below.

First we define the two (dimensionless) parameters α and β as follows:

$$\alpha = \frac{A\ell^2}{I} \text{ and } \beta = \frac{AG\kappa^2\ell^2}{EI}.$$

To obtain the forces and moment in dimensionless form, set

$$V^*(\xi,\tau) = \frac{V(x,t)}{AG\kappa^2},\ M^*(\xi,\tau) = \frac{M(x,t)}{AG\kappa^2\ell} \text{ and } P^*(\xi,\tau) = \frac{P(x,t)\ell}{AG\kappa^2}.$$

Then we define the parameter T by

$$T = \ell\sqrt{\frac{\rho}{G\kappa^2}}. \tag{1.2.5}$$

We find the dimensionless problem using the above expressions. Using the original notation, the problem is as follows:

The equations of motion are

$$\partial_t^2 w = \partial_x V + P, \tag{1.2.6}$$

$$\frac{1}{\alpha}\partial_t^2\phi = V + \partial_x M, \tag{1.2.7}$$

with constitutive equations

$$M = \frac{1}{\beta}\partial_x\phi, \tag{1.2.8}$$

$$V = \partial_x w - \phi. \tag{1.2.9}$$

Remark 1.2.2. The constant α is a measure of the length of the beam compared to its thickness; that is, a larger value of α corresponds to a more slender beam. As a result, α can vary greatly in size [ZVV04], as can β, since $\frac{\beta}{\alpha} = \frac{G\kappa^2}{E}$. The parameter $\frac{\beta}{\alpha}$ depends only on the shape of the cross section and the material of the beam [ZVV04], and realistic values for a homogeneous beam are between $\frac{1}{6}$ and $\frac{1}{2}$ [LVV09]. Note that a beam may be tapered, and consequently values of α and β can vary across the length of the beam.

Remark 1.2.3. The Timoshenko beam model can also be considered with several types of damping, such as viscous or material damping, where damping terms are then added to the equations of motion or the constitutive equations. The dimensionless forms can be derived in much the same way as was done above. Damping is not considered in detail in this dissertation.

Several boundary conditions may be considered for the model, but in this dissertation, the focus was on the pinned-pinned and cantilever cases.

Problem T-P (Pinned-pinned)
The model consists of the equations of motion (1.2.6) and (1.2.7), with constitutive equations (1.2.8) and (1.2.9), and boundary conditions

$$w(0,t) = w(1,t) = M(0,t) = M(1,t) = 0.$$

Problem T-C (Cantilever)
The problem is the same as Problem T-P above, except we consider instead the boundary conditions

$$w(0,t) = \phi(0,t) = V(1,t) = M(1,t) = 0.$$

For both problems, the initial conditions are

$$w(\cdot,0) = w_0,\ \phi(\cdot,0) = \phi_0,\ \partial_t w(\cdot,0) = w_d,\ \partial_t \phi(\cdot,0) = \phi_d.$$

1.2.2 Variational forms for the original Timoshenko model

We derive the variational forms for Problems T-P and T-C in Section 1.2.1 above. To this end, multiply Equations (1.2.6) and (1.2.7) by arbitrary functions v and ψ in $C^1[0,1]$ respectively, and integrate.

Using integration by parts, we obtain

$$\int_0^1 \partial_t^2 w(\cdot,t)v = V(1,t)v(1) - V(0,t)v(0) - \int_0^1 \left(V(\cdot,t)v' - P(\cdot,t)v\right) \text{ and}$$
$$\int_0^1 \frac{1}{\alpha}\partial_t^2\phi(\cdot,t)\psi = M(1,t)\psi(1) - M(0,t)\psi(0) - \int_0^1 \left(M(\cdot,t)\psi' - V(\cdot,t)\psi\right).$$

Define the class of test functions for the pinned-pinned case by

$$T_P[0,1] = \left\{v \in C^1[0,1] : v(0) = v(1) = 0\right\}.$$

For the cantilever case, define the class of test functions by

$$T_C[0,1] = \left\{v \in C^1[0,1] : v(0) = 0\right\}.$$

Then we can use the boundary conditions and constitutive equations to obtain the variational problems.

Problem TV-P

Find $\langle w, \phi\rangle$ such that for each $t > 0$, $w(\cdot,t) \in T_P[0,1]$, $\phi(\cdot,t) \in C^1[0,1]$, and

$$\begin{aligned}\int_0^1 \partial_t^2 w(\cdot,t)v + \int_0^1 \frac{1}{\alpha}\partial_t^2\phi(\cdot,t)\psi = &-\int_0^1 \left(\partial_x w(\cdot,t) - \phi(\cdot,t)\right)v' + \int_0^1 P(\cdot,t)v \\ &- \int_0^1 \frac{1}{\beta}\partial_x\phi(\cdot,t)\psi' + \int_0^1 \left(\partial_x w(\cdot,t) - \phi(\cdot,t)\right)\psi\end{aligned} \tag{1.2.10}$$

for each pair $\langle v, \psi\rangle \in T_P[0,1] \times C^1[0,1]$.

Problem TV-C

Find $\langle w, \phi\rangle$ such that for each $t > 0$, $w(\cdot,t) \in T_C[0,1]$, $\phi(\cdot,t) \in T_C[0,1]$, and Equation (1.2.10) holds for each pair $\langle v, \psi\rangle \in T_C[0,1] \times T_C[0,1]$.

For both problems, the initial conditions are

$$w(\cdot,0) = w_0,\ \phi(\cdot,0) = \phi_0,\ \partial_t w(\cdot,0) = w_d,\ \partial_t\phi(\cdot,0) = \phi_d.$$

1.2.3 The Timoshenko model with axial force

We also consider the Timoshenko beam model with an axial force due to gravity in the first equation of motion. The model in dimensionless form is almost the same as Equations (1.2.6)-(1.2.9) above. In this case, Equation (1.2.6) becomes

$$\partial_t^2 w = \partial_x(S\partial_x w) + \partial_x V + P,$$

where P is the load density, and S denotes the axial force.

The resulting model then has the equations of motion

$$\partial_t^2 w = \partial_x(S\partial_x w) + \partial_x V + P, \tag{1.2.11}$$

$$\frac{1}{\alpha}\partial_t^2 \phi = V + \partial_x M. \tag{1.2.12}$$

The constitutive equations are

$$M = \frac{1}{\beta}\partial_x \phi, \tag{1.2.13}$$

$$V = \partial_x w - \phi, \tag{1.2.14}$$

and a third constitutive equation for S, which depends on the application of the model.

The dimensionless form was derived in the same way as was done in Section 1.2.1. Note that if $S = 0$, then the model above is the same as Equations (1.2.6)-(1.2.9).

The boundary conditions considered are for both the pinned-pinned and cantilever cases, as in Section 1.2.1. The cantilever conditions here are slightly different from those introduced in Problem T-C in Section 1.2.1.

Problem TM-P

The model consists of the equations of motion (1.2.11) and (1.2.12), with constitutive equations (1.2.13), (1.2.14) and a constitutive equation for S, and boundary conditions

$$w(0,t) = w(1,t) = M(0,t) = M(1,t) = 0.$$

Problem TM-C

The problem is the same as Problem TM-P above, except we consider instead the boundary conditions

$$w(0,t) = \phi(0,t) = S(1,t)\partial_x w(1,t) + V(1,t) = M(1,t) = 0.$$

For both problems, we consider the initial conditions

$$w(\cdot,0) = w_0,\ \phi(\cdot,0) = \phi_0,\ \partial_t w(\cdot,0) = w_d,\ \partial_t \phi(\cdot,0) = \phi_d.$$

1.2.4 Variational forms for the Timoshenko model with axial force

The process of deriving the variational forms for the two problems is the same as in Subsection 1.2.2. Multiply equations (1.2.11) and (1.2.12) by arbitrary functions v and ψ in $C^1[0,1]$ respectively, and integrate.

From integration by parts, we obtain

$$\begin{aligned}\int_0^1 \partial_t^2 w(\cdot,t)v = S(1,t)\partial_x w(1,t)v(1) - S(0,t)\partial_x w(0,t)v(0) - \int_0^1 S(\cdot,t)\partial_x w(\cdot,t)v' \\ + V(1,t)v(1) - V(0,t)v(0) - \int_0^1 (V(\cdot,t)v' - P(\cdot,t)v) \text{ and} \\ \int_0^1 \frac{1}{\alpha}\partial_t^2 \phi(\cdot,t)\psi = M(1,t)\psi(1) - M(0,t)\psi(0) - \int_0^1 (M(\cdot,t)\psi' - V(\cdot,t)\psi)\,.\end{aligned}$$

Define the class of test functions for the pinned-pinned case by

$$T_P[0,1] = \left\{v \in C^1[0,1] : v(0) = v(1) = 0\right\}.$$

For the cantilever case, define the class of test functions by

$$T_C[0,1] = \left\{v \in C^1[0,1] : v(0) = 0\right\}.$$

Remark 1.2.4. The classes of test functions defined here are the same as those in Subsection 1.2.2.

In this subsection, two approaches are used to derive the variational forms for Problems TM-P and TM-C above. The first approach will be used in applications of existence theory (see Chapter 2), while the second is convenient for applying the mixed finite element method to approximate solutions of the problems (see Chapter 4).

In the first approach, the variational problems are derived in exactly the same way as in Subsection 1.2.2. We use the constitutive equations and boundary conditions to obtain the variational form. For both cases of boundary conditions, the variational problems look the same, except for the definition of the test functions. To this end, let $\mathcal{T}$ denote either $T_P[0,1] \times C^1[0,1]$ or $T_C[0,1] \times T_C[0,1]$. Then we obtain the variational problem.

Problem T-V

Find $\langle w, \phi \rangle$ such that for each $t > 0$, $\langle w(\cdot,t)\phi(\cdot,t) \rangle \in \mathcal{T}$, and

$$\begin{aligned} \int_0^1 \partial_t^2 w(\cdot,t)v &= -\int_0^1 S(\cdot,t)\partial_x w(\cdot,t)v' - \int_0^1 \left(\partial_x w(\cdot,t) - \phi(\cdot,t)\right)v' + \int_0^1 P(\cdot,t)v \\ \int_0^1 \frac{1}{\alpha}\partial_t^2 \phi(\cdot,t)\psi &= -\int_0^1 \frac{1}{\beta}\partial_x \phi(\cdot,t)\psi' - \int_0^1 \left(\partial_x w(\cdot,t) - \phi(\cdot,t)\right)\psi \end{aligned} \tag{1.2.15}$$

for each pair $\langle v, \psi \rangle \in \mathcal{T}$, while

$$w(\cdot,0) = w_0, \ \phi(\cdot,0) = \phi_0, \ \partial_t w(\cdot,t) = w_d, \text{ and } \partial_t \phi(\cdot,0) = \phi_d.$$

For the second approach, a slightly different method is used. We again use the boundary conditions and constitutive equations, but instead of substituting Equation (1.2.14) after integration by parts, we multiply it by an arbitrary function $\xi \in C^1[0,1]$ and integrate. Again, the variational problems look the same for both cases of boundary conditions, except for the definition of the test functions. Here, let $\mathcal{T}$ denote either $T_P[0,1] \times C^1[0,1] \times C^1[0,1]$ or $T_C[0,1] \times T_C[0,1] \times C^1[0,1]$. To avoid confusion with notation later in the dissertation, we will denote the shear force by F instead of V for this method.

Problem TM-V

Find $\langle w, \phi \rangle$ and a function F such that for each $t > 0$, $\langle w(\cdot,t), \phi(\cdot,t), F(\cdot,t) \rangle \in \mathcal{T}$ and

$$\begin{aligned} \int_0^1 \partial_t^2 w(\cdot,t) v &= -\int_0^1 S(\cdot,t)\partial_x w(\cdot,t) v' - \int_0^1 F(\cdot,t)v' + \int_0^1 P(\cdot,t)v \\ \int_0^1 \frac{1}{\alpha}\partial_t^2 \phi(\cdot,t)\psi &= -\int_0^1 \left(\frac{1}{\beta}\partial_x \phi(\cdot,t)\psi' - F(\cdot,t)\psi \right) \\ \int_0^1 F(\cdot,t)\xi &= \int_0^1 \left(\partial_x w(\cdot,t) - \phi(\cdot,t)\right)\xi \end{aligned} \tag{1.2.16}$$

for each triple $\langle v, \psi, \xi \rangle \in \mathcal{T}$, while

$$w(\cdot,0) = w_0,\ \phi(\cdot,0) = \phi_0,\ \partial_t w(\cdot,0) = w_d,\ \text{and } \partial_t \phi(\cdot,0) = \phi_d.$$

1.3 Euler-Bernoulli Beam

As mentioned above, the Euler-Bernoulli beam is considered as an alternative to the Timoshenko beam. In [LVV09] and [ZVV04] it was noted that the Timoshenko model is considered to be more realistic. However, in many applications, the Euler-Bernoulli beam model is completely sufficient. Sansour et. al. [SNH15], for example, noted that in applications for spatial deformations and micro mechanics, where out-of-plane shear is not well defined, it is preferred to use a beam model that considers only displacement, and it is ideal to use Euler-Bernoulli type beams. We show in this section how the Euler-Bernoulli model can be derived from the Timoshenko model, by making some additional assumptions. We also derive the variational forms of the model.

Consider again the Timoshenko beam model, Equations (1.2.6)-(1.2.9).

First, we rewrite Equation (1.2.7) as

$$V = \frac{1}{\alpha}\partial_t^2 \phi - \partial_x M. \tag{1.3.1}$$

Now substitute Equation (1.3.1) into Equation (1.2.6) to obtain

$$\partial_t^2 w = \partial_x \left(\frac{1}{\alpha}\partial_t^2 \phi - \partial_x M \right) + P.$$

The assumption for the Euler-Bernoulli model is that cross sections remain plane after beam deformation; that is, $\partial_x w = \phi$. As a result, we have the following equation of motion and constitutive equation:

$$\partial_t^2 w = \partial_x \left(\frac{1}{\alpha} \partial_t^2 (\partial_x w) - \partial_x M \right) + P, \tag{1.3.2}$$

$$M = \frac{1}{\beta} \partial_x^2 w. \tag{1.3.3}$$

A further assumption is that the rotary inertia term $\frac{1}{\alpha} \partial_t^2 (\partial_x^2 w)$ is ignored in Equation (1.3.2), resulting in the equation of motion

$$\partial_t^2 w = -\partial_x^2 M + P. \tag{1.3.4}$$

Remark 1.3.1. Equations (1.3.2)-(1.3.3) are referred to as the Rayleigh beam model [LVV09].

Remark 1.3.2. By substituting the constitutive equation (1.3.3) into the equation of motion (1.3.4), the partial differential equation for the Euler-Bernoulli model can be obtained, and is

$$\partial_t^2 w = -\frac{1}{\beta} \partial_x^4 w + P.$$

We consider the same boundary conditions as for the Timoshenko beam above. Using the assumptions for this model as described above, the boundary conditions can be rewritten as well.

Problem E-P (Pinned-pinned)
The model consists of the equation of motion (1.3.4) with constitutive equation (1.3.3) and boundary conditions

$$w(0,t) = w(1,t) = M(0,t) = M(1,t) = 0.$$

Problem E-C (Cantilever)
The problem is the same as Problem E-P above, except we consider instead the boundary conditions

$$w(0,t) = \partial_x w(0,t) = M(1,t) = \partial_x M(1,t).$$

For both problems, the initial conditions are

$$w(\cdot,0) = w_0,\ \partial_x w(\cdot,0) = w_{0x},\ \partial_t w(\cdot,0) = w_d,\ \partial_t \partial_x w(\cdot,0) = w_{dx}.$$

For the variational form, multiply Equation (1.3.4) by an arbitrary function v in $C^1[0,1]$ and integrate. Using integration by parts twice, we obtain

$$\begin{aligned}\int_0^1 \partial_t^2 w(\cdot,t)v = &-\partial_x M(1,t)v(1) + \partial_x M(0,t)v(0) + M(1,t)v'(1) - M(0,t)v'(0) \\ &- \int_0^1 \left(M(\cdot,t)v'' - P(\cdot,t)v\right).\end{aligned}$$

For the pinned-pinned case, define the class of test functions by

$$T_P[0,1] = \left\{v \in C^1[0,1] : v(0) = v(1) = 0\right\}.$$

For the cantilever case, the class of test functions is

$$T_C[0,1] = \left\{v \in C^1[0,1] : v(0) = v'(0) = 0\right\}.$$

Then we use the constitutive equation (1.3.3) and the boundary conditions to derive the variational problems.

Problem EV-P

Find w such that for each $t > 0$, $w(\cdot,t) \in T_P[0,1]$ and

$$\int_0^1 \partial_t^2 w(\cdot,t)v = -\int_0^1 \left(\frac{1}{\beta}\partial_x^2 w(\cdot,t)v'' - P(\cdot,t)v\right) \tag{1.3.5}$$

for each $v \in T_P[0,1]$, while

$$w(\cdot,0) = w_0,\ \partial_x w(\cdot,0) = w_{0x},\ \partial_t w(\cdot,0) = w_d,\ \partial_t \partial_x w(\cdot,0) = w_{dx}.$$

Problem EV-C

Find w such that for each $t > 0$, $w(\cdot,t) \in T_C[0,1]$ and Equation (1.3.5) holds for each $v \in T_C[0,1]$, while

$$w(\cdot,0) = w_0,\ \partial_x w(\cdot,0) = w_{0x},\ \partial_t w(\cdot,0) = w_d,\ \partial_t \partial_x w(\cdot,0) = w_{dx}.$$

1.4 The local linear Timoshenko rod

The study of large deformations of slender, flexible structures remains a challenging problem. A rod is described in [VDL21] as a one-dimensional solid, for example a cable, string or beam. In this section, the local linear Timoshenko (LLT) rod, introduced in [VDL21], is considered. There, the authors refer to a rod model as local linear if "large deflections and rotations of the rod are possible, but the rod strains are sufficiently small that linear elasticity theory still applies for the constitutive equations". The LLT rod model is based on the Simo-Reissner theory for a rod (briefly mentioned in Section 1.6 below). It is restricted to shear, flexure and extension, but not torsion; that is, the model considers only two-dimensional motion. Its name is indicative of the nature of the constitutive equations, which are based on those of the linear Timoshenko model, but are adapted for large deformations.

In this section, the LLT model in dimensionless form is introduced, and several special cases for small vibrations are derived from it, under additional assumptions, as was done in [VDL21]. Finally, the variational forms of the model are derived. Details on the derivation of the model itself, as well as its finite element method implementation, are provided in Chapter 5.

1.4.1 The LLT model

The model is presented here for reference, in dimensionless form.

The equations of motion are

$$\partial_t^2 u = \partial_x F_1 + P_1, \tag{1.4.1}$$

$$\partial_t^2 w = \partial_x F_2 + P_2, \tag{1.4.2}$$

$$\frac{1}{\alpha}\partial_t^2 \phi = (1 + \partial_x u) F_2 - \partial_x w F_1 + \partial_x M, \tag{1.4.3}$$

where

$$F_1 = S\cos\theta - V\sin\theta, \tag{1.4.4}$$

$$F_2 = S\sin\theta + V\cos\theta, \tag{1.4.5}$$

and $\partial_x s$ and θ are determined from

$$(\partial_x s)^2 = (1+\partial_x u)^2 + (\partial_x w)^2\,, \tag{1.4.6}$$

$$\cos\theta = (\partial_x s)^{-1}(1+\partial_x u)\,, \tag{1.4.7}$$

$$\sin\theta = (\partial_x s)^{-1}\partial_x w. \tag{1.4.8}$$

The constitutive equations are

$$M = \frac{1}{\beta}\partial_x \phi, \tag{1.4.9}$$

$$V = \theta - \phi, \tag{1.4.10}$$

$$S = \frac{1}{\gamma}(\partial_x s - 1)\,. \tag{1.4.11}$$

We explain the notation here for completeness. The details are in Chapter 5. In the above equations, u and w represent longitudinal and transverse displacements respectively, and ϕ is the angle of a cross-section. The arc length function of the displacement curve is s, and θ is the rotation of the tangent vector. The variables F_1 and F_2 are the components of the force acting on a part of the rod, M is the moment, and V and S are the shear force and axial force respectively. P_1 and P_2 are load forces.

Again we consider one of the following boundary conditions:
Pinned-pinned:

$$u(0,t) = w(0,t) = u(1,t) = w(1,t) = 0 \text{ and } M(0,t) = M(1,t) = 0. \tag{1.4.12}$$

Cantilever:

$$u(0,t) = w(0,t) = \phi(0,t) = 0 \text{ and } F_1(1,t) = F_2(1,t) = M(1,t) = 0. \tag{1.4.13}$$

In each case, the initial conditions are

$$u(\cdot,0) = \alpha_0,\ \partial_t u(\cdot,0) = \alpha_d,\ w(\cdot,0) = \beta_0,\ \partial_t w(\cdot,0) = \beta_d,\ \phi(\cdot,0) = \gamma_0,\ \partial_t \phi(\cdot,0) = \gamma_d.$$

Remark 1.4.1. In [VDL21], boundary conditions for a pivoted beam are also given, but since the above-mentioned boundary conditions are the main ones considered throughout this dissertation, the pivoted case was not studied in detail.

1.4.2 Variational Problems for the LLT model

In this section, the variational problems for the pinned-pinned and cantilever cases of the LLT model, introduced in Section 1.4.1, are derived.

First, multiply Equations (1.4.1)-(1.4.3) by functions $v, z, \psi \in C^1[0,1]$ respectively and integrate. Then, using integration by parts, it follows that

$$\int_0^1 \partial_t^2 u(\cdot,t)v = F_1(\cdot,t)v|_0^1 - \int_0^1 F_1(\cdot,t)v' + \int_0^1 P_1(\cdot,t)v, \tag{1.4.14}$$

$$\int_0^1 \partial_t^2 w(\cdot,t)z = F_2(\cdot,t)z|_0^1 - \int_0^1 F_2(\cdot,t)z' + \int_0^1 P_2(\cdot,t)z, \tag{1.4.15}$$

$$\begin{aligned}\int_0^1 \frac{1}{\alpha}\partial_t^2 \phi(\cdot,t)\psi = &\int_0^1 (1+\partial_x u(\cdot,t))\, F_2(\cdot,t)\psi - \int_0^1 \partial_x w(\cdot,t)F_1(\cdot,t)\psi \\ &+ M(\cdot,t)\psi|_0^1 - \int_0^1 M(\cdot,t)\psi'.\end{aligned} \tag{1.4.16}$$

The classes of test functions for the pinned-pinned and cantilever cases are T_P and T_C, defined in Section 1.2.2, respectively.

Finally, by substituting the boundary conditions, the variational forms are obtained.

Problem LLTV-P

Find $\langle u, w, \phi\rangle$ such that for each $t > 0$, $u(\cdot,t), w(\cdot,t) \in T_P[0,1]$, $\phi(\cdot,t) \in C^1[0,1]$ and

$$\begin{aligned}\int_0^1 \partial_t^2 u(\cdot,t)v &= -\int_0^1 F_1(\cdot,t)v' + \int_0^1 P_1(\cdot,t)v, \\ \int_0^1 \partial_t^2 w(\cdot,t)z &= -\int_0^1 F_2(\cdot,t)z' + \int_0^1 P_2(\cdot,t)z, \\ \int_0^1 \frac{1}{\alpha}\partial_t^2 \phi(\cdot,t)\psi &= \int_0^1 (1+\partial_x u(\cdot,t))\, F_2(\cdot,t)\psi - \int_0^1 \partial_x w(\cdot,t)F_1(\cdot,t)\psi \\ &\quad - \int_0^1 M(\cdot,t)\psi'\end{aligned} \tag{1.4.17}$$

for all $\langle v, z, \psi \rangle \in T_P[0,1] \times T_P[0,1] \times C^1[0,1]$.

Problem LLTV-C

Find $\langle u, w, \phi \rangle$ such that for each $t > 0$, $u(\cdot,t), w(\cdot,t), \phi(\cdot,t) \in T_C[0,1]$ and the equations in (1.4.17) hold for all $\langle v, z, \psi \rangle \in T_C[0,1] \times T_C[0,1] \times T_C[0,1]$.

For both problems, the initial conditions are

$$u(\cdot,0) = \alpha_0,\ \partial_t u(\cdot,0) = \alpha_d,\ w(\cdot,0) = \beta_0,\ \partial_t w(\cdot,0) = \beta_d,\ \phi(\cdot,0) = \gamma_0,\ \partial_t \phi(\cdot,0) = \gamma_d.$$

Remark 1.4.2. These variational forms for the LLT model are only presented in the unpublished work [DLV22]. In [VDL21], variational forms are derived for the special cases of the model.

1.4.3 Special cases of the LLT rod for small vibrations

As was noted in [VDL21], when small vibrations are considered, the assumption is usually that $\partial_x u$ and $\partial_x w$ are small, or that θ is small enough that $\sin\theta \approx \theta$ and $\cos\theta \approx 1$.

Suppose first that θ is small enough that $\sin\theta \approx \theta$ and $\cos\theta \approx 1$. Then Equation (1.4.7) can be replaced with

$$\partial_x s = 1 + \partial_x u. \tag{1.4.18}$$

In the other case, assume that $\partial_x u$ and $\partial_x w$ are small. We prove that the assumption

$$\begin{aligned} \partial_x s &= \sqrt{1 + 2\partial_x u + (\partial_x u)^2 + (\partial_x w)^2} \\ &\approx 1 + \partial_x u + \frac{1}{2}(\partial_x u)^2 + \frac{1}{2}(\partial_x w)^2. \end{aligned}$$

from [VDL21] is justified.

Suppose a variable y is small enough that

$$y^2 \approx 0.$$

Then

$$1 + y \approx 1 + y + \frac{1}{4}y^2; \text{ that is, } 1 + y \approx \left(1 + \frac{y}{2}\right)^2.$$

Since y is small, it is reasonable to assume that

$$1 + y \geq 0 \text{ and } 1 + \frac{y}{2} \geq 0,$$

and hence

$$\sqrt{1 + y} \approx 1 + \frac{y}{2}.$$

Now, since we assume that $\partial_x u$ and $\partial_x w$ are small, it is justified to replace y with $2\partial_x u + (\partial_x u)^2 + (\partial_x w)^2$ above. Thus we have that

$$\partial_x s \approx 1 + \partial_x u + \frac{1}{2}(\partial_x u)^2 + \frac{1}{2}(\partial_x w)^2,$$

and since $(\partial_x u)^2$ and $(\partial_x w)^2$ can be neglected, we again arrive at

$$\partial_x s = 1 + \partial_x u.$$

An alternative assumption, used for example in [SR79] and [WFH01], is that

$$\partial_x s = 1 + \partial_x u + \frac{1}{2}(\partial_x w)^2, \tag{1.4.19}$$

where the term $\frac{1}{2}(\partial_x w)^2$ is used to account for large geometric transverse displacements [WFH01].

In the following sections, these assumptions will be used to derive some special cases of the LLT model. The naming convention for models from [VDL21] will be used for easy reference. Note that in all cases, suitable initial conditions have to be chosen.

1.4.3.1 A nonlinear model for small vibrations

Under the above assumptions, $\sin\theta \approx \theta$ and $\cos\theta \approx 1$, and so we use θ and 1 in Equations (1.4.4) and (1.4.5). As a result we get

$$F_1 = S - V\theta \text{ and } F_2 = S\theta + V.$$

Further, we assume that $\theta \approx \partial_x w$, and hence replace θ to obtain

$$F_1 = S - V\partial_x w,$$
$$F_2 = S\partial_x w + V.$$

Substituting the above two equations into Equations (1.4.1)-(1.4.3), we get

$$\begin{aligned}
\partial_t^2 u &= \partial_x \left(S - V\partial_x w\right) + P_1, \\
\partial_t^2 w &= \partial_x \left(S\partial_x w + V\right) + P_2 \text{ and} \\
\frac{1}{\alpha}\partial_t^2 \phi &= \left(1 + \partial_x u\right)\left(S\partial_x w + V\right) - \partial_x w \left(S - V\partial_x w\right) + \partial_x M \\
&= S\partial_x w + V + \partial_x u \partial_x w S + \partial_x u V - \partial_x w S - V\left(\partial_x w\right)^2 + \partial_x M. \qquad (1.4.20)
\end{aligned}$$

Now, by assumption, $\partial_x u$ and $\partial_x w$ are small, so $\partial_x u \partial_x w$ and $(\partial_x w)^2$ can be neglected. Further, due to the scaling performed to arrive at the dimensionless form (details in Chapter 5), S and V are also small. Therefore Equation (1.4.20) becomes

$$\frac{1}{\alpha}\partial_t^2 \phi = \left(1 + \partial_x u\right) V + \partial_x M.$$

Finally, we substitute one of Equation (1.4.18) or (1.4.19) into Equation (1.4.11), and use the approximation $\theta = \partial_x w$ in Equation (1.4.10). The model is then as follows:

Model SLLT

The equations of motion for the model are

$$\partial_t^2 u = \partial_x \left(S - V\partial_x w\right) + P_1, \qquad (1.4.21)$$
$$\partial_t^2 w = \partial_x \left(S\partial_x w + V\right) + P_2, \qquad (1.4.22)$$
$$\frac{1}{\alpha}\partial_t^2 \phi = \left(1 + \partial_x u\right) V + \partial_x M, \qquad (1.4.23)$$

together with the constitutive equations

$$M = \frac{1}{\beta}\partial_x \phi, \tag{1.4.24}$$

$$V = \partial_x w - \phi, \tag{1.4.25}$$

$$S = \frac{1}{\gamma}\partial_x u \text{ or} \tag{1.4.26}$$

$$S = \frac{1}{\gamma}\partial_x u + \frac{1}{2\gamma}(\partial_x w)^2. \tag{1.4.27}$$

We again consider one of the boundary conditions (1.4.12) or (1.4.13).

Remark 1.4.3. In [VDL21], it was noted that for the case of boundary conditions for a pivoted beam, the solutions may exhibit large displacements, and the assumptions made in this section, which are for small vibrations only, are no longer suitable.

Note that Model SLLT is non-linear. In the following sections, it is shown how simpler models, which may be linear, can be derived with some additional assumptions. This reduces the challenge of analysis of these models, and makes the simpler LLT models convenient for the study of slender structures.

1.4.3.2 A model for transverse vibrations

A model for transverse vibrations can easily be derived from Model SLLT by neglecting the term $-V\partial_x w$ in Equation (1.4.21). Then the model is as follows:

Model LLT-T

The equations of motion are

$$\partial_t^2 u = \partial_x S + P_1, \tag{1.4.28}$$

$$\partial_t^2 w = \partial_x \left(S\partial_x w + V\right) + P_2, \tag{1.4.29}$$

$$\frac{1}{\alpha}\partial_t^2 \phi = \left(1 + \partial_x u\right) V + \partial_x M. \tag{1.4.30}$$

The constitutive equations are Equations (1.4.24)-(1.4.26), and the boundary conditions are as before.

Note that if the boundary conditions for u and S do not contain other variables of the model, and Equation (1.4.26) is used as the constitutive equation for S, then the system is decoupled.

For example, for the cantilever rod, we have the boundary conditions

$$u(0,t) = S(1,t) = 0.$$

Using these together with the system

$$\partial_t^2 u = \partial_x S + P_1,$$
$$S = \frac{1}{\gamma}\partial_x u,$$

u and S can be found.

The remaining system then has the equations of motion

$$\partial_t^2 w = \partial_x \left(S\partial_x w + V\right) + P_2,$$
$$\frac{1}{\alpha}\partial_t^2 \phi = \left(1 + \partial_x u\right) V + \partial_x M,$$

and constitutive equations

$$M = \frac{1}{\beta}\partial_x \phi,$$
$$V = \partial_x w - \phi,$$

and since u and S are already known, this system is linear.

1.4.3.3 Adapted linear Timoshenko models

Consider Model LLT-T. Suppose $\partial_t P_1 = 0$. Then there is no boundary forcing, and hence $\partial_t S = 0$ and Equation (1.4.28) becomes

$$0 = \partial_x S + P_1. \tag{1.4.31}$$

As noted above, the model is decoupled, and the last two equations of motion form a linear system. The resulting model is an adapted version of the linear Timoshenko beam model with axial force introduced in Section 1.2.3.

Model Tim-Ad1

The equations of motion are

$$\begin{aligned} 0 &= \partial_x S + P_1 \\ \partial_t^2 w &= \partial_x \left(S \partial_x w \right) + \partial_x V + P_2, \\ \frac{1}{\alpha} \partial_t^2 \phi &= \gamma S V + V + \partial_x M. \end{aligned} \tag{1.4.32}$$

Note that Equation (1.4.26) was substituted into Equation (1.4.30). The constitutive equations and boundary conditions are as before.

Remark 1.4.4. As was noted in [VDL21], it may be justified to use the approximation

$$(1 + \gamma S) V = V. \tag{1.4.33}$$

If this is the case, then Equation (1.4.32) becomes

$$\frac{1}{\alpha} \partial_t^2 \phi = V + \partial_x M,$$

and then Model Tim-Ad1 is the linear Timoshenko model with axial force from Section 1.2.3.

Another linear model can be obtained by instead assuming that $F_1 = S$ and $F_2 = V$ in Equations (1.4.2) and (1.4.3). Equation (1.4.26) is still used as constitutive equation so that the system is decoupled as before.

Model Tim-Ad2

The model has equations of motion

$$\begin{aligned} 0 &= \partial_x S + P_1, \\ \partial_t^2 w &= \partial_x V + P_2, \\ \frac{1}{\alpha} \partial_t^2 \phi &= (1 + \gamma S) V - S \partial_x w + \partial_x M. \end{aligned}$$

The constitutive equations and boundary conditions are the same as for Model SLLT.

1.4.3.4 Nonlinear Timoshenko model of Sapir and Reiss

A nonlinear Timoshenko model similar to Model LLT-T is derived in [SR79]. To derive this model in the same approach as was done above, some additional assumptions must be made. Suppose that $\partial_t^2 u$ and $\partial_x u V$ are neglected and assume that $P_1 = P_2 = 0$ and $\partial_x S = 0$ in Model LLT-T. The resulting equations of motion are

$$\begin{aligned} \partial_t^2 w &= S\partial_x^2 w + \partial_x V, \\ \frac{1}{\alpha}\partial_t^2 \phi &= V + \partial_x M. \end{aligned}$$

Note that, as discussed for Model LLT-T, if Equation (1.4.18) is used, then the system above is linear. However, since Equation (1.4.19) is used in [SR79] instead, it is necessary to use the assumption $\partial_x S = 0$ and the Fundamental Theorem of Calculus to obtain

$$\begin{aligned} S(t) &= S(\cdot, t) \\ &= \int_0^1 \partial_x S(\cdot, t) \\ &= \int_0^1 \frac{1}{\gamma}\partial_x u(\cdot, t) + \frac{1}{2\gamma}(\partial_x w(\cdot, t))^2 \\ &= \frac{1}{\gamma}\left(u(1, t) - u(0, t)\right) + \frac{1}{2\gamma}\int_0^1 (\partial_x w(\cdot, t))^2 \end{aligned}$$

for each t.

For the pinned-pinned case, [VDL21] uses the boundary conditions

$$w(0, t) = \partial_x \phi(0, t) = w(1, t) = \partial_x \phi(1, t) = 0.$$

1.4.3.5 Euler-Bernoulli model

Recall that in Section 1.3 it was shown how the linear Rayleigh and Euler-Bernoulli beam models can be derived from the linear Timoshenko model. A similar approach can be taken using Model SLLT introduced above.

Note that from Equation (1.4.26) we have that Equation (1.4.23) becomes

$$\frac{1}{\alpha}\partial_t^2\phi = (1+\gamma S)\,V + \partial_x M.$$

Then, using Equation (1.4.33), we obtain

$$\frac{1}{\alpha}\partial_t^2\phi = V + \partial_x M.$$

Substitution into Equation (1.4.22) yields

$$\partial_t^2 w = \partial_x\left(S\partial_x w + \frac{1}{\alpha}\partial_t^2\phi - \partial_x M\right),$$

and together with Equation (1.4.24), we have

$$\partial_t^2 w - \frac{1}{\alpha}\partial_x\partial_t^2\phi = \partial_x(S\partial_x w) - \frac{1}{\beta}\partial_x^3\phi.$$

As before, assume that cross-sections remain plane after deformation, so that $\partial_x w = \phi$. Then we obtain

$$\partial_t^2 w - \frac{1}{\alpha}\partial_t^2\partial_x^2 w = \partial_x(S\partial_x w) - \frac{1}{\beta}\partial_x^4 w. \tag{1.4.34}$$

The above equation is the Rayleigh beam model with axial force. Similar to the case of the linear model, if the term $\frac{1}{\alpha}\partial_t^2\partial_x^2 w$ is neglected, the above becomes the Euler-Bernoulli model with axial force.

Suppose Equation (1.4.27) is used instead of (1.4.26) as above. Then Equation (1.4.23) becomes

$$\frac{1}{\alpha}\partial_t^2\phi = \left(1+\gamma S - \frac{1}{2}(\partial_x w)^2\right)V + \partial_x M.$$

As before, we neglect $(\partial_x w)^2$ since $\partial_x w$ is small by assumption, and then the rest of the derivation is the same, and we again arrive at Equation (1.4.34). However, note that in this case, due to (1.4.27), the system is nonlinear.

1.5 The multi-dimensional wave equation

Although the focus of the dissertation is on models concerning flexible structures, the multi-dimensional wave equation is included in the study since it is a frequently considered problem in publications on existence theory and convergence theory of the finite element method. In applications, the multi-dimensional wave equation models the vibration of a membrane (in the two dimensional case, see e.g. [Inm94]) or even the propagation of sound waves (in the three-dimensional case, see e.g. [PR05]). In this dissertation, the multi-dimensional wave equation will be considered as an illustrative example for the application of existence theory and of finite element approximation convergence theory. For simplicity, the wave equation is considered with Dirichlet boundary conditions over the whole boundary. In this section, the variational form is derived.

Consider the following problem for the wave equation with viscous damping on a bounded domain Ω with boundary $\partial\Omega$.

Problem MWE

Given functions f, k, u_0, and u_1, find u defined on $\Omega \times [0,T]$ such that

$$\begin{aligned} \partial_t^2 u &= \nabla^2 u - k\partial_t u + f \text{ in } \Omega \times (0,T), \\ u &= 0 \text{ on } \partial\Omega, \end{aligned} \tag{1.5.1}$$

while $u(\cdot,0) = u_0$ and $\partial_t u(\cdot,0) = u_1$.

For simplicity, we use the following throughout this dissertation:

Assumption There exists a constant $c^* > 0$ such that

$$0 \leq k \leq c^*.$$

In this case, the class of test functions, denoted by $T(\Omega)$, is the space of all functions in $C(\bar{\Omega})$ that are zero on $\partial\Omega$ and have integrable partial derivatives.

1.5.1 Variational form

We multiply both sides of Equation (1.5.1) by an arbitrary function $v \in C(\bar{\Omega})$ with integrable partial derivatives, and integrate both sides. We also need Green's formula,

$$\iint_{\Omega} -(\nabla^2 u)v dA = \iint_{\Omega} \partial_x u \partial_x v + \partial_y u \partial_y v dA - \int_{\partial\Omega} v \nabla u \cdot n ds.$$

The boundary conditions and Green's formula are used to obtain the problem in variational form.

Problem MWE-V

Find u such that for each $t > 0$, $u(\cdot, t) \in T(\Omega)$ and

$$\iint_{\Omega} \partial_t^2 u(\cdot, t) v dA = -\iint_{\Omega} \partial_x u(\cdot, t)\partial_x v + \partial_y u(\cdot, t)\partial_y v dA - \iint_{\Omega} k\partial_t u(\cdot, t) v dA + \iint_{\Omega} f v dA$$

for each $v \in T(\Omega)$, while $u(\cdot, 0) = u_0$ and $\partial_t u(\cdot, 0) = u_1$.

1.6 Nonlinear models

While the models considered in this dissertation are those introduced in the above sections, other theories and models exist. Geometrically exact beam theories are beam theories in which "the relationships between the configuration and the strain measures are consistent with the virtual work principle and the equilibrium equations at a deformed state regardless of the magnitude of displacements, rotations and strains" [CJ99]. A very detailed survey of geometrically exact beam models can be found in the introduction of [MPW19]. In this section, we highlight a few key differences between the models that are most frequently used.

Cosserat and Kirchhoff models are ideal for modelling nonlinear deformation of slender beams [LA12]. Extension, bending and torsion are just some examples of rod deformation, and can be studied with classical geometrically exact Kirchhoff models, and shearing effects can additionally be incorporated by using Cosserat models [Cos09].

The Kirchhoff and Euler-Bernoulli theory models a beam with no shear strains. The Kirchhoff beam was the first model that allowed arbitrary initial curvature and bending and torsion deformations [MPW19]. The theory was enhanced by Love to include axial strain [MPW19], [CJ99]. Reissner later extended the theory to include shear deformation [MPW19]. Simo finally extended the work of Reissner to a semi-induced beam theory [MPW19]. Note that for Euler-type beams, cross-sections remain orthogonal to the axis of the beam after deformation due to the exclusion of shear strain. Including shear deformation in the model means that there is an angle between the center axis and the cross-sections, and these types of beams are Cosserat- and Timoshenko-type beams [CJ99].

The Kirchhoff and Cosserat rod models are nonlinear generalisations of linear Euler–Bernoulli and Timoshenko–Reissner beam models [LA12]. Mathematical analysis of these types of models can become quite complex, and is beyond the scope of this dissertation. The focus was on simpler models, for which existence theory and finite element applications are well-known and can be studied in detail, as an initial investigation.

Chapter 2

Existence

2.1 Introduction

Existence theory for models of vibration problems is an important research topic and also has practical significance. These model problems do not necessarily have classical solutions. However, so-called weak solutions are accepted, while regularity conditions could still be restrictive. In a practical sense, researchers often approximate "solutions" to model problems which are ill-posed and might not have a solution, but then attribute the numerical method's poor performance to the method, and not to the fact that there might not even be a solution to approximate. For this reason, existence theory is an important topic to consider when working with finite element approximations.

Additionally, a general existence theory that can be applied to a variety of problems, is important. Many articles (on convergence theory) cite existence results from [LM72] or [Eva97], which are not general and are restricted to problems similar to the multi-dimensional wave equation. In the book of Showalter [Sho77] and the article [AKS96], more general existence theory is available, but is given in terms of linear operators, which could be inconvenient for practical applications of the theory.

In [VV02], a general theory for linear second order hyperbolic type problems is derived, where the so-called general linear vibration problem is given in an abstract variational form. This theory is convenient in applications, since methods such as the FEM already require derivation of the variational form of the problem, which can then be used when applying the existence theory. There are restrictions to this theory, namely that the problem has to be linear, and that the bilinear form b, which contains the terms that have to do with elasticity, has to be symmetric. This theory (and the follow up paper [VS19], where the latter restriction is relaxed) is considered in this dissertation, since it is convenient to use for the problems considered.

In this chapter, the results from [VV02] are summarised, and some comparisons are made with [VS19]. As mentioned above, one restriction of [VV02] is that the bilinear form b in the abstract variational form need to be symmetric; in [VS19] this assumption is relaxed, and some proofs must be adapted to achieve the same results. The main existence theorem, which is important in Chapter 3, is from [VV02]. These articles can be consulted for detailed proofs of the results presented here.

In Section 2.2, the general linear second order hyperbolic problem in abstract form is presented, followed by the main existence theory in Section 2.3. The necessary theory to prove the main result, as well as comparisons between [VV02] and [VS19], are in Subsection 2.3.1. The chapter is concluded with a section on the application of some of this existence theory to the Timoshenko model with axial force and to the multi-dimensional wave equation.

2.2 The general linear vibration problem

First, the general linear second-order hyperbolic equation, introduced in [VV02], which involves different types of damping, is given. The notation to be used in the remainder of this chapter and Chapter 3 is also introduced.

1. Let V be a Hilbert space with inner product $b(\cdot,\cdot)$ and norm $\|\cdot\|_V$.

2. Let W be a Hilbert space with inner product $c(\cdot,\cdot)$ and norm $\|\cdot\|_W$.

3. Let X be a Hilbert space with inner product $(\cdot,\cdot)$ and norm $\|\cdot\|_X$.

Here V, W and X are such that $V \subset W \subset X$.

Additionally, let a denote a bilinear form on V.

Remark 2.2.1. The above definitions were changed slightly in [VS19], where it was assumed that b may be non-symmetric. It was still assumed that c is the inner product for W, but the inner product for V was denoted by $(\cdot,\cdot)_V$, and b was merely a bilinear form on V. Note that $b(\cdot,\cdot) = (\cdot,\cdot)_V$ may not be true, since b is not symmetric.

Also denote by J the interval of type $[0,T)$ or $[0,\infty)$, or an open interval containing 0, and let Y denote a Hilbert space. We write $u'(t) \in Y$ if the derivative of u exists with respect to the norm of Y, and write $u \in C^{(k)}(J;Y)$ if $u^{(k)} \in C(J;Y)$.

The general linear vibration problem is Problem G:

Problem G

Given a function $f : [0,T] \to X$, find a function $u \in C([0,T);V)$ such that u' is continuous at 0, and for each $t \in (0,T)$, $u(t) \in V$, $u'(t) \in V$, $u''(t) \in W$ and

$$c(u''(t),v) + a(u'(t),v) + b(u(t),v) = (f(t),v)_X \tag{2.2.1}$$

for each $v \in V$, while $u(0) = u_0$ and $u'(0) = u_1$.

The following four assumptions (from [VV02]) are necessary for the theory in this chapter, and will also play a role in convergence (discussed in Chapter 3):

E1 V is dense in W, and W is dense in X.

E2 There exists a constant $\kappa_1 > 0$ such that $\|v\|_W \leq \kappa_1 \|v\|_V$ for each $v \in V$.

E3 There exists a constant $\kappa_2 > 0$ such that $\|w\|_X \leq \kappa_2 \|w\|_W$ for each $w \in W$.

E4 The bilinear form a is symmetric, non-negative and bounded on V; that is, there exists a constant $K_a > 0$ such that $|a(u,v)| \leq K_a \|u\|_V \|v\|_V$ for all $u, v \in V$.

Remark 2.2.2. In [VS19], an additional assumption, which becomes necessary later, was introduced to accommodate the fact that b may be non-symmetric. Note that we may write $b = b_0 + b_1$, where b_0 is the symmetric part, and b_1 the non-symmetric part, of b. Then we have the following assumption:

E5 The bilinear form b_1 is bounded as follows: there exists a positive constant $K_1 < \frac{1}{\kappa_2}$ such that

$$|b_1(u,v)| \leq K_1 ||u||_V ||u||_W \text{ for all } u, v \in V.$$

Remark 2.2.3. Assumption E4 has to be changed slightly for the case of weak damping. The bilinear form a is then bounded on W instead of on V. The following is again from [VV02]:

E4W The bilinear form $a(\cdot,\cdot)$ is non-negative, symmetric and bounded on W; that is, there exists a constant $K_a > 0$ such that $|a(u,v)| \leq K_a \|u\|_W \|v\|_W$ for all $u, v \in W$.

In the remaining sections of this chapter, assumptions E1 to E4 (and E5 where necessary for the comparison with [VS19]) are assumed to be satisfied.

2.3 Main existence results

The existence theorem for general damping is given in [VV02], but the notation from [BSV17] (where the existence theory is used for convergence of finite element approximations) will be used in this section, for consistency of notation with Chapter 3. For easy reference, the theorem is given as Theorem 2.3.1 below. The results required to prove it are from [VV02], and are given in Section 2.3.1, where comparisons with [VS19] are made.

Theorem 2.3.1. Suppose assumptions E1, E2, E3 and E4 hold. If $u_0 \in V$ and $u_1 \in V$ and there exists some $y \in W$ such that

$$b(u_0, v) + a(u_1, v) = c(y, v) \text{ for each } v \in V, \tag{2.3.1}$$

then for each $f \in C^1([0,T]; X)$, there exists a unique solution

$$u \in C([0,T); V) \cap C^1([0,T); W) \cap C^1((0,T); V) \cap C^2((0,T); W)$$

for Problem G. If $f = 0$, then $u \in C^1([0,\infty); V) \cap C^2([0,\infty); W)$.

Remark 2.3.1. If b is not symmetric, then, assuming instead that assumptions E1 to E5 hold, together with Equation (2.3.1), the result of Theorem 2.3.1 still holds.

Remark 2.3.2. Note that in [VV02] there is a typo in this theorem (Theorem 1 in the article), namely that $u_1 \in W$. It should be $u_1 \in V$, as above, which is also pointed out in [VZV09].

Now define

$$E_b = \{x \in V : \text{ there exists a } y \in W \text{ such that } c(y,v) = b(x,v) \text{ for all } v \in V\}.$$

Using assumption E4W instead of E4, we have the existence theorem for weak damping from [VV02]:

Theorem 2.3.2. Suppose assumptions E1, E2, E3 and E4W hold. Then there exists a unique solution $u \in C^1((-\infty,\infty); V) \cap C^2((-\infty,\infty); W)$ for Problem G for each $u_0 \in E_b$, $u_1 \in V$ and each $f \in C^1((-\infty,\infty); X)$.

If we assume in addition that assumption E5 holds, then we have the existence theorem for weak damping from [VS19], for the case that b is not symmetric:

Theorem 2.3.3. Suppose assumptions E1, E2, E3, E4W and E5 hold. Then there exists a unique solution $u \in C^1(J; V) \cap C^2(J; W)$ for Problem G for each $u_0 \in E_b, u_1 \in V$ and each $f \in C^1(J, X)$. If $f = 0$, then $u \in C^1((-\infty,\infty); V) \cap C^2((-\infty,\infty); W)$.

2.3.1 Important results for the existence theorem

In this subsection, the theory used to prove Theorem 2.3.1 is given.

First note that we can write Problem G as a first-order system. For each $t \in (0,T)$, let $w(t) = u'(t)$. Then we write

$$c(w'(t), v) + a(w(t), v) + b(u(t), v) = (f(t), v)_X$$

for each $v \in V$.

Define the Hilbert space $H = V \times W$. Denote an element x of H by $x = \langle x_1, x_2 \rangle$, where $x_1 \in V$ and $x_2 \in W$. Define the inner product $(\cdot, \cdot)_H$ on H by

$$(x, y)_H = b(x_1, y_1) + c(x_2, y_2) \text{ for all } x, y \in H.$$

The idea is to define an infinitesimal generator of a C_0 semigroup in H, and then semigroup theory can be used to prove Theorem 2.3.1.

The following results are the same in [VV02] and [VS19].

Lemma 2.3.1. Suppose $\lambda \geq 0$. For each $y \in H$, there exists a unique $x \in H$ such that

$$\lambda x_1 - x_2 = y_1, \text{ and} \tag{2.3.2}$$

$$b(x_1, v) + a(x_2, v) + \lambda c(x_2, v) = c(y_2, v) \text{ for all } v \in V. \tag{2.3.3}$$

Definition. For $\lambda = 0$, define the operator Λ on H by $\Lambda y = -x$, if Equations (2.3.2) and (2.3.3) are satisfied.

Lemma 2.3.2. Λ is a bounded linear operator with trivial nullspace.

It follows from Lemma 2.3.2 that Λ^{-1} exists.

Definition. Operator $A = \Lambda^{-1}$.

Lemma 2.3.3. A is a densely defined closed linear operator on H.

The proof of Lemma 2.3.3 differs in [VV02] and [VS19]. Note that in both cases, the proof that A is closed is simple. However, if b is not symmetric, the proof that $D(A) = R(\Lambda)$ is dense in H is not as simple.

Outline of the proof of Lemma 2.3.3. Start by assuming that b is symmetric, and suppose for a contradiction that $R(\Lambda)$ is not dense in H. Then there exists $w \in H$ such that $w \neq 0$ and $(w, z)_H = 0$ for each $z \in \bar{R}$, the closure of $R(\Lambda)$ in H.

In [VV02] it is shown that, if $x = \Lambda\langle w_1, w_2 + w_1\rangle$, then

$$b\left(w_1, z_1\right) + c\left(w_2, z_2\right) = 0 \text{ for each } z \in \bar{R}, \tag{2.3.4}$$

and also

$$x_2 = w_1, \text{ and} \tag{2.3.5}$$

$$b\left(x_1, v\right) + a\left(x_2, v\right) = -c\left(w_2 + w_1, v\right) \text{ for all } v \in V. \tag{2.3.6}$$

From Equation (2.3.4) it follows that

$$b\left(w_1, x_1\right) + c\left(w_2, x_2\right) = 0 \tag{2.3.7}$$

from the definition of $(\cdot, \cdot)_H$.

Equations (2.3.5) and (2.3.6) imply that

$$b\left(x_1, w_1\right) + c\left(w_2, x_2\right) = -a\left(x_2, x_2\right) - c\left(x_2, x_2\right),$$

and then the symmetry of b, that is, the fact that $b\left(w_1, x_1\right) = b\left(x_1, w_1\right)$, and Equation (2.3.7) can be used to prove that $c\left(x_2, x_2\right) = 0$ and hence $x_2 = w_1 = 0$.

This will no longer work if b is not symmetric. Assume again that $R(\Lambda)$ is not dense in H, i.e. there exists $y \in H$ such that $y \neq 0$ and $(y, z)_H = 0$ for each $z \in \bar{R}$ (note here the change of notation from $w \in H$ above to $y \in H$, which is introduced for easy comparison between the two proofs).

In [VS19] it is shown, using the Lax-Milgram Theorem, and the fact that for any $z \in H$, we may write $z = z^0 + z^\perp$, where $z^0 \in \bar{R}$ and $z^\perp \in \bar{R}^\perp$, that there is a unique $w \in H$ such that $b\left(z_1^0, w_1\right) + c\left(z_2^0, w_2\right) = \left(z^0, y\right)_H$ for every $z^0 \in \bar{R}$.

Since $y \in \bar{R}^\perp$ and $z^0 \in \bar{R}$, we have that $\left(z^0, y\right)_H = 0$, and thus there exists a $w \in \bar{R}^\perp$ such that $w \neq 0$ and $b\left(z_1, w_1\right) + c\left(z_2, w_2\right) = 0$ for any $z \in \bar{R}$. Using this instead of Equation (2.3.4), the same procedure as above can now be followed to prove that $w_2 = 0$, since the symmetry of b is no longer required.

The next part of the proof is the same in both articles:
It can be shown that $c(v, w_2) = c(w_2, v) = 0$ for any $v \in W$ using that V is dense in W, and hence $w_2 = 0$.

This proves that $w = 0$. In the case of [VV02], this is the contradiction. In the case of [VS19], this can be used to show that $y = 0$, which is a contradiction.

The following four results can then be obtained.

Lemma 2.3.4. For any $x \in D(A)$, $Ax = y$ if and only if

$$x_2 = y_1 \text{ and}$$
$$b(x_1, v) + a(x_2, v) = -c(y_2, v) \text{ for all } v \in V.$$

Corollary 2.3.1. For any $\lambda \geq 0$, $R(\lambda I - A) = H$.

Corollary 2.3.2. $x \in D(A)$ if and only if there exists a $y \in W$ such that

$$b(x_1, v) + a(x_2, v) = c(y, v) \text{ for all } v \in V.$$

Lemma 2.3.5. $(Ax, y)_H = b(x_2, y_1) - a(x_2, y_2)$ for all $x, y \in D(A)$.

Finally, this leads to the following result:

Lemma 2.3.6. A is the infinitesimal generator of a C_0 semigroup of contractions in H.

The proof of this lemma differs for the cases that b is symmetric and not symmetric.

If b is symmetric, then we have the following:

Corollary 2.3.3. $(Ax, x)_H = -a(x_2, x_2)$ for all $x \in D(A)$.

Corollary 2.3.3 implies that A is dissipative, i.e. $(Ax, x)_H \leq 0$ for every $x \in D(A)$, from the nonnegativity of a. Then, using Lemma 2.3.3 and Corollaries 2.3.3 and 2.3.1, it can be shown that A is the infinitesimal generator of a C_0 semigroup of contractions in H.

If b is not symmetric, the approach in [VS19] must be taken. There, it is shown that $(\lambda - A)^{-1}$ is bounded for all real $\lambda > \frac{1}{2}K_1$. Then

$$\left|\left|\left((\lambda I - A)^{-1}\right)^n\right|\right| \leq \left(\lambda - \frac{1}{2}K_1\right)^{-n} \text{ for each } n \in \mathbb{N}.$$

The fact that A is the infinitesimal generator of a C_0 semigroup of contractions in H follows from Lemma 2.3.3 and Corollary 3.8 p.12 in [Paz83].

Finally, we give the initial value problem for the first-order system defined at the beginning of this subsection.

Problem G-IVP

Given a function $G : J \to H$, find $w \in C(J, H)$ such that for each $t \in J$, $w(t) \in D(A)$, $w'(t) \in H$ and

$$w'(t) = Aw(t) + G(t), \tag{2.3.8}$$

$$w(0) = w_0. \tag{2.3.9}$$

Remark 2.3.3. The problem is written as it is in [VS19], since it uses the same notation as [BSV17] and Chapter 3 of this dissertation. Recall that J is of the form $[0, T)$ or $[0, \infty)$, or an open interval containing 0. Thus, the initial value problem as it is given in [VV02] is essentially the same.

We obtain the following from Lemma 2.3.4:

Lemma 2.3.7. Suppose $G(t) = \langle 0, g(t)\rangle$ for each $t \in J$.

1. If u is a solution of Problem G, then $w = \langle u, u'\rangle$ is a solution of Problem G-IVP with $w_0 = \langle u_0, u_1\rangle$.
2. If w is a solution of Problem G-IVP with $u_0 = \langle u_0, u_1\rangle$, then the first component $u = w_1$ of w is a solution of Problem G.

Finally, using the fact that A is the infinitesimal generator of a C_0 semigroup in H, together with Corollary 2.3.2 and Lemma 2.3.7, Theorem 2.3.1 can be proven.

2.4 Applications

The theory of [VV02] (and [VS19]) can be used in a variety of applications. An example is given in [DD20], where a model for the study of heat transfer in biological tissues is given. Its variational form was derived, and Theorem 2 of [VV02] was applied to prove that the problem has a unique solution. Further, the theory was also applied in [VVS21], to prove the well-posedness of two models for heat transfer of short-pulse lasers. The theory of [VV02] and [VS19] was also applied to the adapted Timoshenko models derived in [VDL21]. In [VZV09], the theory of [VV02] was applied to the variational problem of a vibration model for a plate-beam system consisting of a Reissner-Midlin plate and a Timoshenko beam. Such a system was also analysed in [PRT14], but in this article, the authors derived their own theory for existence of local and global weak solutions.

In this section, the multi-dimensional wave equation and the linear Timoshenko model with axial force introduced in Chapter 1 are used as further illustrative examples of how the theory introduced in Chapter 2 can be used in applications.

2.4.1 The multi-dimensional wave equation without damping

We first consider the multi-dimensional wave equation without damping, as it will be used again in later sections of the dissertation in applications. Thus we ignore the term $k\partial_t u$ in Equation (1.5.1). The aim is to first write the wave equation in the form of Equation (2.2.1) of Problem G.

Let $X = \mathcal{L}^2(\Omega)$ and let V be the closure of the class of test functions $T(\Omega)$ in the Sobolev space $H^1(\Omega)$ (see Appendix A for details on Sobolev spaces). The norm on $H^1(\Omega)$ is denoted by $||\cdot||_1$, and the norm on $\mathcal{L}^2(\Omega)$ is denoted by $||\cdot||$.

For any $u, v \in H^1(\Omega)$, define the bilinear form b by

$$b(u,v) = \iint_\Omega \partial_x u \partial_x v + \partial_y u \partial_y v dA, \tag{2.4.1}$$

and for any $u, v \in \mathcal{L}^2(\Omega)$, define the bilinear form c by

$$c(u,v) = \iint_\Omega uv dA. \tag{2.4.2}$$

Remark 2.4.1. A definition of a bilinear form a as given in Equation (2.2.1) is not necessary here, as we do not consider damping.

Note that for any $u \in H^1(\Omega)$,

$$b(u,u) = \iint_\Omega (\partial_x u)^2 + (\partial_y u)^2 \, dA \geq 0$$

by properties of integrals, since $(\partial_x u)^2 \geq 0$ and $(\partial_y u)^2 \geq 0$.

Proposition 2.4.1. There exists a constant $\kappa_1 > 0$ such that

$$||v||_1 \leq \kappa_1 \sqrt{b(v,v)} \text{ for each } v \in V. \tag{2.4.3}$$

Proof. Note that since $\partial\Omega$ is non-empty, the Poincaré-Friedrichs inequality (see for example Theorem 2 pg.300 of [Eva97]) holds. That is, there exists a constant $\beta > 0$ such that

$$b(v,v) \geq \beta \, ||v||_1^2 \text{ for all } v \in V. \tag{2.4.4}$$

It follows from the definition of $||\cdot||_1$ and Inequality (2.4.4) that for any $v \in V$, we have

$$\begin{aligned} ||v||_W^2 &\leq ||v||_1^2 \\ &\leq \frac{1}{\beta} b(v,v) \end{aligned}$$

and hence

$$||v||_W \leq \kappa_1 \sqrt{b(v,v)} \text{ for all } v \in V,$$

where $\kappa_1 = \sqrt{\dfrac{1}{\beta}} > 0$.

□

Proposition 2.4.2. The bilinear form b is an inner product on V.

Proof. Let $u, v, w \in V$ and let a_1, a_2 be positive constants.

Recall from above that $b(u,u) \geq 0$. Further, by properties of bilinear forms, we know that

$$b(u,v) = b(v,u) \text{ and } b(a_1u + a_2v, w) = a_1b(u,w) + a_2b(v,w).$$

Finally, suppose $b(u,u) = 0$. Then it follows from Inequality (2.4.4) and the fact that $||u||_1^2 \geq 0$, that we must have $||u||_1^2 = 0$. Properties of the norm then imply that $u = 0$.

Hence by definition, $b(\cdot,\cdot)$ is an inner product for V. □

The norm on V is now defined as

$$||v||_V = \sqrt{b(v,v)} \text{ for each } v \in V.$$

Remark 2.4.2. From this definition, Inequality (2.4.3) can be written as

$$||v||_1 \leq \kappa_1 ||v||_V \text{ for each } v \in V. \tag{2.4.5}$$

The bilinear form c is just the inner product on $\mathcal{L}^2(\Omega)$, so $W = X$ and consequently

$$||u||_W = ||u|| \text{ for each } u \in W.$$

To apply the existence theory, it must be shown that assumptions **E1** to **E3** are satisfied.

Remark 2.4.3. Assumption **E4W** is not required here since we do not consider damping, and therefore do not have a bilinear form $a(\cdot,\cdot)$.

First note that since $C_0^\infty(\Omega)$ is dense in $\mathcal{L}^2(\Omega)$ and $C_0^\infty(\Omega) \subset V$, it follows that V is dense in $W = \mathcal{L}^2(\Omega)$. Since $W = \mathcal{L}^2(\Omega) = X$, trivially W is dense in X.

Assumption **E2** follows from Proposition 2.4.1, and Assumption **E3** follows trivially since $W = X$.

Recall that we defined J as an open interval containing 0, or an interval of the form $[0,T)$ or $[0,\infty)$. Then we have the following problem for the wave equation on a multi-dimensional domain, which is the weak variational problem of Problem MWE-V without damping.

Problem MWE-W

Find u such that for each $t \in J$, $u(t) \in V$, $u''(t) \in X$ and

$$c\left(u''(t), v\right) + b\left(u(t), v\right) = c\left(f(\cdot, t), v\right) \text{ for each } v \in V,$$

while $u(0) = u_0$ and $u'(0) = u_1$.

Recall also that we defined

$$E_b = \{x \in V : \text{ there exists a } y \in W \text{ such that } c\left(y, v\right) = b\left(x, v\right) \text{ for all } v \in V\}.$$

Finally, since assumptions **E1** to **E3** are satisfied, it follows from Theorem 2.3.2 that there exists a unique solution

$$u \in C^1((-\infty, \infty); V) \cap C^2((-\infty, \infty); W)$$

for Problem MWE-W for each $u_0 \in E_b$, $u_1 \in V$ and each $f \in C^1\left((-\infty, \infty); X\right)$.

2.4.2 The multi-dimensional wave equation with viscous damping

We again investigate the application of the existence theory to the multi-dimensional wave equation, but now with viscous damping included. Note that most of the argument remains the same as in Section 2.4.1 above.

Recall that we defined $X = \mathcal{L}^2(\Omega)$ and V to be the closure of the class of test functions $T(\Omega)$ in the Sobolev space $H^1(\Omega)$. Also recall the definitions of the bilinear forms b and c from Equations (2.4.1) and (2.4.2).

Now we additionally define for any $u, v \in H^1(\Omega)$ the bilinear form a as follows:

$$a(u, v) = \iint_{\Omega} kuvdA.$$

We proved in Proposition 2.4.2 that b is an inner product for V, and defined its corresponding norm $||\cdot||_V$. Further, we had that the bilinear form c is just the inner product on $\mathcal{L}^2(\Omega)$, so

$W = X$ and

$$||u||_W = ||u|| \text{ for each } u \in W.$$

The proof that assumptions **E1** to **E3** are satisfied is the same as in Section 2.4.1. It remains to prove that assumption **E4W** is satisfied. This is done in the following proposition.

Proposition 2.4.3. The bilinear form a is non-negative, symmetric and bounded on W.

Proof. It is clear from properties of integrals that for any $u, v \in W$,

$$a(u, v) = a(v, u),$$

and that

$$a(u, u) \geq 0,$$

since $u^2 \geq 0$ and $k \geq 0$ from the assumption on k (see Section 1.5).

It remains to prove that a is bounded. Using the Cauchy-Schwarz inequality and since it is assumed that $0 \leq k \leq c^*$ on Ω, we have that

$$\begin{aligned} |a(u, v)| &= \left| \iint_\Omega kuv dA \right| \\ &\leq \iint_\Omega |k| \, |uv| \, dA \\ &\leq c^* \iint_\Omega |uv| \, dA \\ &\leq c^* \, ||u|| \, ||v|| \end{aligned}$$

for any $u, v \in W$.

Since $W = X$, it follows that for any $u, v \in W$

$$|a(u, v)| \leq c^* \, ||u||_W \, ||v||_W .$$

□

Recall that we defined J as an open interval containing 0, or an interval of the form $[0, T)$ or $[0, \infty)$. Then we have the following problem for the wave equation on a multi-dimensional domain, which is the weak variational problem of Problem MWE-V with damping.

Problem MWED-W

Find u such that for each $t \in J$, $u(t) \in V$, $u''(t) \in X$ and

$$c\left(u''(t), v\right) + a(u'(t), v) + b\left(u(t), v\right) = c\left(f(\cdot, t), v\right) \text{ for each } v \in V,$$

while $u(0) = u_0$ and $u'(0) = u_1$.

Recall again that

$$E_b = \{x \in V : \text{ there exists a } y \in W \text{ such that } c\left(y, v\right) = b\left(x, v\right) \text{ for all } v \in V\}.$$

Since assumptions **E1** to **E4W** are satisfied, it follows from Theorem 2.3.2 that there exists a unique solution

$$u \in C^1((-\infty, \infty); V) \cap C^2((-\infty, \infty); W)$$

for Problem MWED-W for each $u_0 \in E_b$, $u_1 \in V$ and each $f \in C^1\left((-\infty, \infty); X\right)$.

2.4.3 The Timoshenko model with axial force

The aim is to first write Problem T-V in the form of Equation (2.2.1) of Problem G.

Some notation is introduced to facilitate the derivations. We denote the inner product on $\mathcal{L}^2(0,1)$ by $(\cdot, \cdot)$, and its corresponding norm by $||\cdot||$. Recall that the inner product and norm on the Sobolev space $H^1(0,1)$ are denoted by $(\cdot, \cdot)_1$ and $||\cdot||_1$ respectively (see Appendix A). Let $X = \mathcal{L}^2(0,1) \times \mathcal{L}^2(0,1)$ and $H^1 = H^1(0,1) \times H^1(0,1)$. An element y of X or H^1 is denoted by $y = \langle y_1, y_2 \rangle$.

Define an inner product on X by

$$(x, y) = (x_1, y_1) + (x_2, y_2).$$

The corresponding norm is denoted by $||\cdot||_X$.

The inner product on H^1 is

$$(x, y)_{H^1} = (x_1, y_1)_1 + (x_2, y_2)_1,$$

with corresponding norm $||\cdot||_{H^1}$.

Also define the following bilinear forms: For any $f, g \in X$ and any $u, v \in H^1$,

$$c(f,g) = (f_1, g_1) + \left(\frac{1}{\alpha} f_2, g_2\right)$$
$$b(u,v) = \left(\frac{1}{\beta} u_2', v_2'\right) + (u_1' - u_2, v_1' - v_2) + (Su_1', v_1'),$$

where the derivatives are weak derivatives. Note that these bilinear forms are symmetric.

Also denote

$$b_T(u,v) = \left(\frac{1}{\beta} u_2', v_2'\right) + (u_1' - u_2, v_1' - v_2).$$

Note then that

$$b(u,v) = b_T(u,v) + (Su_1', v_1').$$

Remark 2.4.4. We do not consider damping in this case, and so there is no need to define a bilinear form a as it appears in Equation (2.2.1).

For simplicity of notation, it is assumed that the area of a cross-section of the beam remains constant. This does not affect the theory.

Proposition 2.4.4. The bilinear form c is an inner product for X.

Proof. Let $u, v, w \in X$ and $a_1, a_2 \in \mathbb{R}$.

First note that

$$c(u,u) = ||u_1||^2 + \frac{1}{\alpha} ||u_2||^2 \geq min\left\{1, \frac{1}{\alpha}\right\} ||u||_X^2 \geq 0. \tag{2.4.6}$$

Since c is a bilinear form, we know that

$$c(u,v) = c(v,u) \text{ and } c(a_1 u + a_2 v, w) = a_1 c(u,w) + a_2 c(v,w).$$

Finally, if $c(u,u) = 0$, then the Inequality (2.4.6) implies that $||u||_X^2 = 0$. Consequently $u = 0$.

Hence by definition, c is an inner product for X. □

Definition. We denote the space X with the inner product c by W. The norm on W is defined by

$$||u||_W = \sqrt{c(u,u)} \text{ for each } u \in W.$$

Proposition 2.4.5. The norms $||\cdot||_W$ and $||\cdot||_X$ are equivalent on W.

Proof. Let $u \in W$. From Inequality (2.4.6) we have that

$$||u||_W^2 \geq min\left\{1, \frac{1}{\alpha}\right\} ||u||_X^2 .$$

Further, it is easy to see that

$$||u||_W^2 \leq max\left\{1, \frac{1}{\alpha}\right\} ||u||_X^2 .$$

Since u is arbitrary, this holds for all $u \in W$, and the result follows. □

Next, we aim to define the space V, which will depend on the boundary conditions used. Recall that two sets of homogeneous boundary conditions were considered for the problem. For the pinned-pinned case, let $V_P(0,1)$ be the closure of $T_P[0,1]$ in $H^1(0,1)$, and define $V_P = V_P(0,1) \times H^1(0,1)$. For the cantilever case, let $V_C(0,1)$ be the closure of $T_C[0,1]$ in $H^1(0,1)$, and define $V_C = V_C(0,1) \times V_C(0,1)$.

Remark 2.4.5. By definition, the spaces $V_P(0,1)$ and $V_C(0,1)$ are Hilbert spaces.

Proposition 2.4.6. The spaces V_P and V_C are dense subsets of W.

Proof. $V_P(0,1)$ and $V_C(0,1)$ are dense in $\mathcal{L}^2(0,1)$ since $C_0^\infty(0,1)$ is dense in $\mathcal{L}^2(0,1)$. Hence V_P and V_C are dense subsets of X. The result then follows from the equivalence of the norms $||\cdot||_W$ and $||\cdot||_X$. □

Similar to the approach for the multi-dimensional wave equation in Section 2.4.1, we use a Poincaré-type inequality to find an upper bound for $b_T(\cdot,\cdot)$ in terms of $||\cdot||_X$:
If $f \in C^1[0,1]$ has a zero in $[0,1]$, then $|f(x)| \leq ||f'||$ for each $x \in [0,1]$.

Using the definitions of $V_C(0,1)$ and $V_P(0,1)$ and the above inequality, we have the following result, by taking limits:

Proposition 2.4.7. For any $u \in V_C(0,1)$ or $V_P(0,1)$,

$$||u|| \leq ||u'|| \,. \tag{2.4.7}$$

We will also need the following proposition:

Proposition 2.4.8. For any $u \in V_C$ or V_P,

$$||u_1||^2 \leq ||u_1'||^2 \leq 2\beta \left(||u_1' - u_2||^2 + \frac{1}{\beta} ||u_2||^2 \right).$$

Proof. Since $u \in V_C$ or V_P, it follows from Proposition 2.4.7 that $||u_1|| \leq ||u_1'||$.

From the triangle inequality, and the fact that for any $a_1, a_2 \in \mathbb{R}$, $2|a_1 a_2| \leq a_1^2 + a_2^2$, it follows that

$$\begin{aligned} ||u_1'||^2 &\leq 2 ||u_1' - u_2||^2 + 2 ||u_2||^2 \\ &\leq 2\beta \left(||u_1' - u_2||^2 + \frac{1}{\beta} ||u_2||^2 \right). \end{aligned}$$

□

Proposition 2.4.7 is also used to prove the following result.

Proposition 2.4.9. There exists a constant $C_b > 0$ such that

$$b_T(u,u) \geq C_b^2 ||u||_X^2 \text{ for each } u \in V_P \text{ or } V_C. \tag{2.4.8}$$

Proof. The case that $u \in V_C$ is simple.

Suppose $u \in V_C$. From the definition of $||\cdot||_X$ and from Proposition 2.4.7 we have

$$\begin{aligned} ||u||_X^2 &\leq ||u_1'||^2 + ||u_2'||^2 \\ &\leq 2 \left(||u_1' - u_2||^2 + ||u_2'||^2 \right). \end{aligned}$$

The result then follows from the definition of b, letting

$$C_b^2 = \frac{1}{2} min \left\{ 1, \frac{1}{\beta} \right\}.$$

The proof for the case that $u \in V_P$ is more complicated. The idea of the proof is from the appendix of [VZV09].

First note that if $u = 0$, then Proposition 2.4.9 holds trivially. The rest of the proof is done by contradiction.

Assume that there is $u \in V_P$ such that

$$b_T(u, u) < C_b^2 \, ||u||_X \tag{2.4.9}$$

for every constant C_b.

Note that for $u \neq 0$ we have that

$$b_T(w, w) = \frac{b_T(u, u)}{||u||_X^2},$$

where $w = \dfrac{u}{||u||_X}$. Then $b_T(w, w) < C_b^2$ for each C_b by assumption, and $w \in B(0, 1) \cap V_P$. Here $B(0, 1)$ denotes the unit sphere in $\mathcal{L}^2(0, 1)$.

It follows that there exists a sequence $(w^n) = (w_1^n, w_2^n)$ in $B(0, 1) \cap T_P[0, 1] \times C^1[0, 1]$ such that

$$||w_1^n||^2 + ||w_2^n||^2 = 1 \text{ for every } n \in \mathbb{N}. \tag{2.4.10}$$

Since Inequality (2.4.9) holds for every C_b, it follows form the definition of b_T that we must have

$$||(w_2^n)'||^2 + ||(w_1^n)' - w_2^n||^2 \to 0 \text{ as } n \to \infty. \tag{2.4.11}$$

First we show that $||w_2^n|| > \dfrac{1}{2}$ for n sufficiently large. Note that since $w_1^n \in T_P[0, 1]$ for each $n \in \mathbb{N}$, we have from Proposition 2.4.7 and the triangle inequality that

$$\begin{aligned} ||w_1^n|| &\leq ||(w_1^n)'|| \\ &\leq ||(w_1^n)' - w_2^n|| + ||w_2^n|| \end{aligned}$$

for each $n \in \mathbb{N}$.

Note that from (2.4.11) we know that

$$||(w_1^n)' - w_2^n|| \to 0 \text{ as } n \to \infty.$$

Then by definition, there exists $n_0 \in \mathbb{N}$ such that

$$||(w_1^n)' - w_2^n|| < \frac{1}{4} \text{ for all } n \geq n_0.$$

Then

$$||w_1^n|| < \frac{1}{4} + ||w_2^n|| \text{ for all } n \geq n_0.$$

From Equation (2.4.10) it follows that

$$\left|\left|w_2^n + \frac{1}{4}\right|\right|^2 + ||w_2^n||^2 > 1.$$

It follows from property of norms that

$$||w_2^n||^2 + \frac{1}{2}||w_2^n|| + \frac{1}{16} + ||w_2^n||^2 > 1$$

and hence $||w_2^n|| > \frac{1}{2}$ for all $n \geq n_0$.

Next we show that $\int_0^1 w_2^n > \frac{1}{3}$ for sufficiently large n. First, suppose $w_2^n(x) = 0$ for some $x \in [0,1]$ for each $n \in \mathbb{N}$. Then from Proposition 2.4.7 we have that

$$||w_2^n|| \leq ||(w_2^n)'|| \text{ for each } n \in \mathbb{N}.$$

From Equation (2.4.11) we know that

$$||(w_2^n)'|| \to 0 \text{ as } n \to \infty, \text{ so } ||w_2^n|| \to 0 \text{ as } n \to \infty.$$

But we showed that $||w_2^n|| > \frac{1}{2}$ for all $n \geq n_0$, a contradiction.

Thus we know that $w_2^n(x) \neq 0$ for every $x \in [0,1]$, for all $n \in \mathbb{N}$. Hence we assume without loss of generality that $w_2^n > 0$ for all $n \in \mathbb{N}$.

Using the Cauchy-Schwarz inequality and the fact that $||w_2^n|| \leq 1$ from Equation (2.4.10), we have

$$\begin{aligned}\left|(w_2^n(b))^2 - (w_2^n(a))^2\right| &= \left|\int_a^b 2w_2^n(w_2^n)'\right| \\ &\leq 2\int_a^b |w_2^n|\,|(w_2^n)'| \\ &\leq ||w_2^n||\,||(w_2^n)'|| \\ &\leq 2\,||(w_2^n)'||\,,\end{aligned}$$

for every subinterval (a, b) of $[0, 1]$.

Again, we know from (2.4.11) that

$$||(w_2^n)'|| \to 0 \text{ as } n \to \infty,$$

so by definition there exists $n_1 \in \mathbb{N}$ such that

$$||(w_2^n)'|| < \frac{1}{10} \text{ for all } n \geq n_1.$$

Let $N = max\{n_0, n_1\}$.

It then follows that $w_{max}^2 - w_{min}^2 < \frac{1}{10}$, where w_{max} and w_{min} are the maximum and minimum values of w_2^n respectively, for all $n \geq N$. Then

$$\begin{aligned}w_{min}^2 &= \int_0^1 w_{min}^2 \\ &= \int_0^1 (w_2^n)^2 - \int_0^1 (w_2^n)^2 - w_{min}^2 \\ &\geq \int_0^1 (w_2^n)^2 - \int_0^1 w_{max}^2 - w_{min}^2 \\ &> \frac{1}{4} - \frac{1}{10} \\ &> \frac{1}{9}.\end{aligned}$$

Hence $\int_0^1 w_2^n > \int_0^1 w_{min} = w_{min} > \frac{1}{3}$ for all $n \geq N$.

Next, we show that $\int_0^1 (w_1^n)' > 0$ for sufficiently large n. Using the Cauchy-Schwarz inequality, we have that

$$\begin{aligned}\left|(w_1^n)' - \int_0^1 w_2^n\right| &= \left|\int_0^1 (w_1^n)' - w_2^n\right| \\ &\leq \int_0^1 |(w_1^n)' - w_2^n| \\ &\leq ||(w_1^n)' - w_2^n||\end{aligned}$$

for all $n \in \mathbb{N}$.

Again, since

$$||(w_1^n)' - w_2^n|| \to 0 \text{ as } n \to \infty,$$

by definition there exists $n_2 \in \mathbb{N}$ such that

$$||(w_1^n)' - w_2^n|| < \frac{1}{3} \text{ for all } n \geq n_2.$$

Then $\left|\int_0^1 (w_1^n)' - \int_0^1 w_2^n\right| < \frac{1}{3}$ for all $n \geq n_2$.

Let $N^* = max\{N, n_2\}$. Since $\int_0^1 w_2^n > \frac{1}{3}$ for all $n \geq N$, it follows that $\int_0^1 (w_1^n)' > 0$ for all $n \geq N^*$.

Finally, we have from the Fundamental Theorem of Calculus that for all $n \in \mathbb{N}$,

$$w_1^n(1) - w_1^n(0) = \int_0^1 (w_1^n)' > 0.$$

Since $w_1^n(0) = 0$, it follows that $w_1^n(1) > 0$ for all $n \geq N^*$. But $w_1^n \in T_P[0,1]$, so $w_1^n(1) = 0$, for all $n \in \mathbb{N}$, a contradiction. Hence Inequality (2.4.8) holds for all $u \in V_P$. □

Now let $K^* = max\{\beta, C_b^{-2}\}$.

Proposition 2.4.10. If

1. $S \geq 0$ or

2. $S < 0$ and $sup\,|S| \leq \dfrac{1}{2K^* + 1}$,

then b is an inner product for V_P or V_C.

Proof. Let $u, v, w \in V_P$ or V_C, and let $a_1, a_2 \in \mathbb{R}$.

First note that since b is a bilinear form, we know that

$$b\,(u, v) = b\,(v, u) \text{ and}$$
$$b\,(a_1 u + a_2 v, w) = a_1 b\,(u, w) + a_2 b\,(v, w)\,.$$

1. Now suppose $S \geq 0$.

   From Proposition 2.4.9 we know that $b_T(u, u) \geq 0$. Then using the definition of b, it follows that

   $$b(u, u) = b_T(u, u) + (Su_1', u_1') \geq 0$$

   by property of integrals.

   Further, if $b(u, u) = 0$ then $b_T(u, u) = -\,(Su_1', u_1') = 0$. Proposition 2.4.9 then implies that $||u||_X^2 = 0$, and hence $u = 0$ by property of norms.

2. Next, suppose $S < 0$ and $sup\,|S| \leq \dfrac{1}{2K^* + 1}$.

   Note that from Proposition 2.4.8 and the definition of K^* we have

   $$\begin{aligned} |(Su_1', u_1')| &\leq sup\,|S|\,||u_1'||^2 \\ &\leq \frac{1}{2K^* + 1} 2\beta b_T(u, u) \\ &\leq \frac{2K^*}{2K^* + 1} b_T(u, u). \end{aligned}$$

   Then

   $$\begin{aligned} b(u, u) &= b_T(u, u) + (Su_1', u_1') \\ &\geq b_T(u, u) - \frac{2K^*}{2K^* + 1} b_T(u, u), \end{aligned}$$

and hence

$$b(u,u) \geq \frac{1}{2K^* + 1} b_T(u,u).$$

Since $b_T(u,u) \geq 0$ from Proposition 2.4.9, it follows that $b(u,u) \geq 0$, and if $b(u,u) = 0$, then $b_T(u,u) = 0$, implying $u = 0$ (in the same way as before).

It follows by definition that b is indeed an inner product for V_P or V_C. □

Remark 2.4.6. We assume that either $S \geq 0$ or $S < 0$, since for this model it is unrealistic in practice for S to change sign in $(0,1)$.

Assumption. In the remainder of this section we assume that $sup\,|S| \leq \frac{1}{2K^* + 1}$ if $S < 0$.

Definition. We define V as the space V_P or V_C in H^1 with inner product b. The norm on V is defined by

$$||u||_V = \sqrt{b(u,u)} \text{ for each } u \in V.$$

Proposition 2.4.11. The norms $||\cdot||_V$ and $||\cdot||_{H^1}$ are equivalent on V.

Proof. Let $u \in V$. Now

$$\begin{aligned} ||u||_V^2 = b(u,u) &\leq max\left\{1, \frac{1}{\beta}\right\}\left(||u_2'||^2 + ||u_1' - u_2||^2\right) + sup\,|S|\,||u_1'||^2 \\ &\leq K_1^*\,||u||_{H^1}^2 \end{aligned}$$

where $K_1^* = max\left\{1, \frac{1}{\beta}, sup\,|S|\right\}$.

Next, note that

$$||u||_{H^1}^2 = ||u||_X^2 + ||u_1'||^2 + ||u_2'||^2 \tag{2.4.12}$$

and that

$$||u_1'||^2 + ||u_2'||^2 \leq ||u_1' - u_2||^2 + ||u_1'||^2 + ||u_2'||^2,$$

since $||u_1' - u_2||^2 \geq 0$.

From the definition of b we have that

$$b(u,u) \geq K_2^*\left(||u_1'||^2 + ||u_2'||^2 + ||u_1' - u_2||^2\right),$$

where $K_2^* = min\left\{1, \frac{1}{\beta}, inf\,|S|\right\}$.

Hence

$$||u_1'||^2 + ||u_2'||^2 \leq (K_2^*)^{-1}\, b(u,u). \tag{2.4.13}$$

Further, recall from Proposition 2.4.9 that

$$b_T(u,u) \geq C_b^2\, ||u||_X^2\,,$$

and from what we showed in the proof of Proposition 2.4.10 above, we know that there is some constant $C^* > 0$ such that

$$b(u,u) \geq C^* b_T(u,u).$$

Hence

$$b(u,u) \geq C_1^*\, ||u||_X^2\,,$$

where $C_1^* = C_b^2 C^*$.

It follows from this, Equation (2.4.12) and Equation (2.4.13) that

$$\begin{aligned} ||u||_{H^1}^2 &= ||u||_X^2 + ||u_1'||^2 + ||u_2'||^2 \\ &\leq (C_1^*)^{-1} b(u,u) + (K_2^*)^{-1} b(u,u) \\ &= K_b\, ||u||_V^2\,, \end{aligned}$$

where $K_b = (K_2^*)^{-1} + (C_1^*)^{-1}$.

This concludes the proof. □

Corollary 2.4.1. The space V is complete.

Finally, we can construct the weak variational problem. Let $\tilde{Q}(t) = Q(\cdot, t)$ for each t.

Problem T-W

Find u such that for each $t \in J$, $u(t) \in V$, $u''(t) \in W$ and

$$c(u''(t), v) + b(u(t), v) = \left(\tilde{Q}(t), v\right) \text{ for each } v \in V,$$

while $u(0) = u_0 = \langle w_0, \phi_0 \rangle$ and $u'(0) = u_d = \langle w_d, \phi_d \rangle$.

Now we apply the existence theory from Chapter 2. To this end, it must again be shown first that assumptions **E1** to **E3** are satisfied.

From Proposition 2.4.6 we know that V is a dense subset of W. Trivially W is a dense subset of X. Further, from the equivalence of $||\cdot||_W$ and $||\cdot||_X$, the equivalence of $||\cdot||_X$ and $||\cdot||_{H^1}$ and from the equivalence of $||\cdot||_V$ and $||\cdot||_{H^1}$, it follows that there exists $\kappa_1 > 0$ such that

$$||v||_W \leq \kappa_1 ||v||_V \text{ for each } v \in V.$$

Further, from the equivalence of $||\cdot||_W$ and $||\cdot||_X$ it follows that there exists $\kappa_2 > 0$ such that

$$||w||_X \leq \kappa_2 ||w||_W \text{ for each } w \in W.$$

Hence assumptions **E1** to **E3** are satisfied. Now define $f(t) = \langle \tilde{Q}(t), 0 \rangle$ for each t. Note that $f \in C^1([0,T); X)$ if $\tilde{Q} \in C^1([0,T); \mathcal{L}^2(0,1))$.

Then it follows from Theorem 2.3.2 that there exists a unique solution

$$u \in C^1((-\infty, \infty); V) \cap C^2((-\infty, \infty); W)$$

for Problem T-W for each $u_0 \in E_b$, $u_d \in V$ and each $\tilde{Q} \in C^1((-\infty, \infty); \mathcal{L}^2(0,1))$.

Chapter 3

Convergence of Solutions of the General Linear Vibration Problem

3.1 Introduction

The finite element method (FEM) can be used to approximate the solution of various problems. It is important to consider whether the approximate solutions converge to the exact solution of the problem. It is often the case that solutions which are not 'smooth' may lead to slow convergence of numerical methods, and especially in finite element applications, very restrictive assumptions, such as existence of third or fourth order time derivatives for the solution, are necessary [VS19]. In [Dup73] and [Bak76], estimates for the errors of the semi-discrete and fully discrete problems for the undamped wave equation were derived, using the standard FEM. In [Sem94] and [FXX99], such estimates were derived for a vibrating Timoshenko beam model, but using mixed FEM. However, as pointed out in [BSV17] and [BV13], the errors for the fully discrete problems were derived without making use of the results obtained for the semi-discrete problem, at the expense of very restrictive regularity assumptions on the exact solution. For example, the existence of the fourth order derivative of the exact solution to the Timoshenko beam model was assumed to guarantee convergence.

Such assumptions are not feasible in practice. The authors of [BSV17] and [BV13] therefore introduced an alternative way of deriving error estimates, by using results already obtained for the semi-discrete error estimate, the final result following easily from the triangle inequality. The results from the existence theory (discussed in Chapter 2) are needed for the convergence theory. Some additional assumptions are also required, but these are much less restrictive than those mentioned above.

In [BV13] and [BSV17], error estimates were derived for the semi-discrete problems of the general linear second order hyperbolic problem. Error estimates for the fully-discrete problem were also presented. In [BV13], the theory holds for weak damping while in [BSV17], general damping was considered, under some additional assumptions. In the following sections, the derivations of the error estimates in [BSV17] are reproduced and analysed. Naturally there is some overlap with results from [BV13], as these papers complement each other. The general linear model under consideration was introduced in Section 2.2. Section 3.2 introduces the semi-discrete problem and derivation of the error estimates. The error estimates for the fully discrete problem are considered in Section 3.4. Where appropriate, comparisons between [BV13] and [BSV17] are made.

Remark 3.1.1. In the sections that follow, it is assumed that the assumptions E1 to E4, as well as the additional assumption of Theorem 2.3.1 in Section 2.2, are satisfied. Thus we assume that the solution u of Problem G exists and satisfies

$$u \in C([0,T);V) \cap C^1([0,T);W) \cap C^1((0,T);V) \cap C^2([0,T);W). \tag{3.1.1}$$

Note that this is also assumed in [BSV17], though it is not explicitly mentioned.

3.2 The semi-discrete problem

In this section, some results from [BSV17] that will be useful in the other sections of this chapter are proved. First it is necessary to introduce the semi-discrete problem, Problem G^h, associated with Problem G.

Let S^h be a finite-dimensional subspace of V.

Problem G^h

Given a function $f : [0,T] \to X$, find a function $u_h \in C^2[0,T]$ such that for each $t \in (0,T)$,

$$c\left(u_h''(t), v\right) + a\left(u_h'(t), v\right) + b\left(u_h(t), v\right) = \left(f(t), v\right)_X \tag{3.2.1}$$

for each $v \in S^h$, while $u_h(0) = u_0^h \in S^h$ and $u_h'(0) = u_1^h \in S^h$.

Now let u be the solution of Problem G, and u_h the solution of Problem G^h. The aim is to derive an estimate for the error $e_h(t) = u(t) - u_h(t)$. As in [BSV17], we start by introducing a projection operator.

Define the operator P by

$$b\left(u - Pu, v\right) = 0 \text{ for all } v \in S^h.$$

Note here that $(Pu)(t) = Pu(t)$ for each $t \in (0,T)$.

Then we can write

$$e_h(t) = e(t) + e_p(t),$$

where

$$e(t) = Pu(t) - u_h(t) \text{ and } e_p(t) = u(t) - Pu(t),$$

for each $t \in (0,T)$. An estimate for e_h can thus be obtained, by finding estimates for e and e_p.

3.2.1 Error estimate for e

Consider the following assumptions:

C1 The solution u of Problem G has the property that $(Pu) \in C^2(0,T)$.

C2 The solution u of Problem G satisfies $u \in C^1([0,T);V) \cap C^2((0,T);V)$.

Remark 3.2.1. In the remainder of this subsection, only Assumption C1 is needed. Assumption C2 is only used later in this chapter, but to avoid confusion when comparing with [BSV17], it is mentioned here for consistency.

Remark 3.2.2. Assumption C2 was not necessary in [BV13], as will become evident in Section 3.3.

Proposition 3.2.1. If $u \in C^2((0,T);W)$ and u satisfies assumption C1, then $e_p \in C^2((0,T);W)$.

Proof. Note that $e_p(t) = u(t) - Pu(t)$ for each $t \in (0,T)$. Now, by definition, $Pu \in S^h$, and by assumption C1, we have that $Pu \in C^2((0,T);V)$. Since S^h is a finite-dimensional subspace of V, all norms on S^h are equivalent. Then by definition, there exist constants $c_1, c_2 > 0$ such that

$$\|x\|_V \leq c_1\|x\|_W \leq c_2\|x\|_V \text{ for each } x \in S^h.$$

Let $t_0 \in (0,T)$. Then for each $t \in (0,T)$, we have that

$$\|Pu(t) - Pu(t_0)\|_V \leq c_1\|Pu(t) - Pu(t_0)\|_W \leq c_2\|Pu(t) - Pu(t_0)\|_V. \tag{3.2.2}$$

Fix $\epsilon > 0$. Since $Pu \in C((0,T);V)$, by definition there exists $\delta > 0$ such that for $t \in (0,T)$, if $|t - t_0| < \delta$, then $\|Pu(t) - Pu(t_0)\|_V < \dfrac{c_1\epsilon}{c_2}$. It follows from Equation (3.2.2) that if $|t - t_0| < \delta$, then $\|Pu(t) - Pu(t_0)\|_W < \epsilon$, and hence by definition, $Pu \in C((0,T);W)$.

Further, since $Pu \in C^1((0,T);V)$, by definition there exists $\delta_1 > 0$ such that for $t \in (0,T)$, if $0 < |\delta t| < \delta_1$, then $\left\|\dfrac{1}{\delta t}(Pu(t+\delta t) - Pu(t)) - (Pu)'(t)\right\|_V < \dfrac{c_1\epsilon}{c_2}$. It follows that if $0 < |\delta t| < \delta_1$, then $\left\|\dfrac{1}{\delta t}(Pu(t+\delta t) - Pu(t)) - (Pu)'(t)\right\|_W < \epsilon$, and hence by definition, $(Pu)' \in W$. In the same way as above, we can prove that $(Pu)' \in C((0,T);W)$. Hence $Pu \in C^1((0,T);W)$.

Repeating the above argument with $(Pu)'$ instead of Pu, it follows that $Pu \in C^2((0,T);W)$. Since $u \in C^2((0,T);W)$ by assumption, it follows by properties of continuous functions that $e_p \in C^2((0,T);W)$. □

Finally, we reach the main result of this subsection, which is Lemma 3.1 in [BSV17]:

Lemma 3.2.1. If the solution u of Problem G satisfies assumption C1, then for all $t \in (0,T)$,

$$c\left(e_p''(t), v\right) + a\left(e_p'(t), v\right) + c\left(e''(t), v\right) + a\left(e'(t), v\right) + b\left(e(t), v\right) = 0 \text{ for all } v \in S^h.$$

Proof. Recall that $u'(t) \in V$ and $u''(t) \in W$. Now from assumption C1, $(Pu) \in C^2((0,T);V)$. Then $(Pu) \in C^1((0,T);V)$, and it follows that $e_p' \in V$. Further, in the proof of Proposition 3.2.1, we showed that $Pu \in C^2((0,T);W)$, and hence $e_p'' \in W$. By the same argument, using u_h instead of u, we find that $e' \in V$ and $e'' \in W$.

It follows that for all $v \in S^h$,

$$\begin{aligned}
&c\left(e_p''(t), v\right) + a\left(e_p'(t), v\right) + c\left(e''(t), v\right) + a\left(e'(t), v\right) + b\left(e(t), v\right) \\
&= c\left(u''(t) - u_h''(t), v\right) + a\left(u'(t) - u_h'(t), v\right) + b\left(u(t) - u_h(t), v\right) + b\left(Pu(t) - u(t), v\right) \\
&= (f, v)_X - (f, v)_X \\
&= 0.
\end{aligned}$$

The second equality follows from the fact that u and u_h are solutions of Problems G and G^h respectively and since $b(Pu - u, v) = 0$ by definition of P. □

Note here that in this version of the proof, the result of Proposition 3.2.1 was not used, as is suggested in [BSV17], but only a part of its proof - Assumption C1 is sufficient to obtain the result of Lemma 3.2.1. To satisfy the assumption $u \in C^2((0,T);W)$ of Proposition 3.2.1, note that the assumption that u satisfies (3.1.1) must be used. However, in the proof above, we only needed the fact that $u''(t) \in W$, i.e. u'' exists with respect to $||\cdot||_W$.

Remark 3.2.3. The result for weak damping corresponding to Lemma 3.2.1 is given as Proposition 3.1 in [BV13].

3.2.2 Error estimate for e_p

The error estimate for $e_p(t) = u(t) - Pu(t)$ is obtained exactly as in [BSV17]. To this end, we require the following definition and assumption.

Definition. $\Pi u = \sum_{k=1}^{n} \phi_k(u) w_k$ where w_k is a basis for S^h and ϕ_k are linear functionals.

We refer to Πu as the generalised interpolation operator.

Suppose that h is such that $h \to 0$ as $n \to \infty$. Then we formulate assumption C3:

C3 There exists a subspace $H(V,k)$ of V, an interpolation operator Π and constants $C_\Pi > 0$ and $\alpha > 0$, depending on V and k, such that for $u \in H(V,k)$,

$$||u - \Pi u||_V \leq C_\Pi h^\alpha \, ||u||_{H(V,k)} \,,$$

where $||\cdot||_{H(V,k)}$ is a norm or semi-norm associated with $H(V,k)$.

Then the following proposition follows immediately from assumption C3.

Proposition 3.2.2. There exists a subspace $H(V,k)$ of V and constants $C_\Pi > 0$ and $\alpha > 0$, depending on V and k, such that for $u \in H(V,k)$,

$$||u - Pu||_V \leq C_\Pi h^\alpha \, ||u||_{H(V,k)} \,,$$

where $||\cdot||_{H(V,k)}$ is a norm or semi-norm associated with $H(V,k)$.

Remark 3.2.4. Note that in [BV13], the corresponding assumption is called Assumption C2. The assumption there is slightly different, in that an upper bound is given for $\inf ||u - v||_V$ instead. In [BV13], it was shown how their Assumption C2 can be used to obtain the same result as in Proposition 3.2.2, and it was noted that in applications, the interpolation error is used to obtain the error estimate of the assumption. Thus, it is reasonable to use the interpolation operator instead, as in C3 above, since the same estimates for the projection errors are obtained.

3.3 Error estimates for the semi-discrete problem

In this section, an error estimate for the semi-discrete approximation is derived. Several results are required, which are proven first, followed by the main results in Subsection 3.3.2.

3.3.1 Initial estimates

The following expression will be useful throughout this section:

$$E(t) = \frac{1}{2}c\left(e'(t), e'(t)\right) + \frac{1}{2}b\left(e(t), e(t)\right) \tag{3.3.1}$$

$$= \frac{1}{2}\left|\left|e'(t)\right|\right|_W^2 + \frac{1}{2}\left|\left|e(t)\right|\right|_V^2, \tag{3.3.2}$$

provided that $e' \in W$.

The idea here is to obtain an estimate for $E(t)$ in terms of the projection errors, and then use the fact that $||e'(t)||_W^2 + ||e(t)||_V^2 = 2E(t)$ to obtain an estimate for $e(t)$.

We start by obtaining an upper bound for $E'(t)$.

Lemma 3.3.1. If the solution u of Problem G satisfies assumption C1, then for any $t \in (0, T)$,

$$E'(t) \leq -c\left(e_p''(t), e'(t)\right) - a\left(e_p'(t), e'(t)\right). \tag{3.3.3}$$

Proof. The solution u_h of Problem G^h is in $C^2[0,T]$, and $(Pu) \in C^2(0,T)$ from assumption C1, so $e \in C^2(0,T)$. Further, u_h and Pu are in S^h by definition, and so $e(t) \in S^h$. Hence $e'(t) \in S^h$ for each $t \in (0,T)$.

Now let $t \in (0,T)$. Since the result of Lemma 3.2.1 holds for all $v \in S^h$, it follows that

$$c\left(e_p''(t), e'(t)\right) + a\left(e_p'(t), e'(t)\right) + c\left(e''(t), e'(t)\right) + a\left(e'(t), e'(t)\right) + b\left(e(t), e'(t)\right) = 0. \tag{3.3.4}$$

By property of the inner products b and c, it follows from Equation (3.3.1) that

$$\begin{aligned} E'(t) &= \frac{1}{2}c\left(e''(t), e'(t)\right) + \frac{1}{2}c\left(e'(t), e''(t)\right) + \frac{1}{2}b\left(e'(t), e(t)\right) + \frac{1}{2}b\left(e(t), e'(t)\right) \\ &= c\left(e''(t), e'(t)\right) + b\left(e(t), e'(t)\right). \end{aligned}$$

Then, substituting Equation (3.3.4), we obtain

$$E'(t) = -c\left(e_p''(t), e'(t)\right) - a\left(e_p'(t), e'(t)\right) - a\left(e'(t), e'(t)\right).$$

Since $a\left(e'(t), e'(t)\right) \geq 0$ by assumption E4, it follows then that

$$E'(t) \leq -c\left(e_p''(t), e'(t)\right) - a\left(e_p'(t), e'(t)\right).$$

Since $t \in (0,T)$ is arbitrary, this holds for any $t \in (0,T)$. □

Equation (3.3.3) will be used to obtain an estimate for $E(t)$. However, as pointed out in [BSV17], the second term of the equation is problematic, since

$$a\left(e_p'(t), e'(t)\right) \leq K_a \left|\left|e_p'(t)\right|\right|_V ||e'(t)||_V$$

from assumption E4, and $||e'(t)||_V$ is not bounded by $E(t)$.

Instead, the following result will be used, and its use will become clear in the proof of Lemma 3.3.3 below.

Proposition 3.3.1. If $e_p \in C^1([0,T);V) \cap C^2((0,T);V)$, then for any $t \in (0,T)$,

$$\int_0^t a\left(e_p'(\cdot), e'(\cdot)\right) = a\left(e_p'(t), e(t)\right) - a\left(e_p'(0), e(0)\right) - \int_0^t a\left(e_p''(\cdot), e(\cdot)\right).$$

To prove this result, we use the following theorem and lemma. Note that Lemma 3.3.2 is from [BV13].

Theorem 3.3.1. Let $\{a_1, a_2, \ldots, a_k\}$ be a linearly independent set in the k-dimensional vector space U. Then any $x \in U$ can be written as $\sum_{i=1}^{k} x_i a_i$, and the set of real numbers $\{x_i\}$ is uniquely determined.

Lemma 3.3.2. If $u \in C^1(J;V)$, then $(Pu) \in C^1(J;V)$ and $(Pu)'(t) = Pu'(t)$ for each $t \in J$.

Proof of Proposition 3.3.1. Recall that in the proof of Lemma 3.3.1 we showed that $e(t) \in S^h$. Let $\{\phi_1, \phi_2, \ldots, \phi_n\}$ be a basis for S^h. Then by Theorem 3.3.1, we can write

$$e(t) = \sum_{i=1}^{n} e_i(t)\phi_i \tag{3.3.5}$$

for any $t \in (0,T)$.

It follows from properties of the inner product a that

$$a\left(e_p'(t), e(t)\right) = \sum_{i=1}^{n} e_i(t) a\left(e_p'(t), \phi_i\right) \tag{3.3.6}$$

for any $t \in (0, T)$.

Recall that $e(t) = Pu(t) - u_h(t)$. At this point, the proof in [BSV17] points out that $e \in C^1(0, T)$. It should be shown why this is the case. We assume that u satisfies Equation (3.1.1). Then by Lemma 3.3.2, we have that $(Pu) \in C^2((0, T); V)$. Since $u_h \in C^2[0, T]$, it follows that $e \in C^2(0, T)$, and so $e \in C^1(0, T)$.

Hence $e_i \in C^1(0, T)$ for each $i = 1, 2, \ldots, n$. From Equation (3.3.5) it follows that $e'(t) = \sum_{i=1}^{n} e_i'(t)\phi_i$, and hence we conclude, like above, that for any $t \in (0, T)$,

$$a\left(e_p'(t), e'(t)\right) = \sum_{i=1}^{n} e_i'(t) a\left(e_p'(t), \phi_i\right). \tag{3.3.7}$$

Since $e_p \in C^2((0, T); V)$ we have by definition that

$$\begin{aligned} 0 &\leq \left| \frac{1}{\delta t} \left(a\left(e_p'(t + \delta t), \phi_i\right) - a\left(e_p'(t), \phi_i\right)\right) - a\left(e_p''(t), \phi_i\right) \right| \\ &\leq K_a \left|\left| \frac{1}{\delta t} \left(e_p'(t + \delta t) - e_p'(t)\right) - e_p''(t) \right|\right|_V ||\phi_i||_V \\ &\to 0 \text{ as } \delta t \to 0 \end{aligned}$$

for any $t \in (0, T)$, where the second inequality follows from assumption E4.

Then $\left| \frac{1}{\delta t} \left(a\left(e_p'(t + \delta t), \phi_i\right) - a\left(e_p'(t), \phi_i\right)\right) - a\left(e_p''(t), \phi_i\right) \right| \to 0$ as $\delta t \to 0$ from the squeeze theorem, and it follows by definition that $a\left(e_p'(\cdot), \phi_i\right)$ is differentiable on $(0, T)$, and

$$\frac{d}{dt} a\left(e_p'(t), \phi_i\right) = a\left(e_p''(t), \phi_i\right) \text{ for each } t \in (0, T) \text{ and for } i = 1, 2, \ldots, n. \tag{3.3.8}$$

Finally, we can combine Equations (3.3.6), (3.3.7) and (3.3.8) to obtain

$$\begin{aligned} \frac{d}{dt} a\left(e_p'(t), e(t)\right) &= \frac{d}{dt} \sum_{i=1}^{n} e_i(t) a\left(e_p'(t), \phi_i\right) \\ &= \sum_{i=1}^{n} e_i'(t) a\left(e_p'(t), \phi_i\right) + \sum_{i=1}^{n} e_i(t) a\left(e_p''(t), \phi_i\right) \\ &= a\left(e_p'(t), e'(t)\right) + a\left(e_p''(t), e(t)\right) \end{aligned}$$

for each $t \in (0,T)$.

Integrating both sides, and using the Fundamental Theorem of Calculus, it follows that for each $t \in (0,T)$,

$$\begin{aligned}\int_0^t a\left(e_p'(\cdot),e'(\cdot)\right) &= \int_0^t \frac{d}{dt}a\left(e_p'(\cdot),e(\cdot)\right) - a\left(e_p''(\cdot),e'(\cdot)\right)dt \\ &= a\left(e_p'(t),e(t)\right) - a\left(e_p'(0),e(0)\right) - \int_0^t a\left(e_p''(\cdot),e(\cdot)\right)dt\end{aligned}$$

□

Remark 3.3.1. It should briefly be pointed out why the Fundamental Theorem of Calculus may be used above. We showed above that $e \in C^1(0,T)$, and by assumption, $e_p \in C^2((0,T);V)$. By continuity of the inner product, it follows that $a\left(e_p'(t),e'(t)\right) + a\left(e_p''(t),e(t)\right)$ is continuous at each $t \in (0,T)$, and hence $\frac{d}{dt}a\left(e_p'(\cdot),e(\cdot)\right)$ is continuous on $[0,t]$ for any $t \in (0,T)$. Therefore $\frac{d}{dt}a\left(e_p'(\cdot),e(\cdot)\right)$ is integrable on $[0,t]$ and hence the requirement for the Fundamental Theorem of Calculus is satisfied.

Finally, we obtain the following useful result:

Lemma 3.3.3. If the solution u of Problem G satisfies assumption C2, then for any $t \in (0,T)$,

$$||e(t)||_V + ||e'(t)||_W \leq \sqrt{24e^{3t}}K_T,$$

where

$$\begin{aligned}K_T = &\int_0^T \left|\left|e_p''(\cdot)\right|\right|_W + 3K_a max\left|\left|e_p'(t)\right|\right|_V + 3K_a\int_0^T \left|\left|e_p''(\cdot)\right|\right|_V + ||e'(0)||_W \\ &+ \sqrt{1+K_a}\,||e(0)||_V + \sqrt{K_a}\left|\left|e_p'(0)\right|\right|.\end{aligned}$$

To prove the lemma, the following two well-known results are used.

Theorem 3.3.2. Young's inequality

If a and b are nonnegative real numbers and if p and q are real numbers such that $p > 1$, $q > 1$, and $\frac{1}{p} + \frac{1}{q} = 1$, then $ab \leq \frac{a^p}{p} + \frac{b^q}{q}$.

Theorem 3.3.3. Gronwall's inequality

If α is a real constant, $\beta(t) \geq 0$ and $g(t)$ are continuous real functions for $t \in [a, b]$ such that

$$g(t) \leq \alpha + \int_a^t \beta(\cdot)g(\cdot) \text{ for each } t \in [a, b],$$

then

$$g(t) \leq \alpha e^{\int_a^t \beta(\cdot)} \text{ for each } t \in [a, b].$$

Proof of Lemma 3.3.3. First note that by assumption, $u \in C^1([0, T); V) \cap C^2((0, T); V)$. Then so is Pu, from Lemma 3.3.2, and hence e_p satisfies the assumption of Proposition 3.3.1. Also note that u then satisfies assumption C1, and as a result we can show as in the proof of Lemma 3.2.1 that $e' \in V$ and $e_p'' \in W$. Let $t \in (0, T)$.

Now from the Cauchy-Schwarz inequality and Theorem 3.3.2, we have that

$$\begin{aligned} \left|c\left(e_p''(t), e'(t)\right)\right| &\leq \left|\left|e_p''(t)\right|\right|_W ||e'(t)||_W \\ &\leq \frac{1}{2}\left|\left|e_p''(t)\right|\right|_W^2 + \frac{1}{2}||e'(t)||_W^2, \end{aligned}$$

and from Equation (3.3.1), we have

$$||e'(t)||_W^2 \leq 2E(t) \text{ and } ||e(t)||_V^2 \leq 2E(t)$$

since $||e(t)||_V^2 \geq 0$ and $||e(t)||_W^2 \geq 0$.

Since u satisfies assumption C1, we substitute the above into Inequality (3.3.3) to obtain

$$E'(t) \leq \frac{1}{2}\left|\left|e_p''(t)\right|\right|_W^2 + E(t) - a\left(e_p'(t), e'(t)\right). \tag{3.3.9}$$

Recall that $E'(t) = c\left(e''(t), e'(t)\right) + b(e(t), e'(t))$, as was shown in the proof of Lemma 3.3.1. Since $Pu, u_h \in C^2(0, T)$, it follows that $e \in C^2(0, T)$, and hence by the continuity of the inner product, $E'(t) \in C^2(0, T)$. Thus E' is continuous, and hence integrable, on $[0, t]$, and thus by the Fundamental Theorem of Calculus, it follows that $\int_0^t E'(t) = E(t) - E(0)$.

Then, integrating both sides of Equation (3.3.9) and using the above result with that of Proposition 3.3.1, it follows that

$$\begin{aligned} E(t) &\leq E(0) + \frac{1}{2}\int_0^t \left|\left|e_p''(\cdot)\right|\right|_W^2 + \int_0^t E(\cdot) - \int_0^t a\left(e_p'(\cdot), e'(\cdot)\right) \\ &= E(0) + \frac{1}{2}\int_0^t \left|\left|e_p''(\cdot)\right|\right|_W^2 + \int_0^t E(\cdot) - \left[a\left(e_p'(t), e(t)\right) - a\left(e_p'(0), e(0)\right) - \int_0^t a\left(e_p''(t), e(t)\right)\right]. \end{aligned}$$

Now, using assumption E4 and Theorem 3.3.2, we have

$$\begin{aligned} \left|a\left(e_p'(t), e(t)\right)\right| &\leq K_a \left|\left|e_p'(t)\right|\right|_V ||e(t)||_V \\ &\leq K_a \frac{1}{\epsilon^2}\left|\left|e_p'(t)\right|\right|_V^2 + K_a\epsilon^2 ||e(t)||_V^2 \\ &\leq K_a \frac{1}{\epsilon^2}\left|\left|e_p'(t)\right|\right|_V^2 + 2K_a\epsilon^2 E(t) \end{aligned}$$

where $\epsilon > 0$ is arbitrary.

Further, by similar argument,

$$\begin{aligned} \left|a\left(e_p''(t), e(t)\right)\right| &\leq \int_0^t \left|a\left(e_p''(\cdot), e(\cdot)\right)\right| \\ &\leq K_a \frac{1}{\epsilon^2}\int_0^t \left|\left|e_p''(\cdot)\right|\right|_V^2 + K_a\epsilon^2 \int_0^t ||e(\cdot)||_V^2 \\ &\leq K_a \frac{1}{\epsilon^2}\int_0^t \left|\left|e_p''(\cdot)\right|\right|_V^2 + 2K_a\epsilon^2 \int_0^t E(t). \end{aligned}$$

Additionally,

$$\left|a\left(e_p'(0), e(0)\right)\right| \leq \frac{1}{2}K_a \left|\left|e_p'(0)\right|\right|_W^2 + \frac{1}{2}K_a ||e(0)||_V^2. \tag{3.3.10}$$

Now

$$\begin{aligned} E(t) &\leq E(0) + \frac{1}{2}\int_0^t \left|\left|e_p''(\cdot)\right|\right|_W^2 + \int_0^t E(\cdot) + 2K_a\epsilon^2 \int_0^t E(\cdot) \\ &\quad + 2K_a\epsilon^2 \int_0^t E(\cdot) + 2K_a\epsilon^2 E(t) + K_a \frac{1}{\epsilon^2}\left|\left|e_p'(t)\right|\right|_V^2 \\ &\leq E(0) + \frac{1}{2}\int_0^t \left|\left|e_p''(\cdot)\right|\right|_W^2 + \frac{3}{2}\int_0^t E(\cdot) + \frac{1}{2} + 4K_a^2 \left|\left|e_p'(t)\right|\right|_V^2 + a\left(e_p'(0), e(0)\right) \\ &\quad + 4K_a^2 \int_0^t \left|\left|e_p''(\cdot)\right|\right|_V^2 \text{ by choosing } \epsilon \text{ such that } 2K_a\epsilon^2 = \frac{1}{2}. \end{aligned}$$

Combining this with Equation (3.3.10), we have

$$\frac{1}{2}E(t) \leq \frac{3}{2}\int_0^t E(\cdot) + \frac{1}{2}\int_0^t \left|\left|e_p''(\cdot)\right|\right|_W^2 + 4K_a^2\left|\left|e_p'(t)\right|\right|_V^2 + 4K_a\int_0^t \left|\left|e_p''(\cdot)\right|\right|_V^2 + E(0)$$
$$+ \frac{1}{2}K_a\left|\left|e_p'(0)\right|\right|_V^2 + \frac{1}{2}K_a\left|\left|e(0)\right|\right|_V^2,$$

which we rewrite as

$$E(t) \leq 3\int_0^t E(\cdot) + K_T^*,$$

where

$$K_T^* = \int_0^T \left|\left|e_p''(\cdot)\right|\right|_W^2 + 8K_a^2 max\left|\left|e_p'(t)\right|\right|_V^2 + 8K_a^2\int_0^T \left|\left|e_p''(\cdot)\right|\right|_V^2 + \left|\left|e'(0)\right|\right|_W^2 \tag{3.3.11}$$
$$+ (1+K_a)\left|\left|e(0)\right|\right|_V^2 + K_a\left|\left|e_p'(0)\right|\right|_V^2.$$

Above it was shown that $E' \in C^2(0,T)$, so we know E is continuous on $[0,t]$ for each $t \in (0,T)$. Then, using Theorem 3.3.3 (with $\beta(s) = 1$ for $s \in (0,t)$), it follows that

$$E(t) \leq e^{3t}K_T^*,$$

and hence from the definition of E we get

$$\frac{1}{2}\left|\left|e'(t)\right|\right|_W^2 + \frac{1}{2}\left|\left|e(t)\right|\right|_V^2 \leq e^{3t}K_T^*. \tag{3.3.12}$$

Using Equation (3.3.11) and the equality of norms, we have that

$$K_T^* \leq 6\left[\int_0^T \left|\left|e_p''(\cdot)\right|\right|_W + \sqrt{8}K_a max\left|\left|e_p'(t)\right|\right|_V + \sqrt{8}K_a\int_0^T \left|\left|e_p''(\cdot)\right|\right|_V\right.$$
$$\left. + \left|\left|e_p'(0)\right|\right|_W + \sqrt{1+K_a}\left|\left|e(0)\right|\right|_V + \sqrt{K_a}\left|\left|e_p'(0)\right|\right|_V\right]^2.$$

Finally, let

$$K_T = \int_0^T \left|\left|e_p''(\cdot)\right|\right|_W + 3K_a max\left|\left|e_p'(t)\right|\right|_V + 3K_a\int_0^T \left|\left|e_p''(\cdot)\right|\right|_V + \left|\left|e'(0)\right|\right|_W$$
$$+ \sqrt{1+K_a}\left|\left|e(0)\right|\right|_V + \sqrt{K_a}\left|\left|e_p'(0)\right|\right|.$$

Since $(A+B)^2 \leq 2A^2 + 2B^2$ for any $A, B \in \mathbb{R}$, it then follows from Equation (3.3.12) that

$$\begin{aligned}
&||e(t)||_V + ||e'(t)||_W \\
&\leq \sqrt{2\,||e(t)||_V^2 + 2\,||e'(t)||_W^2} \\
&\leq \sqrt{4e^{3t}K_T^*} \\
&= \sqrt{24e^{3t}}K_T.
\end{aligned}$$

□

Remark 3.3.2. The result of Lemma 3.3.3 is different from that obtained in Lemma 4.1 of [BV13]. There, the result of Lemma 3.2.1 (which is Proposition 3.1 in [BV13]) is used to obtain an expression for

$$\frac{d}{dt}\left[\frac{1}{2}c\,(e,e) - \frac{1}{2}b\,(v,v) - c\,(e_h',v) - a\,(e_h,v)\right],$$

with $v'(t) = e(t)$, whereas above, the result was used to obtain an upper bound for

$$\frac{d}{dt}E(t) = \frac{d}{dt}\left[\frac{1}{2}c\,(e',e') + \frac{1}{2}b\,(e,e)\right].$$

In both cases, integration and the Fundamental Theorem of Calculus were used to obtain approximation errors. However in [BV13], the estimate is for $||e(t)||_W$, whereas above the estimate is for $||e(t)||_V + ||e'(t)||_W$. Note that in [BV13], the error estimate was only in terms of the norm $||\cdot||_W$. In the proof, assumption E4 (the boundedness of a on W), was used. The same result cannot be obtained here, since assumption E4 in this case is that a is bounded on V.

Remark 3.3.3. As mentioned, assumption C2 was not necessary in [BV13], since upper bounds for the terms on the right-hand side of equation (4.4) in the article could be obtained using merely that $e_p' \in W$. Here however, the assumption was necessary to use the result of Proposition 3.3.1, which in turn was necessary to obtain the upper bound for $E(t)$.

3.3.2 Error estimates and convergence for the semi-discrete approximation

Lemma 3.3.4. Assume that the solution u of Problem G satisfies Assumption C2. Then for any $t \in (0,T)$,

$$||u(t)-u_h(t)||_V+||u'(t)-u_h'(t)||_W \leq ||u(t)-Pu(t)||_V+||u'(t)-Pu'(t)||_W+\sqrt{24e^{3t}}K_T,$$

where

$$K_T = \int_0^T ||u''-(Pu)''||_W + 3K_a max\,||u'(t)-Pu'(t)||_V + 3K_a\int_0^T ||u''-(Pu)''||_V \\ + \left|\left|Pu_1-u_1^h\right|\right|_W + \sqrt{1+K_a}\left|\left|Pu_0-u_0^h\right|\right|_V + \sqrt{K_a}\,||u_1-Pu_1||_V\,.$$

Proof. Substituting the expressions for e and e_p, the result follows immediately from Lemma 3.3.3. □

Remark 3.3.4. An error bound for $||u(t)-u_h(t)||_W$ was obtained in [BV13] by using the triangle inequality and the result of Lemma 4.1 in the article, which, as mentioned, was obtained instead of Lemma 3.3.3.

Lemma 3.3.4 allows us to prove the following theorem.

Theorem 3.3.4. Suppose assumption C3 holds for the space V, and that the solution u of Problem G satisfies assumption C2, and that $u'' \in \mathcal{L}^2([0,T];H(V,k))$. Then for any $t \in (0,T)$,

$$||u(t)-u_h(t)||_V + ||u'(t)-u_h'(t)||_W \leq C_\Pi h^\alpha\left(||u(t)||_{H(V,k)} + C_b\,||u'(t)||_{H(V,k)}\right) \\ + \sqrt{24e^{3t}}C_\Pi h^\alpha\left[\int_0^T C_b\,||u''(\cdot)||_{H(V,k)} + 3K_a max\,||u'(t)||_{H(V,k)} + 3K_a\int_0^T ||u''(\cdot)||_{H(V,k)}\right] \\ + \sqrt{24e^{3t}}\left[\left|\left|Pu_1-u_1^h\right|\right|_W + \sqrt{1+K_a}\left|\left|Pu_0-u_0^h\right|\right|_V + \sqrt{K_a}\,||u_1-Pu_1||_V\right]$$

Proof. Since u satisfies the given assumptions, it follows from Lemma 3.3.4 and assumption

E2 that

$$
\begin{aligned}
&||u(t)-u_h(t)||_V + ||u'(t)-u_h'(t)||_W \\
&\leq ||u(t)-Pu(t)||_V + ||u'(t)-Pu'(t)||_W \\
&+ \sqrt{24e^{3t}}\left[\int_0^T ||u''-(Pu)''||_W + 3K_a max\,||u'(t)-Pu'(t)||_V + 3K_a\int_0^T ||u''-(Pu)''||_V\right. \\
&\left.+ \left|\left|Pu_1-u_1^h\right|\right|_W + \sqrt{1+K_a}\left|\left|Pu_0-u_0^h\right|\right|_V + \sqrt{K_a}\,||u_1-Pu_1||_V\right] \\
&\leq ||u(t)-Pu(t)||_V + \kappa_1\,||u'(t)-Pu'(t)||_V \\
&+ \sqrt{24e^{3t}}\left[\int_0^T \kappa_1\,||u''-(Pu)''||_V + 3K_a max\,||u'(t)-Pu'(t)||_V + 3K_a\int_0^T ||u''-(Pu)''||_V\right. \\
&\left.+\kappa_1\left|\left|Pu_1-u_1^h\right|\right|_W + \sqrt{1+K_a}\left|\left|Pu_0-u_0^h\right|\right|_V + \sqrt{K_a}\,||u_1-Pu_1||_V\right].
\end{aligned}
$$

It follows, with Proposition 3.2.2, that

$$
\begin{aligned}
&||u(t)-u_h(t)||_V + ||u'(t)-u_h'(t)||_W \\
&\leq C_\Pi h^\alpha\,||u(t)||_{H(V,k)} + C_\Pi\kappa_1 h^\alpha\,||u'(t)||_{H(V,k)} \\
&+ \sqrt{24e^{3t}}C_\Pi h^\alpha\left[\int_0^T \kappa_1\,||u''(\cdot)||_{H(V,k)} + 3K_a max\,||u'(t)||_{H(V,k)} + 3K_a\int_0^T ||u''(\cdot)||_{H(V,k)}\right] \\
&+ \sqrt{24e^{3t}}\left[\left|\left|Pu_1-u_1^h\right|\right|_W + \sqrt{1+K_a}\left|\left|Pu_0-u_0^h\right|\right|_V + \sqrt{K_a}\,||u_1-Pu_1||_V\right] \\
&\leq C_\Pi h^\alpha\left(||u(t)||_{H(V,k)} + C_b\,||u'(t)||_{H(V,k)}\right) \\
&+ \sqrt{24e^{3t}}C_\Pi h^\alpha\left[\int_0^T C_b\,||u''(\cdot)||_{H(V,k)} + 3K_a max\,||u'(t)||_{H(V,k)} + 3K_a\int_0^T ||u''(\cdot)||_{H(V,k)}\right] \\
&+ \sqrt{24e^{3t}}\left[\left|\left|Pu_1-u_1^h\right|\right|_W + \sqrt{1+K_a}\left|\left|Pu_0-u_0^h\right|\right|_V + \sqrt{K_a}\,||u_1-Pu_1||_V\right]
\end{aligned}
$$

where we denote $C_b = \kappa_1 > 0$. □

Note that the above estimate depends on u_0^h and u_1^h, and thus these values must be chosen carefully. As suggested in [BSV17], one may choose the interpolants of u_0 and u_1, and then Corollary 3.3.1 follows.

Corollary 3.3.1. Suppose assumption C3 holds for the space V and that u_0 and u_1 are in $H(V,k)$. Let $u_0^h = \Pi u_0$ and $u_1^h = \Pi u_1$. Also assume that the solution u of Problem G

satisfies assumption C2 and that $u'' \in \mathcal{L}^2([0,T];H(V,k))$. Then for each $t \in (0,T)$,

$$||u(t)-u_h(t)||_V + ||u'(t)-u_h'(t)||_W \leq C_\Pi h^\alpha \left(||u(t)||_{H(V,k)} + C_b \, ||u'(t)||_{H(V,k)} \right)$$
$$+ \sqrt{24e^{3t}} C_\Pi h^\alpha \left[\int_0^T C_b \, ||u''(\cdot)||_{H(V,k)} + 3K_a max \, ||u'(t)||_{H(V,k)} + 3K_a \int_0^T ||u''(\cdot)||_{H(V,k)} \right.$$
$$\left. + 2C_b \, ||u_1||_{H(V,k)} + 2\sqrt{1+K_a} \, ||u_0||_{H(V,k)} + \sqrt{K_a} \, ||u_1||_{H(V,k)} \right].$$

Proof. The proof is exactly as in [BSV17]. □

Remark 3.3.5. Since Lemma 3.3.4 differs from Theorem 5.1 in [BV13], and assumption C3 was different, the results of Theorem 3.3.4 and Corollary 3.3.1 are not the same as those of Theorem 5.2 in [BV13]. There, an upper bound for $||u(t)-u_h(t)||_W$ in terms of the norm of $H(V,k)$ was obtained. In both cases, the same general interpolation operator was used.

3.4 The fully discrete approximation

The fully discrete problem is derived as in [BSV17] and [BV13], following a similar approach to [Bak76], using a finite difference scheme. In [Bak76], the finite difference approximation is compared directly to the exact solution of Problem G. As mentioned in [BSV17] and [BV13], an estimate of the error between the semi-discrete and fully discrete approximations was derived instead, and the error estimate between the fully-discrete approximation and the exact solution follows from the triangle inequality. This removes the need for unnecessary and unrealistic regularity assumptions on the exact solution.

To derive the fully discrete problem, divide the interval $[0,T]$ into N subintervals of equal length $\tau = \frac{T}{N}$. Denote the approximation of $u_h(t_k)$ by u_h^k. We use u_k if no confusion is possible. Consider also the following notation:

For any sequence $\{x_k\} \subset \mathbb{R}^n$, denote

$$\delta_t x_k = \frac{1}{\tau}(x_{k+1} - x_k),$$
$$x_{k+\frac{1}{2}} = \frac{1}{2}(x_{k+1} + x_k) \text{ and}$$
$$v_k \text{ as the approximation of } u_h'(t_k).$$

Then we have the fully discrete problem, Problem G^h-D, in variational form as follows.

Problem G^h-D

Find a sequence $\{u_k^h\} \subset S^h$ such that for $k = 0, 1, \ldots, N-1$,

$$\delta_t u_k^h = v_{k+\frac{1}{2}} \tag{3.4.1}$$
$$c(\delta_t v_k, \psi) + a\left(v_{k+\frac{1}{2}}, \psi\right) + b\left(u_{k+\frac{1}{2}}^h, \psi\right) = \frac{1}{2}(f(t_k) + f(t_{k+1}), \psi)_X \tag{3.4.2}$$

for each $\psi \in S^h$, while $u_0^h = u_h(0)$ and $v_0 = u_h'(0)$.

Problem G^h-D has a unique solution for each pair of vectors u_0^h and v_0 in S^h [BSV17].

In the following two subsections, the main results for the stability and convergence theory of the fully discrete approximation are given. The proofs of these results are given in detail in [BV13] and [BSV17]. Thus below, only the main steps and notation necessary to present the results are provided, and differences between the two articles are pointed out. Note that, with the current approach, the restrictive regularity assumptions on the exact solution, made in [FXX99] and [Sem94] for example, are avoided.

3.4.1 Stability result

Let $e_k = u_h(t_k) - u_k$ and $q_k = v_h(t_k) - v_k$, where $v_h(t) = u_h'(t)$. Note that $e_0 = 0$ and $q_0 = 0$.

Now from Equation (3.2.1), we have

$$c(v_h'(t_{k+1}), \psi) + a(v_h(t_{k+1}), \psi) + b(u_h(t_{k+1}), \psi) = (f(t_{k+1}), \psi)_X$$

and

$$c\left(v_h'(t_k),\psi\right)+a\left(v_h(t_k),\psi\right)+b\left(u_h(t_k),\psi\right)=\left(f(t_k),\psi\right)_X$$

for any $\psi\in S^h$.

Combining these, we obtain

$$\begin{aligned}&c\left(\frac{1}{\tau}\left[v_h(t_{k+1})-v_h(t_k)\right],\psi\right)+\frac{1}{2}a\left(v_h(t_{k+1})+v_h(t_k),\psi\right)+\frac{1}{2}b\left(u_h(t_{k+1})+u_h(t_k),\psi\right)\\&=\frac{1}{2}\left(f(t_{k+1})+f(t_k),\psi\right)_X+c\left(\rho_k,\psi\right)\end{aligned}$$

where

$$\rho_k=\frac{1}{\tau}\left(v_h(t_{k+1})-v_h(t_k)\right)-\frac{1}{2}\left(v_h'(t_{k+1})+v_h'(t_k)\right).$$

Next, use the above equation together with Equations (3.4.1) and (3.4.2) to obtain

$$\frac{1}{\tau}\left(u_h(t_{k+1})-u_h(t_k)\right)=\frac{1}{2}\left(v_h(t_{k+1})+v_h(t_k)\right)+\sigma_k,$$

where

$$\sigma_k=\frac{1}{\tau}\left(u_h(t_{k+1})-u_h(t_k)\right)-\frac{1}{2}\left(v_h(t_{k+1})+v_h(t_k)\right).$$

This, together with Equation (3.4.1), yields

$$\delta_t e_k=q_{k+\frac{1}{2}}+\sigma_k. \tag{3.4.3}$$

It then follows that

$$e_n=\tau\sum_{k=0}^{n-1}q_{k+\frac{1}{2}}+\tau\sum_{k=0}^{n-1}\sigma_k.$$

Let $s_0=0$, $s_n=\tau\sum_{k=0}^{n-1}e_{k+\frac{1}{2}}$ and $\epsilon_n=\frac{\tau}{2}\rho_n+\tau\sum_{k=0}^{n-1}\rho_k+\sigma_n$ for $n=1,2,\ldots,N-1$. Let $\nu\in\mathbb{N}$ such that $2\leq\nu\leq N$.

It was shown in [BV13] that

$$||e_\nu||_W^2-||e_1||_W^2+||s_\nu||_V^2-||s_1||_V^2\leq 4T\tau\sum_{n=1}^{\nu-1}||\epsilon_n||_W^2+\frac{\tau}{4T}\sum_{n=1}^{\nu-1}\left|\left|e_{n+\frac{1}{2}}\right|\right|_W^2 \tag{3.4.4}$$

and that

$$||e_1||_W^2 + ||s_1||_V^2 + \frac{\tau}{2}a\left(e_1, e_1\right) = \frac{\tau^2}{2}c\left(\rho_0, e_1\right) + \tau c\left(\sigma_0, e_1\right) + \frac{\tau^2}{2}a\left(\sigma_0, e_1\right). \tag{3.4.5}$$

In [BSV17] it was further proven that

$$||e_1||_W^2 + ||s_1||_V^2 \leq \tau^4 ||\rho_0||_W^2 + \frac{1}{16}||e_1||_W^2 + 4\tau^2 ||\sigma_0||_W^2 + \frac{1}{16}||e_1||_W^2 \tag{3.4.6}$$

$$+ \tau^4 K_a^2 ||\sigma_0||_V^2 + \frac{1}{16}||e_1||_V^2, \tag{3.4.7}$$

using the Cauchy-Schwarz inequality and Theorem 3.3.2, assumption E4, and the fact that $a(e_1, e_1) \geq 0$ by property of a.

Equation (3.4.6) was combined with Equation (3.4.4), and then it was shown in [BSV17] that

$$||e_\nu||_W^2 \leq 4T\tau \sum_{n=1}^{\nu-1} ||\epsilon_n||_W^2 + \frac{1}{2}max\,||e_n||_W^2 + \frac{1}{16}||e_1||_V^2 + \tau^4 ||\rho_0||_W^2 \tag{3.4.8}$$

$$+ 4\tau^2 ||\sigma_0||_W^2 + \tau^4 K_a^2 ||\sigma_0||_V^2.$$

The stability result finally follows from Equation (3.4.8).

Lemma 3.4.1. Stability

$$max\,||e_n||_W^2 \leq 8T\tau \sum_{n=0}^{N-1} ||\epsilon_n||_W^2 + \frac{1}{8}||e_1||_V^2 + 2\tau^4 ||\rho_0||_W^2$$

$$+ 8\tau^2 ||\sigma_0||_W^2 + 2\tau^4 K_a ||\sigma_0||_V^2. \tag{3.4.9}$$

Remark 3.4.1. As already pointed out in [BSV17], the Inequalities (3.4.6) and (3.4.8) differ from those in [BV13]. Inequality (3.4.6) is obtained using assumption E4, which differs between the two articles due to the different types of damping. Note that in the above case, the term with e_1 remains on the right-hand side of (3.4.6) and (3.4.8), and there are terms with $||\sigma_0||_W$ and $||\sigma_0||_V$. Because a is bounded in terms of the norm on V and not W, the right hand side of Inequality (3.4.6) is in terms of the norms on V and W, and not just the norm on W, as was the case in [BV13]. This will affect the derivation of the convergence result, as will be seen in Subsection 3.4.2 below.

3.4.2 Convergence result

The result is derived using Lemma 3.4.1. It therefore remains to derive estimates for ρ_k, σ_k and e_1. Note that in [BV13], estimates for $||\sigma_0||_V$ and $||e_1||_V$ were not necessary, since the lemma on stability (Lemma 6.1) only involved expressions of $||\rho_0||_W$ and $||\sigma_0||_W$ (as explained in Remark 3.4.1).

The following inequalities are from [BV13]:

$$||\rho_k||_W^2 \leq \tau^4 max\, ||v_h'''||_W^2 \text{ and} \tag{3.4.10}$$

$$||\sigma_k||_W^2 \leq \tau^4 max\, ||u_h'''||_W^2 . \tag{3.4.11}$$

Then

$$||\epsilon_n||_W^2 \leq 5T^2\tau^4 max\, ||v_h'''||_W^2 + 4\tau^4 max\, ||u_h'''||_W^2 .$$

Using the same procedure used in [BV13] to derive Inequality (3.4.11), with an orthonormal basis for V instead of W, it follows that

$$||\sigma_k||_V^2 \leq \tau^4 max\, ||u_h'''||_V^2 . \tag{3.4.12}$$

This can be used to obtain the estimate for $||\sigma_0||_W$.

Next, it is shown in [BSV17], using Equation (3.4.3) with $k = 0$, that

$$||e_1||_V^2 \leq 2\left(\frac{\tau^2}{4}\,||q_1||_V^2 + \tau^2\,||\sigma_0||_V^2\right).$$

Now an estimate for $||q_1||_V^2$ is required. The main steps from [BSV17] are given below. Let $\psi \in S^h$. Subtracting

$$\begin{aligned} &c\,(v_1,\psi) + \frac{\tau}{2}a\,(v_1,\psi) + \frac{\tau^2}{4}b\,(v_1,\psi) \\ &= c\,(v_0,\psi) - \frac{\tau}{2}a\,(v_0,\psi) - \frac{\tau^2}{4}b\,(v_0,\psi) - \tau b\,(u_0,\psi) + \frac{\tau}{2}\,(f(t_0)+f(t_1),\psi)_X \end{aligned}$$

from

$$\begin{aligned} & c\left(v_h(t_1),\psi\right)+\frac{\tau}{2}a\left(v_h(t_1),\psi\right)+\frac{\tau^2}{4}b\left(v_h(t_1),\psi\right) \\ & =c\left(v_h(t_0),\psi\right)-\frac{\tau}{2}a\left(v_h(t_0),\psi\right)-\frac{\tau^2}{4}b\left(v_h(t_0),\psi\right)-\tau b\left(u_h(t_0),\psi\right) \\ & -\frac{\tau^2}{4}b\left(\sigma_0,\psi\right)+\tau c\left(\rho_0,\psi\right)+\frac{\tau}{2}\left(f(t_0)+f(t_1),\psi\right)_X, \end{aligned}$$

we obtain

$$\begin{aligned} & c\left(q_1,\psi\right)+\frac{\tau}{2}a\left(q_1,\psi\right)+\frac{\tau^2}{4}b\left(q_1,\psi\right) \\ & =c\left(q_0,\psi\right)-\frac{\tau}{2}a\left(q_0,\psi\right)-\frac{\tau^2}{4}b\left(q_0,\psi\right)-\tau b\left(q_0,\psi\right)-\frac{\tau^2}{4}b\left(\sigma_0,\psi\right)+\tau c\left(\rho_0,\psi\right) \\ & =\tau c\left(\rho_0,\psi\right)-\frac{\tau^2}{4}b\left(\sigma_0,\psi\right). \end{aligned}$$

Letting $\psi = q_1$ in the above equation and using the Cauchy-Schwarz inequality, Theorem 3.3.2, and the fact that $a\left(q_1,q_1\right)\geq 0$, it follows that

$$||q_1||_W^2+\frac{\tau^2}{4}||q_1||_V^2\leq ||q_1||_W^2+\frac{\tau^2}{4}||\rho_0||_W^2+\frac{\tau^2}{8}||\sigma_0||_V^2+\frac{\tau^2}{8}||q_1||_V^2.$$

Then the estimate for $||e_1||_V^2$ can be obtained, using the estimates for ρ_0 and σ_0:

$$||e_1||_V^2\leq \tau^6 max\,||v_h'''||_W^2+\frac{5\tau^6}{2}max\,||u_h'''||_V^2. \tag{3.4.13}$$

Finally, substituting Equations (3.4.12) and (3.4.13) into Inequality (3.4.9) of Lemma 3.4.1, it follows that

$$\begin{aligned} max\,||e_n||_W^2 \leq\ & 40T^4\tau^4 max\,||v_h'''||_W^2+32T^2\tau^4 max\,||u_h'''||_W^2+\frac{1}{8}\tau^6 max\,||u_h'''||_W^2+\frac{5\tau^6}{16}max\,||u_h'''||_V^2 \\ & +2\tau^8 max\,||v_h'''||_W^2+8\tau^6 max\,||u_h'''||_W^2+2\tau^8 K_a max\,||u_h'''||_V^2. \end{aligned}$$

If $f\in C^2([0,T];X)$, then $u_h\in C^4[0,T]$ and from the inequality above we obtain the following result:

Theorem 3.4.1. If $f \in C^2([0,T];X)$, then for each $t_k \in (0,T)$,

$$\begin{aligned}\left|\left|u_h(t_k) - u_k^h\right|\right|_W \leq \tau^2 &\left(7T^2 max \left|\left|u_h^{(4)}\right|\right|_W + 3(1+2T) max \left|\left|u_h'''\right|\right|_W\right) \\ &+ 2\tau^3 \left(max \left|\left|u_h^{(4)}\right|\right|_W + max \left|\left|u_h'''\right|\right|_V\right) \\ &+ \sqrt{2K_a}\tau^4 max \left|\left|u_h'''\right|\right|_W .\end{aligned}$$

Finally, an estimate can be obtained for the fully discrete approximation by using the results of Section 3.3, Theorem 3.4.1, and the fact that

$$\left|\left|u(t) - u_k^h\right|\right|_W \leq \left|\left|u(t) - u_h(t_k)\right|\right|_W + \left|\left|u_h(t_k) - u_k^h\right|\right|_W$$

from the triangle inequality.

Chapter 4

Applications of the Finite Element Method

4.1 The two-dimensional wave equation

Recall the multi-dimensional wave equation introduced in Section 1.5. The existence theory from Chapter 2 was applied to Problem MWE in Section 2.4.1. In the following sections, the wave equation on a two-dimensional domain is used to demonstrate the use of some of the theory from Chapter 3. Then, a finite element central difference average acceleration scheme is derived, to approximate the solution to the problem, followed by some numerical results.

4.1.1 Application of the convergence theory

In Section 2.4.1 the existence theory was applied to the multi-dimensional wave equation. Recall that we defined the spaces V, W and X, where V was the closure of the space of test functions $T(\Omega)$ in $H^1(\Omega)$, and $W = X = \mathcal{L}^2(\Omega)$. In that section, we also gave definitions of the bilinear forms b, c and a.

A detailed implementation of the finite element method is given in the sections below. For the convergence theory, we consider for simplicity the two-dimensional wave equation, where the domain Ω is a rectangle. Using piecewise linear basis functions and triangle or rectangle elements, we construct the space S^h, which is the span of the basis functions that are in the class of test functions, and is a finite dimensional subspace of V. Note that we assume h is related to the dimension n of S^h, and that $h \to 0$ as $n \to \infty$.

Then we can find the Galerkin approximation of Problem MWE. Note that it is a special case of Problem G^h from Section 3.2.

Problem MWE^h

Find a function u_h such that for each $t \in (0,T)$, $u_h(t) \in S^h$ and

$$c\left(u_h''(t), v\right) + a\left(u_h'(t), v\right) + b\left(u_h(t), v\right) = \left(f(t), v\right)_X$$

for each $v \in S^h$, while $u_h(0) = u_0^h \in S^h$ and $u_h'(0) = u_1^h \in S^h$.

It can be proven that assumptions **C1** and **C2** of Section 3.2.1 are satisfied, depending on the properties of u_0, u_1 and f and on the properties of the boundary $\partial\Omega$. The proofs are beyond the scope of this chapter, and the focus is instead on the interpolation operator that is used to derive error estimates.

The aim is to find an interpolation operator that depends on the space S^h to use instead of assumption **C3** of Section 3.2.2.

For this problem, define $H(V,k) = H^k(\Omega) \cap V$. Then we have the following result for piecewise linear basis functions, which is a special case of a result from [OR76, p. 279].
If $u \in H^k(\Omega)$ for $k \geq 2$, then

$$\left|\left|\Pi u - u\right|\right|_V \leq C_\Pi h \left|u\right|_2,$$

where

$$\left|u\right|_k = \left|\left|u^{(k)}\right|\right|.$$

Finally, if we choose $u_0^h = \Pi u_0 \in H^k(\Omega) \cap V$ and $u_1^h = \Pi u_1 \in H^k(\Omega) \cap V$, then we can obtain an error estimate for the semi-discrete approximation from Corollary 3.3.1, provided that

$u'' \in \mathcal{L}^2([0,T]; H^k(\Omega) \cap V)$, and the error estimate for the fully discrete approximation is obtained using Theorem 3.4.1, provided that $f \in C^2([0,T]; X)$.

4.1.2 Algorithm for the approximation

In this section, assume that Ω is the square $\{\langle x, y\rangle \in \mathbb{R}^2 \mid 0 \leq x \leq 1,\ 0 \leq y \leq 1\}$. For simplicity we do not consider damping. For the finite element method, the domain Ω is divided into N elements. Denote any node in the resulting grid by $\bar{x}_k$, where $k = 1, 2, \ldots, n$. The basis functions δ_i are constructed from binomials, and we choose those that are in our class of test functions. Suppose $\hat{I}$ is the set of all indices k such that $\bar{x}_k$ is not on the boundary of Ω. Let S^h denote the span of all functions δ_i where $i \in \hat{I}$. Then we write Problem MWE^h as follows.

Problem MWE-G

Find a function u_h such that for each $t \in (0,T)$, $u_h(t) \in S^h$, and

$$\iint_\Omega \partial_t^2 u^h(\cdot,t)v = -\iint_\Omega \partial_x u^h(\cdot,t)\partial_x v + \partial_y u^h(\cdot,t)\partial_y v + \iint_\Omega fv$$

for each $v \in S^h$, while $u^h(\cdot,0) = u_0$ and $\partial_t u^h(\cdot,0) = u_1$.

Denote $u^h(\cdot,t) = \sum_{k\in\hat{I}} u_k(t)\delta_k$, and define the matrices K and M by

$$K_{ij} = \iint_\Omega \delta_j'\delta_i' \text{ and } M_{ij} = \iint_\Omega \delta_j\delta_i \text{ for } i,j = 0,1,\ldots,n.$$

Then let

$$M_{ij}^* = M_{ij} \text{ and } K_{ij}^* = K_{ij} \text{ for } i,j = \hat{I}$$

and

$$[M_1]_{ij} = M_{ij} \text{ for } i = \hat{I},\ j = 1,2,\ldots,n.$$

In this case, also define the interpolant, f_I, of the function f by

$$f_I = \sum_{k=1}^{n} f(\bar{x}_k)\delta_k$$

and the vector

$$F = M_1\bar{f}, \text{ where } \bar{f} = [f(\bar{x}_1), f(\bar{x}_2), \ldots, f(\bar{x}_n)]^t$$

Further, we have vectors $\bar{b}$ and $\bar{a}$, which are obtained from the interpolants of u_0 and u_1, such that

$$\bar{b}_j = u_0(\bar{x}_j) \text{ and } \bar{a}_j = u_1(\bar{x}_j) \text{ for } j \in \hat{I}.$$

Then we obtain the system

$$M^*\bar{u}''(t) = -K^*\bar{u}(t) + F \tag{4.1.1}$$

for $t > 0$, with $\bar{u}(0) = \bar{b}$ and $\bar{u}'(0) = \bar{a}$, where $\bar{u}_j(t) = u_j(t)$ for $j \in \hat{I}$.

Finally, we use a central difference average acceleration scheme to approximate the solution of the system (4.1.1). To this end, let m be the number of time steps, and suppose we approximate the solution at a time point t^*. Let $\delta t = \dfrac{t^*}{m}$. We divide the interval $[0, t^*]$ into subintervals $[t_k, t_{k+1}]$ of equal length δt, for $k = 0, 1, \ldots, m-1$. We use $\bar{u}_k$ to denote the approximations for $\bar{u}(t_k)$. Then we obtain the following system:

$$\frac{1}{\delta t^2}M^*\left(\bar{u}_{k+1} - 2\bar{u}_k + \bar{u}_{k-1}\right) = -\frac{1}{4}K^*\left(\bar{u}_{k+1} + 2\bar{u}_k + \bar{u}_{k-1}\right) + F \tag{4.1.2}$$

with $\bar{u}_0 = \bar{b}$ and $\dfrac{1}{2\delta t}(\bar{u}_1 - \bar{u}_{-1}) = \bar{a}$.

For example, at the first step, $k = 1$. Note that $\bar{u}_{-1} = \bar{u}_1 - 2\delta t\bar{a}$. This can be substituted into system (4.1.2), together with $\bar{u}_0 = \bar{b}$. After rearranging, we obtain

$$\left(\frac{1}{\delta t^2}2M^* + \frac{1}{2}K^*\right)\bar{u}_1 = \left(\frac{1}{\delta t^2}2M^* - \frac{1}{2}K^*\right)\bar{b} + \left(\frac{1}{\delta t}2M^* + \frac{1}{2}\delta tK^*\right)\bar{a} + F,$$

which can now be used to solve for $\bar{u}_1$.

4.1.3 Numerical results - rectangle elements

Finally, the finite element central difference average acceleration method described in Subsection 4.1.2 above can be used to approximate the solution of the wave equation on a rectangular domain. N rectangular elements with width and height $h = \dfrac{1}{N}$ are used. Here we assume $f = 0$ and consider the initial conditions $u_0(x, y) = \sin(\pi x)\sin(\pi y)$ and $u_1(x, y) = 0$.

The formal series solution of the wave equation in this case, which can be obtained using separation of variables, is

$$u(x,y,t) = \sum_{j=1}^{\infty}\sum_{k=1}^{\infty} \sin(k\pi x)\sin(j\pi y)\left(B_{kj}\cos\left(\sqrt{(k\pi)^2+(j\pi)^2}t\right)\right. \\ \left. + B^*_{kj}\sin\left(\sqrt{(k\pi)^2+(j\pi)^2}t\right)\right), \tag{4.1.3}$$

where B_{kj} and B^*_{kj} are constants.

Using the initial conditions, the exact solution to the problem is

$$u(x,y,t) = \sin(\pi x)\sin(\pi y)\cos(\sqrt{2\pi^2}t).$$

We can compare the exact solution to the approximations obtained by the scheme. To do this, relative errors were calculated, using the maximum norm.

Table 4.1 gives the relative errors of the exact and approximate solutions at the time point $t = \frac{\pi}{2}$ for various numbers of elements N and time steps m. The number of time steps is doubled each time the total number of elements is quadrupled. The relative errors are given to ten significant digits. Note that, as the number of elements and time steps increases, the relative error decreases, indicating that the approximation converges to the exact solution as the number of elements and time steps is increased.

N	m	relative error
4	50	0.9736663712
16	100	0.2365688958
64	200	0.06930004110
256	400	0.02420949428
1024	800	0.009655514117

Table 4.1: Relative errors of the exact and approximate solutions of the wave equation at the time point $t = \frac{\pi}{2}$ for various numbers of elements N and number of time steps m.

To further compare the exact and approximate solutions, the surface plots of the exact and

approximate solutions at $t = \frac{\pi}{2}$ with 256 elements and 150 time steps were considered. Figures 4.1a and 4.1b depict the approximate and exact solutions on the rectangle respectively. To make a better visual comparison, Figure 4.1c shows both plots on the same axes, "sliced" at the point where $x = \frac{1}{2}$. Some accompanying numerical values are given in Table 4.2. Note that the approximations seem to be less accurate at the nodes closer to the peak of the wave. Further, the values of the exact solution are slightly larger than those of the approximations.

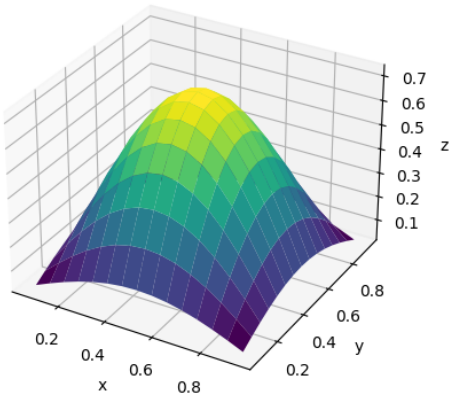

(a) Approximate solution of the wave equation, using 256 elements and 150 time steps.

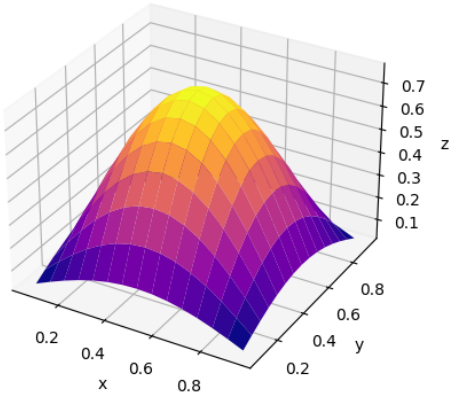

(b) Exact solution of the wave equation.

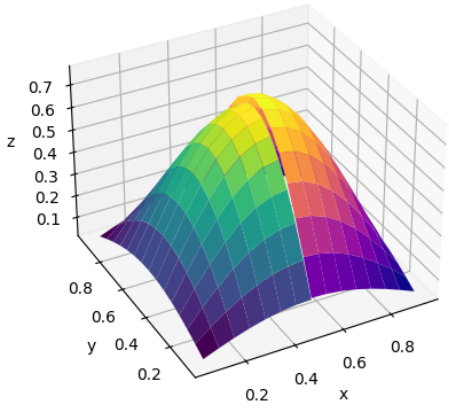

(c) Comparison of the approximate and exact solution.

Figure 4.1: Surface plots of the exact and approximate solutions to the wave equation at the time point $t = \frac{\pi}{2}$ on a rectangle with width and height 1.

(x, y)	$u(x, y, \frac{\pi}{2})$	approximation of $u(x, y, \frac{\pi}{2})$
$(\frac{1}{16}, \frac{1}{16})$	0.02921575	0.02779052
$(\frac{1}{2}, \frac{1}{2})$	0.75286919	0.71614208

Table 4.2: Some numerical values of the exact and approximate solutions of the wave equation at the time point $t = \frac{\pi}{2}$ for 256 elements and 150 time steps.

Although the results in Table 4.1 are indicative that the scheme suffices to approximate the solution of the wave equation, it should be noted that the central difference average acceleration scheme used above may not necessarily be stable, and may lead to some erratic behaviour in numerical results. In general, about 10 times the number of elements should be used for the number of time steps to ensure that the scheme is stable. This was done for the same number of elements as in Table 4.1, and the relative errors are given in Table 4.3. Results are again given to ten significant digits. Note that the errors are smaller than those of Table 4.1 from $N = 16$ onwards, indicating that a larger number of time steps leads to more accurate results.

N	m	relative error
4	40	1.012384088
16	160	0.2104587731
64	640	0.04814715534
256	2560	0.01173755880
1024	10240	0.002915415081

Table 4.3: Relative errors of the exact and approximate solutions of the wave equation at the time point $t = \frac{\pi}{2}$ for various numbers of rectangle elements N and number of time steps $m = 10N$.

Consider again the surface plots of the exact and approximate solutions at 256 elements and 2560 time steps, at the time point $t = \frac{\pi}{2}$ on the same axes, "sliced" at the point where $x = \frac{1}{2}$. The plot is given in Figure 4.2. Contrary to Figure 4.1c, the plots appear almost identical, again an indication that more time steps produce more accurate results.

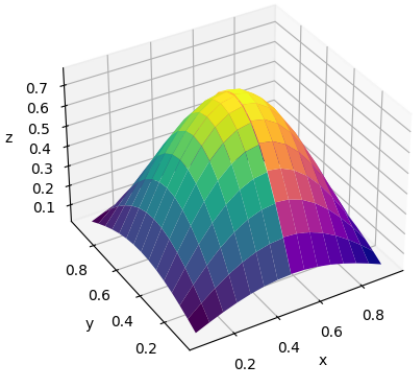

Figure 4.2: Comparison of the surface plots of the exact and approximate solutions to the wave equation at the time point $t = \frac{\pi}{2}$ on a rectangle with width and height 1.

As mentioned above, about 10 times the number of elements should be used for the number of time steps to ensure that the scheme is stable, and the numerical results were given in Table 4.3. As a final comparison, we investigated the convergence of the finite element method when the number of time steps is kept constant, to demonstrate the effects of the number of elements on the convergence. To ensure the stability of the scheme, 1024×10 time steps were used for all calculations. Table 4.4 gives the relative errors (rounded to ten significant digits) of the exact and approximate solutions at the time point $t = \frac{\pi}{2}$ for the same numbers of elements as above. The relative errors decrease as the number of elements is increased, indicating that the finite element approximations converge for the semi-discrete problem.

N	relative error
4	0.7951120889
16	0.1668002022
64	0.03910846099
256	0.01000486911
1024	0.002915415081

Table 4.4: Relative errors of the exact and approximate solutions of the wave equation at the time point $t = \frac{\pi}{2}$ for various numbers of rectangle elements N and 10240 time steps.

4.1.4 Numerical results - triangle elements

Next, the finite element central difference average acceleration method described in Subsection 4.1.2 above was used to approximate the solution with $2N$ right-angled triangle elements with vertical and horizontal sides of length $h = \frac{1}{N}$. An illustration of such a grid is given in Figure 4.3. The formal series solution of the problem is still as in Equation (4.1.3).

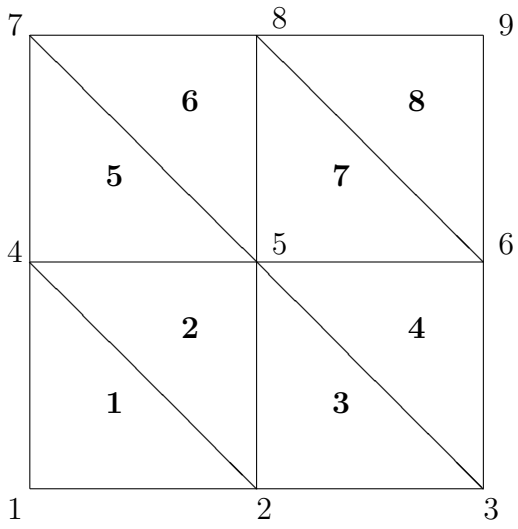

Figure 4.3: Illustration of a finite element grid for a rectangular domain, using 8 triangular elements.

Table 4.5 gives the relative errors of the exact and approximate solutions at the time point $t = \frac{\pi}{2}$ for various numbers of elements $2N$ and time steps m, calculated using the maximum norm. To ensure stability of the scheme, the number of time steps used was ten times the number of elements. The relative errors are given to ten significant digits. Note that, as the number of elements and time steps increases, the relative error decreases, indicating that the approximation converges to the exact solution as the number of elements and time steps is increased. Further, note that the relative errors are larger than those from Table 4.3 for rectangle elements.

$2N$	m	relative error
8	80	2.180211388
32	320	0.5910118528
128	1280	0.1253405896
512	5120	0.03001386653
2048	20480	0.007351744800

Table 4.5: Relative errors of the exact and approximate solutions of the wave equation at the time point $t = \frac{\pi}{2}$ for various numbers of triangle elements $2N$ and number of time steps m.

As for the case of rectangle elements, we also compared the surface plots of the exact and approximate solutions at $2N = 512$ elements and 5120 time steps, at the time point $t = \frac{\pi}{2}$, and also compared the plots on the same axes, "sliced" at the point where $x = \frac{1}{2}$. The plot is given in Figure 4.4. As with Figure 4.2, the plots appear almost identical.

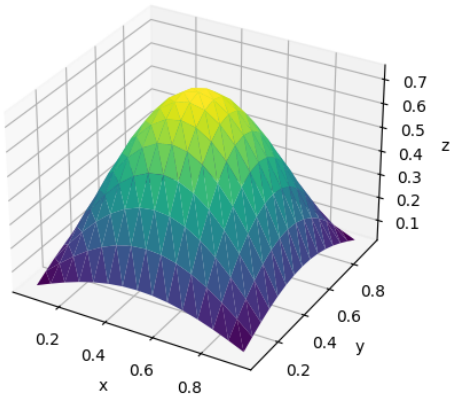

(a) Approximate solution of the wave equation with triangle elements, using 512 elements and 5120 time steps.

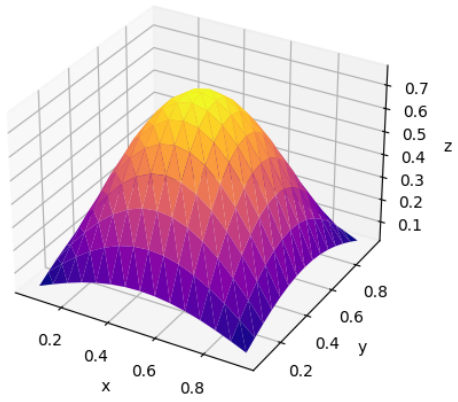

(b) Exact solution of the wave equation.

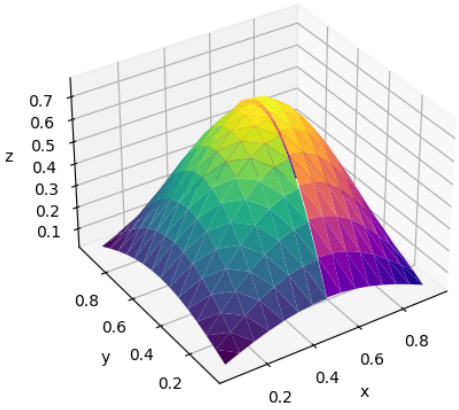

(c) Comparison of the approximate and exact solution.

Figure 4.4: Surface plots of the exact and approximate solutions to the wave equation at the time point $t = \frac{\pi}{2}$ on a rectangle with width and height 1.

As for the case of rectangle elements above, we investigated the convergence of the finite element method when the number of time steps is kept constant, to demonstrate the effects of the number of elements on the convergence. In this case, $2 \times 2048 \times 10$ time steps were used for all calculations. Table 4.6 gives the relative errors (rounded to ten significant digits) of the exact and approximate solutions at the time point $t = \frac{\pi}{2}$ for the same numbers of elements as above. The relative errors decrease as the number of elements is increased, indicating that the finite element approximations converge for the semi-discrete problem.

$2N$	relative error
8	2.118313892
32	0.5616056493
128	0.1203959343
512	0.02912234057
2048	0.007351744800

Table 4.6: Relative errors of the exact and approximate solutions of the wave equation at the time point $t = \frac{\pi}{2}$ for various numbers of triangle elements $2N$ and 20480 time steps.

4.2 The Timoshenko beam with axial force

Recall the Timoshenko beam with axial force introduced in Section 1.2.3. The existence theory for Problem T-V is given in Section 2.4.3. This section starts with a demonstration of the application of some of the theory from Chapter 3 to the Timoshenko model. It should be noted that according to this theory, the standard finite element method with piecewise linear basis functions will give convergence. However, as mentioned in Section 1.1, it is possible that the finite element approximations diverge due to "shear locking" when piecewise linear basis functions are used, making them unsuitable for this model. An alternative would be to use Hermite cubic basis functions, but we will instead consider the mixed finite element method for the model, where shear stress is also considered as a dependent variable, and where piecewise linear basis functions can still be used to obtain accurate results. The derivation of a mixed finite element algorithm for the Timoshenko model is given in Subsection 4.2.2.

4.2.1 Application of the convergence theory

Existence of solutions of the Timoshenko model with axial force was discussed in Section 2.4.3. The pinned-pinned and cantilever boundary conditions were considered. Recall the definitions of the bilinear forms b and c from that section, and also that we defined $X = \mathcal{L}^2(0,1) \times \mathcal{L}^2(0,1)$ and W as the space X with inner product c. We also defined the two spaces $V_P = V_P(0,1) \times H^1(0,1)$ and $V_C = V_C(0,1) \times V_C(0,1)$ for the pinned-pinned and cantilever cases respectively, where $V_P(0,1)$ and $V_C(0,1)$ denoted the closure of $T_P(0,1)$ and $T_C(0,1)$ respectively, in $H^1(0,1)$. For the purposes of this section, we will denote by V either the space V_P or V_C.

A detailed description for the implementation of the finite element method is given in the section below. For the convergence theory, we use piecewise linear basis functions to construct finite dimensional spaces, which are spans of the set of basis functions which are in the class of test functions. We then define the space S^h, which is a product space of these spaces (so S^h depends on the boundary conditions), and is a finite dimensional subspace of V. For

example, if S_0^h denotes the span of the set of basis functions without the first basis function, then the set S^h for the cantilever case is $S^h = S_0^h \times S_0^h$, which is a finite dimensional subspace of V_C. Assume again that h is related to the dimension n of S^h, and that $h \to 0$ as $n \to \infty$.

Then we can find the Galerkin approximation of Problem TM-P or TM-C, which is a special case of Problem G^h:

Problem TM^h

Find a function $u_h = \langle w^h, \phi^h \rangle$ such that for each $t \in (0, T)$, $u_h(t) \in S^h$ and

$$c\left(u_h''(t), v\right) + b\left(u_h(t), v\right) = \left(f(t), v\right)_X$$

for each $v \in S^h$, while $u_h(0) = u_0^h = \langle w_0^h, \phi_0^h \rangle \in S^h$ and $u_h'(0) = u_1^h = \langle w_1^h, \phi_1^h \rangle \in S^h$.

As for the wave equation, we find an interpolation operator that depends on the space S^h to use instead of assumption **C3** of Section 3.2.2.

For $u \in H^k \cap V$, define the operator Π by

$$\Pi u = \langle \Pi_L u_1, \Pi_L u_2 \rangle,$$

where Π_L is the interpolation operator for piecewise linear basis functions.

Define $H(V, k) = H^k \cap V$ and again $|u|_k = \left|\left|u^{(k)}\right|\right|$. Also define

$$|u|_{H^k}^2 = |u_1|_k^2 + |u_2|_k^2 .$$

We have the following estimate.

Proposition 4.2.1. There exists a constant K such that for each $u \in H^2 \cap V$,

$$||\Pi u - u||_V \leq K C_L h \, |u|_{H^2} .$$

Proof. Let $u \in H^2 \cap V$. First note that by definition we have that

$$||\Pi u - u||_{H^1}^2 = ||\Pi_L u_1 - u_1||_1^2 + ||\Pi_L u_2 - u_2||_1^2 .$$

Note also that from a special case of the result from [OR76, p.279] that there exists a constant C_L such that for any $v \in H^2(0,1)$,

$$||\Pi_L v - v||_1 \leq C_L h \, |v|_2 \, .$$

It follows that

$$\begin{aligned} ||\Pi u - u||^2_{H^1} &\leq C_L^2 h^2 \, |u_1|_2^2 + C_L^2 h^2 \, |u_2|_2^2 \\ &= C_L^2 h^2 \, |u|^2_{H^2} \, . \end{aligned}$$

The final result then follows from the equivalence of the norms $||\cdot||_{H^1}$ and $||\cdot||_V$. □

Finally, as for the wave equation above, if we choose $u_0^h = \Pi u_0 \in H^2 \cap V$ and $u_1^h = \Pi u_1 \in H^2 \cap V$, then we can obtain an error estimate for the semi-discrete approximation from Corollary 3.3.1, provided that $u'' \in \mathcal{L}^2([0,T]; H^2 \cap V)$, and the error estimate for the fully discrete approximation is obtained using Theorem 3.4.1, provided that $f \in C^2([0,T]; X)$.

4.2.2 Algorithm for the approximation

In this section, the Galerkin approximation using the mixed finite element method with piecewise linear basis functions is derived for the Timoshenko model for both the pinned-pinned and cantilever boundary conditions. In particular, the case where $S = 0$ (i.e. there is no axial force) is considered, with the aim of obtaining results that can be compared to those that will be presented in Section 5.4.2. Numerical results are therefore not given here, but rather in that section. Recall that we denote the shear force by F instead of V in this case.

For the mixed finite element method, we choose piecewise linear basis functions, and divide the interval $[0,1]$ into n elements, i.e. n subintervals $[x_{k-1}, x_k]$ of equal length $h = \dfrac{1}{n}$, where $k = 1, 2, \ldots, n$. We choose basis functions δ_i, where $i = 1, 2, \ldots, n$, which are in our class of test functions. For the pinned-pinned case, let $S_w^h = span\,\{\delta_1, \delta_2, \ldots, \delta_{n-1}\}$ and $S_\phi^h = span\,\{\delta_0, \delta_1, \ldots, \delta_n\} = S_F^h$. For the cantilever case, we denote $S_w^h = span\,\{\delta_1, \delta_2, \ldots, \delta_n\} = S_\phi^h$ and $S_F^h = span\,\{\delta_0, \delta_1, \ldots, \delta_n\}$.

Then we can write the problem as follows.

Problem TM-G

Find $\langle w^h, \phi^h \rangle \in S_w^h \times S_\phi^h$ and $F^h \in S_F^h$ such that

$$\begin{aligned} \int_0^1 \partial_t^2 w^h(\cdot,t)v &= -\int_0^1 F^h(\cdot,t)v' + \int_0^1 P(\cdot,t)v \\ \int_0^1 \frac{1}{\alpha}\partial_t^2 \phi^h(\cdot,t)\psi &= -\int_0^1 \left(\frac{1}{\beta}\partial_x \phi^h(\cdot,t)\psi' - F^h(\cdot,t)\psi\right) \\ \int_0^1 F^h(\cdot,t)\xi &= \int_0^1 \left(\partial_x w(\cdot,t) - \phi^h(\cdot,t)\right)\xi \end{aligned} \tag{4.2.1}$$

for each triple $\langle v, \psi, \xi \rangle \in S_w^h \times S_\phi^h \times S_F^h$, while $w^h(\cdot,0) = w_0, \phi^h(\cdot,0) = \phi_0, \partial_t w^h(\cdot,0) = w_d$ and $\partial_t \phi^h(\cdot,t) = \phi_d$.

Now, define the matrices K, M and L by

$$K_{ij} = \int_0^1 \delta_j' \delta_i', M_{ij} = \int_0^1 \delta_j \delta_i \text{ and } L_{ij} = \int_0^1 \delta_j \delta_i' \text{ for } i,j = 0,1,\ldots,n.$$

For the pinned-pinned case

Denote $w^h(\cdot,t) = \sum_{k=1}^{n-1} w_k(t)\delta_k$, $\phi^h(\cdot,t) = \sum_{k=0}^{n} \phi_k(t)\delta_k$ and $F^h(\cdot,t) = \sum_{k=0}^{n} F_k(t)\delta_k$.

Then let

$$\begin{aligned} \bar{w}(t) &= [w_1(t), w_2(t), \ldots, w_{n-1}(t)]^t, \\ \bar{\phi}(t) &= [\phi_0(t), \phi_1(t), \ldots, \phi_n(t)]^t \text{ and} \\ \bar{F}(t) &= [F_0(t), F_1(t), \ldots, F_n(t)]^t. \end{aligned}$$

Now let

$$M_{ij}^* = M_{ij} \text{ and } K_{ij}^* = K_{ij} \text{ for } i,j = 1,2,\ldots,n-1$$

and let

$$\begin{aligned} \hat{L}_{ij} &= L_{ij} \text{ for } i = 1,2,\ldots,n-1 \text{ and } j = 0,1,\ldots,n \text{ and} \\ \tilde{L}_{ij} &= L_{ij}^t \text{ for } i = 0,1,\ldots,n \text{ and } j = 1,2,\ldots,n-1. \end{aligned}$$

Also let $\bar{P}(t) = \left[\bar{P}_w(t), \bar{P}_\phi(t), \bar{P}_F(t)\right]^t$ where

$$\bar{P}_\phi = \bar{0},$$
$$\bar{P}_F = \bar{0},$$

and $\left[\bar{P}_w\right]_i(t) = \int_0^1 P(x_i, t)\delta_i$ for each $i = 0, 1, \ldots, n$.

Further, let $\bar{b} = \left[\bar{b}_w, \bar{b}_\phi, \bar{b}_F\right]^t$ where

$$\bar{b}_w = \left[w_0(x_1), w_0(x_2), \ldots, w_0(x_{n-1})\right],$$
$$\bar{b}_\phi = \left[\phi_0(x_0), \phi_0(x_1), \ldots, \phi_0(x_n)\right] \text{ and}$$
$$\bar{b}_F = \left[(w_0' - \phi_0)(x_0), (w_0' - \phi_0)(x_1), \ldots, (w_0' - \phi_0)(x_n)\right],$$

and let $\bar{a} = \left[\bar{a}_w, \bar{a}_\phi, \bar{\phi}_F\right]^t$, where

$$\bar{a}_w = \left[w_d(x_1), w_d(x_2), \ldots, w_d(x_{n-1})\right],$$
$$\bar{b}_\phi = \left[\phi_d(x_0), \phi_d(x_1), \ldots, \phi_d(x_n)\right],$$
$$\bar{a}_F = \left[(w_d' - \phi_d)(x_0), (w_d' - \phi_d)(x_1), \ldots, (w_d' - \phi_d)(x_n)\right].$$

Then we define the matrices

$$A = \begin{bmatrix} M^* & 0 & 0 \\ 0 & \frac{1}{\alpha}M & 0 \\ 0 & 0 & 0 \end{bmatrix} \text{ and } B = \begin{bmatrix} 0 & 0 & \hat{L} \\ 0 & \frac{1}{\beta}K & -M \\ -\tilde{L} & M & M \end{bmatrix}.$$

For the cantilever case

Denote $w^h(\cdot, t) = \sum_{k=1}^{n} w_k(t)\delta_k$, $\phi^h(\cdot, t) = \sum_{k=1}^{n} \phi_k(t)\delta_k$ and $F^h(\cdot, t) = \sum_{k=0}^{n} F_k(t)\delta_k$.

Then let

$$\bar{w}(t) = \left[w_1(t), w_2(t), \ldots, w_n(t)\right]^t,$$
$$\bar{\phi}(t) = \left[\phi_1(t), \phi_2(t), \ldots, \phi_n(t)\right]^t \text{ and}$$
$$\bar{F}(t) = \left[F_0(t), F_1(t), \ldots, F_n(t)\right]^t.$$

Let

$$M^*_{ij} = M_{ij} \text{ and } K^*_{ij} = K_{ij} \text{ for } i, j = 1, 2, \ldots, n$$

and let

$$\hat{L}_{ij} = L_{ij} \text{ for } i = 1, 2, \ldots, n \text{ and } j = 0, 1, \ldots, n, \text{ and}$$
$$\tilde{L}_{ij} = L^t_{ij} \text{ for } i = 0, 1, \ldots, n \text{ and } j = 1, 2, \ldots, n.$$

Further, let

$$\hat{M}_{ij} = M_{ij} \text{ for } i = 0, 1, \ldots, n \text{ and } j = 1, 2, \ldots, n, \text{ and}$$
$$\tilde{M}_{ij} = M_{ij} \text{ for } i = 1, 2, \ldots, n \text{ and } j = 0, 1, \ldots, n.$$

Also let $\bar{P}(t) = \left[\bar{P}_w(t), \bar{P}_\phi(t), \bar{P}_F(t)\right]^t$ where

$$\bar{P}_\phi = \bar{0},$$
$$\bar{P}_F = \bar{0},$$

and $\left[\bar{P}_w\right]_i(t) = \int_0^1 P(x_i, t)\delta_i$ for each $i = 1, 2, \ldots, n$.

Further, let $\bar{b} = \left[\bar{b}_w, \bar{b}_\phi, \bar{b}_F\right]^t$ where

$$\bar{b}_w = \left[w_0(x_1), w_0(x_2), \ldots, w_0(x_n)\right],$$
$$\bar{b}_\phi = \left[\phi_0(x_1), \phi_0(x_2), \ldots, \phi_0(x_n)\right] \text{ and}$$
$$\bar{b}_F = \left[(w'_0 - \phi_0)(x_0), (w'_0 - \phi_0)(x_1), \ldots, (w'_0 - \phi_0)(x_n)\right]$$

and let $\bar{a} = \left[\bar{a}_w, \bar{a}_\phi, \bar{\phi}_F\right]^t$, where

$$\bar{a}_w = \left[w_d(x_1), w_d(x_2), \ldots, w_d(x_n)\right],$$
$$\bar{a}_\phi = \left[\phi_d(x_1), \phi_d(x_2), \ldots, \phi_d(x_n)\right] \text{ and}$$
$$\bar{a}_F = \left[(w'_d - \phi_d)(x_0), (w'_d - \phi_d)(x_1), \ldots, (w'_d - \phi_d)(x_n)\right].$$

Then we define the matrices

$$A = \begin{bmatrix} M^* & 0 & 0 \\ 0 & \frac{1}{\alpha}M^* & 0 \\ 0 & 0 & 0 \end{bmatrix} \text{ and } B = \begin{bmatrix} 0 & 0 & \hat{L} \\ 0 & \frac{1}{\beta}K^* & -\tilde{M} \\ -\tilde{L} & \hat{M} & M \end{bmatrix}.$$

In both cases, we obtain the following system:

$$A \begin{bmatrix} \bar{w}''(t) \\ \bar{\phi}''(t) \\ \bar{F}''(t) \end{bmatrix} = -B \begin{bmatrix} \bar{w}(t) \\ \bar{\phi}(t) \\ \bar{F}(t) \end{bmatrix} + \bar{P}(t). \tag{4.2.2}$$

Finally, we obtain a central difference average acceleration scheme to approximate the solutions $\bar{w}(\cdot, t^*), \bar{\phi}(\cdot, t^*)$ of the system (4.2.2) at a point $t^* > 0$. To this end, let m denote the number of time steps. Let $\delta t = \dfrac{t^*}{m}$. We divide the interval $[0, t^*]$ into subintervals $[t_k, t_{k+1}]$ of equal length δt, for $k = 0, 1, \ldots, m-1$. We use $\bar{w}_y$, $\bar{\phi}_k$, $\bar{F}_k$ and $\bar{P}_k$ to denote approximations for $\bar{w}(t_k)$, $\bar{\phi}(t_k)$, $\bar{F}(t_k)$ and $\bar{P}(t_k)$ respectively, and denote $\bar{z}_k = [\bar{w}_k, \bar{\phi}_k, \bar{F}_k]^t$. Then we obtain the following system:

$$\frac{1}{(\delta t)^2} A \left[\bar{z}_{k+1} - 2\bar{z}_k + \bar{z}_{k-1}\right] = -\frac{1}{4} B \left[\bar{z}_{k+1} + 2\bar{z}_k + \bar{z}_{k-1}\right] + \bar{P}_k \tag{4.2.3}$$

with $\bar{z}_0 = \bar{b}$ and $(2\delta t)^{-1} \left[\bar{z}_1 - \bar{z}_{-1}\right] = \bar{a}$, for $k \leq m - 1$.

For example, at the first step, $k = 1$. Note that $\bar{z}_{-1} = \bar{z}_1 - 2\delta t \bar{a}$. This can be substituted into system (4.2.3), together with $\bar{z}_0 = \bar{b}$. After rearranging, we obtain

$$\left(\frac{1}{\delta t^2} 2A + \frac{1}{2} B\right) \bar{z}_1 = \left(\frac{1}{\delta t^2} A - \frac{1}{2} B\right) \bar{b} + \left(\frac{1}{\delta t} 2A + \frac{1}{2} \delta t B\right) \bar{a} + \bar{P}_1,$$

which can now be used to solve for $\bar{z}_1$.

As mentioned, numerical results from applying this scheme are presented in Section 5.4.2.

Chapter 5

The Local Linear Timoshenko Theory

5.1 Introduction

This chapter provides more details on the local linear Timoshenko (LLT) rod from [VDL21], introduced in Chapter 1. In [VDL21], the equations of motion and constitutive equations for the model were derived. The model was then used to derive special cases, such as LLT rod models for small vibrations, and also adapted versions of the Timoshenko model. Variational forms and weak variational forms were presented for the adapted models, for pinned-pinned, cantilever and pivoted boundary conditions, as well as some existence results.

As a further investigation into the LLT rod model, a finite element algorithm for approximating possible solutions to the LLT rod model was introduced in the (currently unpublished) work [DLV22]. In this chapter, this algorithm is investigated, and some of the results obtained in this work were reproduced. In [DLV22], the variational forms are derived with the same boundary conditions mentioned above for the original model, not just for the special cases in [VDL21], with the intention of drawing comparisons between the LLT and linear Timoshenko models. The variational problems were used to find semi-discrete problems for the model. An algorithm, based on the mixed finite element method, was derived in [DLV22] to solve these problems. Several numerical results are given in the article: for small

vibrations, for LLT rods with beam-like properties, and for highly slender rods, showing the applicability of this model to a wide variety of slender structures. A few problems were considered where comparisons were made between results obtained for the LLT rod and the (linear) Timoshenko beam models. For example, numerical simulations showed that for a pinned-pinned beam with small vibrations, the approximations obtained from the LLT algorithm corresponded to exact solutions obtained for the Timoshenko beam.

The full LLT model, some special cases, and the variational problems for the model were derived in Section 1.4. In the following sections, the model is studied in more detail. In Section 5.2, the derivation of the model from [VDL21] is given, followed by the finite element algorithm for the model, suggested in [DLV22], in Section 5.3. Finally, in Section 5.4, some of the numerical results from [DLV22] are reproduced, and some additional results using the same algorithms are presented.

5.2 The Local Linear Timoshenko rod model

In this section, the model for the Local Linear Timoshenko rod is derived. The procedure is as in [VDL21], but is presented in detail here. Some of the results given here will further be used in Chapter 6.

5.2.1 Conservation of momentum and angular momentum

Before the model is derived, a brief introduction to some notation and concepts of mechanics are provided for reference. The details of these assumptions are beyond the scope of this dissertation.

Consider an elastic body with reference configuration denoted by $\mathcal{B}$ and let $\bar{x}$ denote any point in $\mathcal{B}$. Let $\bar{r}(\bar{x}, t)$ denote the position of the point at a time t. Then the velocity of the point at time t is $\bar{v}(\bar{x}, t) = \partial_t \bar{r}(\bar{x}, t)$. Also let ρ denote the density, as before.

Further, let $\mathcal{R}$ be an arbitrary part of $\mathcal{B}$ with boundary Σ, and let $\bar{t}_{\mathcal{R}}$ and $\bar{b}$ denote the traction and body force respectively. If ρ is constant, then the momentum of $\mathcal{R}$ is

$$\int_{\mathcal{R}} \rho \bar{v} dV$$

and the angular momentum is

$$\int_{\mathcal{R}} \bar{R} \times \rho \bar{v} dV.$$

The following two assumptions form the basis for the theory:

Conservation of momentum

$$\frac{d}{dt} \int_{\mathcal{R}} \rho \bar{v} dV = \int_{\Sigma} \bar{t}_{\mathcal{R}} dS + \int_{\mathcal{R}} \bar{b} dV$$

Conservation of angular momentum

$$\frac{d}{dt} \int_{\mathcal{R}} (\bar{r} - \bar{p}) \times \rho \bar{v} dV = \int_{\Sigma} (\bar{r} - \bar{p}) \times \bar{t}_{\mathcal{R}} dS + \int_{\mathcal{R}} (\bar{r} - \bar{p}) \times \bar{b} dV$$

where $\bar{p}$ is any fixed point. Without loss of generality, it may be assumed that $\bar{p} = \bar{0}$.

The following function convention is followed: $\bar{F}(c,t)$ and $\bar{M}(c,t)$ denote the force and couple acting at the part of the rod where $x \leq c$ respectively.

Finally, we choose the line segment in $\mathcal{B}$ such that every cross section perpendicular to it has its centroid on the line to be the straight line $y = z = 0$. This line is referred to as the axis of the rod.

5.2.2 Model derivation

As in [VDL21], we assume that the position of a point $X(x,y,z)$ in $\mathcal{B}$ at time t is

$$\begin{aligned} \bar{R}(X,t) &= \bar{r}_0(x,t) + y\bar{e}_y(x,t) + z\bar{e}_z(x,t) \\ &= \bar{r}_0(x,t) + \bar{r}(X,t), \end{aligned} \tag{5.2.1}$$

where $\bar{e}_y$ and $\bar{e}_z$ are orthogonal unit vectors and $\bar{r}_0$ is the position of the point $(x, 0, 0)$ at time t.

Now let $\mathcal{R}$ be the part of $\mathcal{B}$ between $x = a$ and $x = b$. Denote the distance between the axis and the edge of the beam in the direction $\bar{e}_y$ by h and in the direction of $\bar{e}_z$ by k. The velocity of a point X at time t is

$$\begin{aligned}\bar{v} &= \partial_t \bar{R} \\ &= \partial_t \bar{r}_0 + \partial_t \bar{r} \\ &= \partial_t \bar{r}_0 + y\partial_t \bar{e}_y + z\partial_t \bar{e}_z.\end{aligned}$$

Then the momentum of $\mathcal{R}$ is

$$\begin{aligned}\int_{\mathcal{R}} \rho \bar{v} dV &= \rho \int_a^b \int_{\mathcal{D}} \partial_t \bar{r}_0 + y\partial_t \bar{e}_y + z\partial_t \bar{e}_z dA dx \\ &= \rho \int_a^b A(x)\partial_t \bar{r}_0 dx + \rho \int_a^b \int_{-h}^{h} \int_{-k}^{k} y\partial_t \bar{e}_y dz dy dx + \int_a^b \int_{-h}^{h} \int_{-k}^{k} z\partial_t \bar{e}_z dz dy dx \\ &= \rho \int_a^b A(x)\partial_t \bar{r}_0 dx + \rho \int_a^b ky^2 \partial_t \bar{e}_y|_{-h}^{h} dx + \rho \int_a^b hz^2 \partial_t \bar{e}_z|_{-k}^{k} dx \\ &= \rho \int_a^b A(x)\partial_t \bar{r}_0 dx + \bar{0},\end{aligned} \tag{5.2.2}$$

where $\mathcal{D} = \mathcal{D}(x)$ denotes a cross-section. Note that it is assumed that $\mathcal{D}$ is symmetric with respect to the y-axis and z-axis.

Further, the angular momentum of $\mathcal{R}$ about $\bar{0}$ is

$$\begin{aligned}\int_{\mathcal{R}} \bar{R}\times\rho\bar{v}dV &= \int_{\mathcal{R}} (\bar{r}_0(x,t)+\bar{r}(X,t))\times\rho\left(\partial_t\bar{r}_0(x,t)+\partial_t\bar{r}(X,t)\right)dV\\ &= \rho\int_{\mathcal{R}}\bar{r}_0(x,t)\times\partial_t\bar{r}_0(x,t)dV+\rho\int_{\mathcal{R}}\bar{r}(X,t)\times\partial_t\bar{r}_0(x,t)dV+\rho\int_{\mathcal{R}}\bar{r}_0(x,t)\times\partial_t\bar{r}(X,t)dV\\ &+\rho\int_{\mathcal{R}}\bar{r}(X,t)\times\partial_t\bar{r}(X,t)dV\\ &= \rho\int_a^b A(x)\bar{r}_0(x,t)\times\partial_t\bar{r}_0(x,t)dV+\rho\int_a^b\int_{\mathcal{D}} y\bar{e}_y(x,t)\times\partial_t\bar{r}_0(x,t)\\ &+ z\bar{e}_z\times\partial_t\bar{r}_0(x,t)dAdx\\ &+\rho\int_a^b\int_{\mathcal{D}} y\bar{r}_0(x,t)\times\partial_t\bar{e}_y(x,t)+z\bar{r}_0(x,t)\times\partial_t\bar{e}_z dAdx\\ &+\rho\int_a^b\int_{\mathcal{D}}\bar{r}(X,t)\times\partial_t\bar{r}(X,t)dAdx.\end{aligned} \tag{5.2.3}$$

Since

$$\int_{\mathcal{D}} ydA = ky^2|_{-h}^{h}=0 \text{ and } \int_{\mathcal{D}} zdA = hz^2|_{-k}^{k}=0,$$

it follows that

$$\begin{aligned}\int_{\mathcal{R}}\bar{R}\times\rho\bar{v}dV &= \rho\int_a^b A(x)\bar{r}_0(x,t)\times\partial_t\bar{r}_0(x,t)dx\\ &+\rho\int_a^b\int_{\mathcal{D}}\bar{r}(X,t)\times\partial_t\bar{r}(X,t)dAdx.\end{aligned}$$

From our function convention above, we have that the forces on $\mathcal{R}$ are $\bar{F}(b,t)$ and $-\bar{F}(a,t)$ and the moments are $\bar{M}(b,t)$ and $-\bar{M}(a,t)$.

From the conservation of momentum and Equation (5.2.2) we then have

$$\frac{d}{dt}\int_a^b \rho A(x)\partial_t\bar{r}_0(x,t)dx = \bar{F}(b,t)-\bar{F}(a,t)+\int_a^b\bar{P}(x,t)dx.$$

For convenience, introduce the following notation:

$$\bar{H}(x,t)=\rho\int_{\mathcal{D}}\bar{r}\times\partial_t\bar{r}dA. \tag{5.2.4}$$

Then from the conservation of angular momentum and Equation (5.2.3) we have

$$\frac{d}{dt}\int_a^b \rho A(x)\bar{r}_0(x,t)\times\partial_t\bar{r}_0(x,t)dx+\frac{d}{dt}\int_a^b \bar{H}(x,t)dx$$
$$=\bar{r}_0(b,t)\times\bar{F}(b,t)-\bar{r}_0(a,t)\times\bar{F}(a,t)+\bar{M}(b,t)-\bar{M}(a,t)+\int_a^b \bar{r}_0(x,t)\times\bar{P}(x,t).$$

From the Fundamental Theorem of Calculus, it then follows that

$$\int_a^b \rho A(x)\partial_t^2\bar{R}_0(x,t)dx=\int_a^b \frac{d}{dx}\bar{F}(x,t)dx+\int_a^b \bar{P}(x,t)$$

and

$$\int_a^b \rho A(x)\bar{r}_0(x,t)\times\partial_t^2\bar{r}_0(x,t)dx+\int_a^b \frac{d}{dt}\bar{H}(x,t)dx$$
$$=\int_a^b \frac{d}{dx}\bar{r}_0(x,t)\times\bar{F}(x,t)+\int_a^b \frac{d}{dx}\bar{M}(x,t)+\int_a^b \bar{r}_0(x,t)\times\bar{P}(x,t)dx.$$

Since $[a,b]$ is arbitrary, it follows that these two equations must hold for any $[a,b]$, and hence we must have

$$\rho A\partial_t^2\bar{r}_0=\partial_x\bar{F}+\bar{P}, \tag{5.2.5}$$
$$\rho A\bar{r}_0\times\partial_t^2\bar{r}_0+\partial_t\bar{H}=\partial_x(\bar{r}_0\times\bar{F})+\partial_x\bar{M}+\bar{r}_0\times\bar{P}. \tag{5.2.6}$$

Substituting Equation (5.2.5) into Equation (5.2.6), we obtain

$$\bar{r}_0\times(\partial_x\bar{F}+\bar{P})+\partial_t\bar{H}=\partial_x(\bar{r}_0\times\bar{F})+\partial_x\bar{M}+\bar{r}_0\times\bar{P},$$

and hence

$$\partial_t\bar{H}=\partial_x\bar{r}_0\times\bar{F}+\partial_x\bar{M},$$

since $\partial_x(\bar{r}_0\times\bar{F})=\partial_x\bar{r}_0\times\bar{F}+\bar{r}_0\times\partial_x\bar{F}$.

Hence we have the equations of motion

$$\rho A\partial_t^2\bar{r}_0=\partial_x\bar{F}+\bar{P}, \tag{5.2.7}$$
$$\partial_t\bar{H}=\partial_x\bar{r}_0\times\bar{F}+\partial_x\bar{M}. \tag{5.2.8}$$

Now let $\{\bar{e}_1, \bar{e}_2, \bar{e}_3\}$ denote a right-hand orthonormal set fixed in space.

We assume that $\bar{r}_0$ has the form

$$\bar{r}_0(x,t) = r_1(x,t)\bar{e}_1 + r_2(x,t)\bar{e}_2,$$

and that $\bar{e}_z(t) = \bar{e}_3(t)$.

Then the tangent vector to the deflection curve is

$$\partial_x \bar{r}_0(x,t) = \partial_x r_1(x,t)\bar{e}_1 + \partial_x r_2(x,t)\bar{e}_2.$$

Denote the angle between this tangent vector and the vector $\bar{e}_1$ by $\theta(x,t)$. Note then that

$$\begin{aligned}\cos(\theta(x,t)) &= \frac{\partial_x r_1}{||\partial_x \bar{r}_0||}\\ \sin(\theta(x,t)) &= \frac{\partial_x r_2}{||\partial_x \bar{r}_0||}.\end{aligned}$$

Then the normalised tangent vector, denoted $\bar{e}_T$, is

$$\begin{aligned}\bar{e}_T(x,t) &= \frac{\partial_x \bar{r}_0(x,t)}{||\partial_x \bar{r}_0(x,t)||}\\ &= \cos(\theta(x,t))\,\bar{e}_1 + \sin(\theta(x,t))\,\bar{e}_2.\end{aligned}$$

Next, note that the angle of rotation, denoted by ϕ, is defined by

$$\begin{aligned}\cos(\phi(x,t)) &= \bar{e}_x(x,t)\cdot\bar{e}_1\\ \sin(\phi(x,t)) &= \bar{e}_y(x,t)\cdot\bar{e}_2,\end{aligned}$$

and hence

$$\bar{e}_y(x,t) = -\sin(\phi(x,t))\,\bar{e}_1 + \cos(\phi(x,t))\,\bar{e}_2 \tag{5.2.9}$$

$$\bar{e}_x(x,t) = \cos(\phi(x,t))\,\bar{e}_1 + \sin(\phi(x,t))\,\bar{e}_2. \tag{5.2.10}$$

From Equations (5.2.1) and (5.2.4), it then follows that

$$\begin{aligned}\bar{H}(x,t) &= \rho \int_{\mathcal{D}} \bar{r}(x,t) \times \partial_t \bar{r}(x,t) \\ &= \rho \int_{\mathcal{D}} (y\bar{e}_y(x,t) + z\bar{e}_z(t)) \times (y\partial_t \bar{e}_y(x,t) + z\partial_t \bar{e}_z(t))\, dA \\ &= \rho \int_{\mathcal{D}} y^2 \bar{e}_y(x,t) \times \partial_t \bar{e}_y(x,t) + yz\bar{e}_y(x,t) \times \partial_t \bar{e}_z(t) + yz\bar{e}_z(t) \times \partial_t \bar{e}_y(x,t) \\ &+ z^2 \bar{e}_z(t) \times \partial_t \bar{e}_z(t) dA.\end{aligned}$$

Now from Equations (5.2.9) and (5.2.10) we know that

$$\partial_t \bar{e}_y = -\partial_t \phi \bar{e}_x \text{ and } \partial_t \bar{e}_x = \partial_t \phi.$$

Then

$$\partial_t \bar{e}_z = \partial_t \bar{e}_y \times \bar{e}_x + \bar{e}_y \times \partial_t \bar{e}_x = \bar{0}.$$

Also note that

$$\bar{e}_y \times \bar{e}_x = -\bar{e}_z = -\bar{e}_3.$$

Further, note that since $\mathcal{D}$ is symmetric with respect to the y-axis, then it follows as was shown in Equations (5.2.2) that

$$\int_{\mathcal{D}} yz dA = \bar{0}.$$

Then it follows that

$$\begin{aligned}\bar{H}(x,t) &= \rho \int_{\mathcal{D}} y^2 \partial_t \phi(x,t) dA \bar{e}_3 \\ &= \rho I \partial_t \phi(x,t) \bar{e}_3,\end{aligned} \tag{5.2.11}$$

where $I = \int_{\mathcal{D}} y^2 dA$.

Equations of motion

Finally, we are able to derive the equations of motion for our problem, using Equations (5.2.7), (5.2.8) and (5.2.11). They are

$$\rho A \partial_t^2 \bar{r}_0 = \partial_x \bar{F} + \bar{P}, \tag{5.2.12}$$

$$\rho I \partial_t^2 \phi \bar{e}_3 = \partial_x \bar{r}_0 \times \bar{F} + \partial_x \bar{M}, \tag{5.2.13}$$

or, using the fact that

$$\partial_t \bar{r}_0 = \partial_t^2 r_1 \bar{e}_1 + \partial_t^2 r_2 \bar{e}_2,$$

we have

$$\rho A \partial_t^2 r_1 = \partial_x F_1 + P_1, \tag{5.2.14}$$

$$\rho A \partial_t^2 r_2 = \partial_x F_2 + P_2, \tag{5.2.15}$$

$$\rho I \partial_t^2 \phi = \partial_x r_1 F_2 - \partial_x r_2 F_1 + \partial_x M_3. \tag{5.2.16}$$

Constitutive Equations

To derive the final model, we require constitutive equations. We use the following equations, as they are in [VDL21].

Firstly,

$$F_1 = S\cos\theta - V\sin\theta,$$

$$F_2 = S\sin\theta + V\cos\theta.$$

The following are similar to the constitutive equations used for the original Timoshenko model in Chapter 1,

$$M = M_3 = EI\partial_x \phi, \tag{5.2.17}$$

$$V = \kappa^2 AG(\theta - \phi). \tag{5.2.18}$$

Finally, we have

$$S = AE\epsilon_s \tag{5.2.19}$$

from Hooke's law, where

$$\epsilon_s = \partial_x s - 1 \text{ and } (\partial_x s)^2 = ||\partial_x \bar{r}_0||\,.$$

Here s is the arc length function.

Dimensionless form

As was done for the Timoshenko model in Chapter 1, it is convenient to derive the model in

dimensionless form. We proceed in much the same way as before, and the main steps of the derivation of the dimensionless form are given below.

To this end, let

$$u(x,t) = r_1(x,t) - x \text{ and } w(x,t) = r_2(x,t).$$

Further, let

$$\tau = \frac{t}{T},\ \xi = \frac{x}{\ell},\ u^*(\xi,\tau) = \frac{u(x,t)}{\ell},\ w^*(\xi,\tau) = \frac{w(x,t)}{\ell},\ \phi^*(\xi,\tau) = \phi(x,t),\ \text{and } s^*(\xi,\tau) = \frac{s(x,t)}{\ell},$$

where T needs to be determined.

Also let

$$F_i^*(\xi,\tau) = \frac{F_i(x,t)}{AG\kappa^2},\ P_i^*(\xi,\tau) = \frac{\ell P_i(x,t)}{AG\kappa^2},\ M^*(\xi,\tau) = \frac{M(x,t)}{AG\kappa^2\ell},$$
$$V^*(\xi,\tau) = \frac{V(x,t)}{AG\kappa^2},\ \text{and } S^*(\xi,\tau) = \frac{S(x,t)}{AG\kappa^2},$$

where $i = 1, 2$.

It follows from Equations (5.2.14)-(5.2.16) that

$$\frac{\rho A}{T^2}\partial_\tau^2 u^* = \frac{AG\kappa^2}{\ell^2}\partial_\xi^2 F_1^* + \frac{AG\kappa^2}{\ell^2}P_1^*,$$
$$\frac{\rho A}{T^2}\partial_\tau^2 w^* = \frac{AG\kappa^2}{\ell^2}\partial_\xi^2 F_2^* + \frac{AG\kappa^2}{\ell^2}P_2^*,$$
$$\frac{\rho I}{T^2}\partial_\xi \phi^* = (1+\partial_\xi u^*)AG\kappa^2 F_2^* - \partial_\xi w^* AG\kappa^2 F_1^* + AG\kappa^2\partial_\xi M^*,$$

or

$$\frac{\rho\ell^2}{G\kappa^2T^2}\partial_\tau^2 u^* = \partial_\xi^2 F_1^* + P_1^*,$$
$$\frac{\rho\ell^2}{G\kappa^2T^2}\partial_\tau^2 w^* = \partial_\xi^2 F_2^* + P_2^*,$$
$$\frac{\rho I}{AG\kappa^2T^2}\partial_\xi \phi^* = (1+\partial_\xi u^*)\partial_\xi F_2^* - \partial_\xi w^* F_1^* + \partial_\xi M^*.$$

Similarly, Equations (5.2.17)-(5.2.19) become

$$AG\kappa^2\ell M^* = \frac{EI}{\ell}\partial_x\phi^*,$$
$$AG\kappa^2 V^* = \kappa^2 AG(\theta^* - \phi^*),$$
$$AG\kappa^2 S^* = EA(\partial_\xi s - 1).$$

Then let $T = \ell\sqrt{\dfrac{\rho}{G\kappa^2}}$ and let

$$\alpha = \frac{A\ell^2}{I},\ \beta = \frac{AG\kappa^2\ell^2}{EI} \text{ and } \gamma = \frac{\beta}{\alpha} = \frac{G\kappa^2}{E}.$$

The full model in dimensionless form is given in the next section, in original notation. It is the same as the model in Section 1.4.1, but is given again for convenience and easy reference.

Remark 5.2.1. The dimensionless constants α and β are exactly the same as for the original Timoshenko model in Section 1.2.1.

5.2.3 Local Linear Timoshenko Model

Consider again the model for the LLT rod in dimensionless form.

The equations of motion are

$$\partial_t^2 u = \partial_x F_1 + P_1, \tag{1.4.1}$$

$$\partial_t^2 w = \partial_x F_2 + P_2, \tag{1.4.2}$$

$$\frac{1}{\alpha}\partial_t^2 \phi = (1 + \partial_x u)\, F_2 - \partial_x w F_1 + \partial_x M, \tag{1.4.3}$$

where

$$F_1 = S\cos\theta - V\sin\theta, \tag{1.4.4}$$

$$F_2 = S\sin\theta + V\cos\theta, \tag{1.4.5}$$

and $\partial_x s$ and θ are determined from

$$(\partial_x s)^2 = (1 + \partial_x u)^2 + (\partial_x w)^2\,, \tag{1.4.6}$$

$$\cos\theta = (\partial_x s)^{-1}\,(1 + \partial_x u)\,, \tag{1.4.7}$$

$$\sin\theta = (\partial_x s)^{-1}\,\partial_x w. \tag{1.4.8}$$

The constitutive equations are

$$M = \frac{1}{\beta}\partial_x \phi, \tag{1.4.9}$$

$$V = \theta - \phi, \tag{1.4.10}$$

$$S = \frac{1}{\gamma}\left(\partial_x s - 1\right). \tag{1.4.11}$$

Recall also the boundary conditions:

Pinned-pinned: $u(0,t) = w(0,t) = u(1,t) = w(1,t) = 0$ and $M(0,t) = M(1,t) = 0$.

Cantilever: $u(0,t) = w(0,t) = \phi(0,t) = 0$ and $F_1(1,t) = F_2(1,t) = M(1,t) = 0$.

5.3 Finite Element Algorithm for the LLT beam

Recall the variational problems derived for the LLT model in Section 1.4.2. In this section, it is shown how a finite element algorithm for the LLT beam model is derived to obtain a linear system whose solution is used to approximate solutions of the original model. The reader is referred to [DLV22] for more details of the derivation of the algorithm, to complement the main steps presented below. We choose piecewise linear functions δ_i as basis functions. Denote $S_0^h = span\left\{\delta_0, \delta_1, \ldots, \delta_n\right\}$, $S_1^h = span\left\{\delta_1, \delta_2, \ldots, \delta_n\right\}$ and $S_2^h = span\left\{\delta_1, \delta_2, \ldots, \delta_{n-1}\right\}$.

5.3.1 The cantilever case

Consider again Problem LLTV-C presented in Section 1.4.2. We write the problem as follows:

Find u^h, w^h, $\phi^h \in S_1^h$ such that for each $t > 0$,

$$\int_0^1 \partial_t^2 u^h(\cdot,t)v = -\int_0^1 F_1^h(\cdot,t)v' + \int_0^1 P_1(\cdot,t)v, \tag{5.3.1}$$

$$\int_0^1 \partial_t^2 w^h(\cdot,t)z = -\int_0^1 F_2^h(\cdot,t)z' + \int_0^1 P_2(\cdot,t)z, \tag{5.3.2}$$

$$\int_0^1 \frac{1}{\alpha}\partial_t^2 \phi^h(\cdot,t)\psi = \int_0^1 \left(1 + \partial_x u^h(\cdot,t)\right) F_2^h(\cdot,t)\psi - \int_0^1 \partial_x w^h(\cdot,t) F_1^h(\cdot,t)\psi - \int_0^1 \frac{1}{\beta}\partial_x \phi^h(\cdot,t)\psi' \tag{5.3.3}$$

for all v, z, $\psi \in S_1^h$, where F_1^h, $F_2^h \in S_0^h$. Note that in Equation (5.3.3), the constitutive equation (1.4.9) was used.

Now, since derivatives of piecewise linear basis functions are discontinuous at the nodes, we introduce functions $g_u^h(t)$ and $g_w^h(t)$ to approximate $\partial_x u(\cdot, t)$ and $\partial_x w(\cdot, t)$ respectively. To this end, define

$$\int_0^1 g_u^h(t)\delta_i = \int_0^1 \partial_x u^h(\cdot, t)\delta_i, \tag{5.3.4}$$

$$\int_0^1 g_w^h(t)\delta_i = \int_0^1 \partial_x w^h(\cdot, t)\delta_i \tag{5.3.5}$$

for $i = 0, 1, \ldots, n$.

Then we may approximate the function $\partial_x s$ in (1.4.6) with the function d_s^h, which is defined by

$$\left(d_s^h\right)^2 = \left(1 + g_u^h\right)^2 + \left(g_w^h\right)^2.$$

As in [DLV22], we assume that

$$d_s^h(x_i, t) = \sqrt{\left(1 + g_u^h(x_i, t)\right)^2 + \left(g_w^h(x_i, t)\right)^2} \tag{5.3.6}$$

holds only at the nodes x_i.

Furthermore, define

$$s_\theta^h(t) = \frac{g_w^h(t)}{d_s^h(t)} \text{ and} \tag{5.3.7}$$

$$c_\theta^h(t) = \frac{1 + g_u^h(t)}{d_s^h(t)} \tag{5.3.8}$$

so that

$$\sin\theta^h = s_\theta^h \text{ and} \tag{5.3.9}$$

$$\cos\theta^h = c_\theta^h. \tag{5.3.10}$$

Then we obtain

$$V^h = \theta^h - \phi^h, \tag{5.3.11}$$

$$S^h = \frac{1}{\gamma}\left(d_s^h - 1\right) \tag{5.3.12}$$

from Equations (1.4.10) and (1.4.11).

Finally, we obtain expressions for F_1^h and F_2^h:

$$F_1^h = S^h c_\theta^h - V^h s_\theta^h \text{ and} \tag{5.3.13}$$

$$F_2^h = S^h c_\theta^h + V^h s_\theta^h. \tag{5.3.14}$$

Now denote

$$\begin{aligned} M_{ij} &= \int_0^1 \delta_j \delta_i \text{ for } i,j = 0,1,\ldots,n, \\ K_{ij} &= \int_0^1 \delta_j' \delta_i' \text{ for } i,j = 0,1,\ldots,n, \\ L_{ij} &= \int_0^1 \delta_j \delta_i' \text{ for } i,j = 0,1,\ldots,n. \end{aligned}$$

We also use the following notation:

$$\begin{aligned} T^h \bar{x} &= \sum_{i=0}^{n} x_i \delta_i \in S_0^h \text{ for any } \bar{x} \in \mathbb{R}^{n+1}, \\ T_1^h \bar{x} &= \sum_{i=1}^{n} x_i \delta_i \in S_1^h \text{ for any } \bar{x} \in \mathbb{R}^{n}, \end{aligned}$$

and

$$\begin{aligned} A_1 &= [A_{ij}] \text{ for } i,j = 1,2,\ldots,n, \\ A_c &= [A_{ij}] \text{ for } i = 0,1,\ldots,n, j = 1,2,\ldots,n, \end{aligned}$$

where A represents matrices K, M or L.

Next, we use integration by parts and properties of the basis functions to write Equations (5.3.4) and (5.3.5) as

$$\begin{aligned} \int_0^1 g_u^h(\cdot,t)\delta_i &= u^h(1,t)\delta_i(1) - \int_0^1 u^h(\cdot,t)\delta_i' \text{ for } i = 0,1,\ldots,n, \\ \int_0^1 g_w^h(\cdot,t)\delta_i &= w^h(1,t)\delta_i(1) - \int_0^1 w^h(\cdot,t)\delta_i' \text{ for } i = 0,1,\ldots,n. \end{aligned}$$

Then we can calculate $\bar{g}_u(t) = \left(T^h\right)^{-1} g_u^h(t)$ and $\bar{g}_w(t) = \left(T^h\right)^{-1} g_w^h(t)$ from

$$M\bar{g}_u(t) = -L_c^*\bar{u}(t),$$
$$M\bar{g}_w(t) = -L_c^*\bar{w}(t)$$

where $L_{ij}^* = L_{ij}$ but $L_{nn}^* = L_{nn} - 1$.

From Equation (5.3.6) we define $\bar{d}_s$ by

$$d_{s,i}(t) = \sqrt{(1 + g_{u,i}(t))^2 + (g_{w,i}(t))^2}.$$

From Equations (5.3.7) and (5.3.8) we have then

$$s_{\theta,i}(t) = \frac{g_{w,i}(t)}{d_{s,i}(t)} \text{ and } c_{\theta,i}(t) = \frac{1 + g_{u,i}(t)}{d_{s,i}(t)}$$

so that $\bar{\theta}$ is defined by

$$\sin\theta_i(t) = s_{\theta,i}(t) \text{ and } \cos\theta_i(t) = c_{\theta,i}(t)$$

from Equations (5.3.9) and (5.3.10).

To define $\bar{V}$ and $\bar{S}$ we first note that since $\bar{\theta} \in \mathbb{R}^{n+1}$ but $\bar{\phi} \in \mathbb{R}^n$, $\bar{\phi}$ is augmented by a first zero component. Then

$$\bar{V}(t) = \bar{\theta}(t) - \bar{\phi}(t) \text{ and}$$
$$\bar{S}(t) = \frac{1}{\gamma}\left(\bar{d}_s(t) - 1\right)$$

from Equations (5.3.11) and (5.3.12).

Finally, Equations (5.3.13) and (5.3.14) imply that

$$F_1^h \approx \left(T^h\bar{S}\right)\left(T^h\bar{c}_\theta\right) - \left(T^h\bar{V}\right)\left(T^h\bar{s}_\theta\right),$$
$$F_2^h \approx \left(T^h\bar{V}\right)\left(T^h\bar{c}_\theta\right) + \left(T^h\bar{S}\right)\left(T^h\bar{s}_\theta\right).$$

Note that $\bar{u}(t) = \left(T_1^h\right)^{-1} u^h(t)$, $\bar{w}(t) = \left(T_1^h\right)^{-1} w^h(t)$, and $\bar{\phi}(t) = \left(T_1^h\right)^{-1} \phi^h(t)$.

Define the vectors $\bar{G}_1$ and $\bar{G}_2$ by

$$G_{1,i}(t) = \int_0^1 F_1^h(\cdot, t)\delta_i',$$
$$G_{2,i}(t) = \int_0^1 F_2^h(\cdot, t)\delta_i'$$

for $i = 1, 2, \ldots, n$, define the vectors $\bar{H}_u$ and $\bar{H}_w$ by

$$H_{u,i}(t) = \int_0^1 F_2^h(\cdot, t)\left(1 + g_u^h(t)\right)\delta_i,$$
$$H_{w,i}(t) = \int_0^1 F_1^h(\cdot, t)g_w^h(t)\delta_i$$

for $i = 1, 2, \ldots, n$, and define $\bar{P}_1$ and $\bar{P}_2$ by

$$P_{1,i}(t) = \int_0^1 P_1(\cdot, t)\delta_i,$$
$$P_{2,i}(t) = \int_0^1 P_2(\cdot, t)\delta_i$$

for $i = 1, 2, \ldots, n$.

Then we obtain a linear system for $\bar{u}, \bar{w}$ and $\bar{\phi}$:

$$M_1\bar{u}'' = -\bar{G}_1 + \bar{P}_1,$$
$$M_1\bar{w}'' = -\bar{G}_2 + \bar{P}_2,$$
$$\frac{1}{\alpha}M_1\bar{\phi}'' = \bar{H}_u - \bar{H}_w - \frac{1}{\beta}K_1\bar{\phi}.$$

A central difference scheme is used to approximate solutions of this system. To this end, let m be the number of time steps, and suppose we approximate the solution at time point t^*. Let $\delta t = \dfrac{t^*}{m}$. Denote $a_{u,i} = \alpha_d(x_i)$ for $i = 1, 2, \ldots, n$ and $b_{u,i} = \alpha_0(x_i)$ for $i = 1, 2, \ldots, n$, and similar notation for w and ϕ respectively. Then we obtain the following system,

$$\frac{1}{\delta t^2}M_1\left[\bar{u}_{k+1} - 2\bar{u}_k + \bar{u}_{k-1}\right] = -\bar{G}_1 + \bar{P}_1,$$
$$\frac{1}{\delta t^2}M_1\left[\bar{w}_{k+1} - 2\bar{w}_k + \bar{w}_{k-1}\right] = -\bar{G}_2 + \bar{P}_2,$$
$$\frac{1}{\delta t^2}\frac{1}{\alpha}M_1\left[\bar{\phi}_{k+1} - 2\bar{\phi}_k + \bar{\phi}_{k-1}\right] = \bar{H}_u - \bar{H}_w - \frac{1}{4\beta}K_1\left[\bar{\phi}_{k+1} + 2\bar{\phi}_k + \bar{\phi}_{k-1}\right]$$

where $\bar{u}_0 = \bar{b}_u$, $\bar{w}_0 = \bar{b}_w$ and $\bar{\phi}_0 = \bar{b}_\phi$ and $\dfrac{1}{2\delta t}\left[\bar{u}_1 - \bar{u}_{-1}\right] = \bar{a}_u$, $\dfrac{1}{2\delta t}\left[\bar{w}_1 - \bar{w}_{-1}\right] = \bar{a}_w$ and $\dfrac{1}{2\delta t}\left[\bar{\phi}_1 - \bar{\phi}_{-1}\right] = \bar{a}_\phi$.

5.3.2 The pinned-pinned case

The procedure to derive the FEM algorithm in this section is similar to the one for the cantilever case above. Consider Problem LLTV-P described in the previous section. We rewrite the problem as follows:
Find $u^h, w^h \in S_2^h$ and $\phi^h \in S_0^h$ such that for each $t > 0$, Equations (5.3.1)-(5.3.3) hold for all $v, z \in S_2^h$ and $\psi \in S_0^h$, where $F_1^h, F_2^h \in S_0^h$.

Equations (5.3.4)-(5.3.14) remain exactly the same.

Again denote

$$M_{ij} = \int_0^1 \delta_j \delta_i \text{ for } i, j = 0, 1, \ldots, n,$$
$$K_{ij} = \int_0^1 \delta_j' \delta_i' \text{ for } i, j = 0, 1, \ldots, n,$$
$$L_{ij} = \int_0^1 \delta_j \delta_i' \text{ for } i, j = 0, 1, \ldots, n.$$

We also use the following notation:

$$T^h \bar{x} = \sum_{i=0}^{n} x_i \delta_i \in S_0^h \text{ for any } \bar{x} \in \mathbb{R}^{n+1},$$
$$T_2^h \bar{x} = \sum_{i=1}^{n-1} x_i \delta_i \in S_2^h \text{ for any } \bar{x} \in \mathbb{R}^{n-1}$$

and

$$A_2 = [A_{ij}] \text{ for } i, j = 1, 2, \ldots, n-1,$$
$$A_d = [A_{ij}] \text{ for } i = 0, 1, \ldots, n, j = 1, 2, \ldots, n-1$$

where A represents matrices K, M or L.

Next, we use integration by parts and properties of the basis functions to write Equations (5.3.4) and (5.3.5) as

$$\int_0^1 g_u^h(\cdot, t)\delta_i = -\int_0^1 u^h(\cdot, t)\delta_i' \text{ for } i = 0, 1, \ldots, n,$$
$$\int_0^1 g_w^h(\cdot, t)\delta_i = -\int_0^1 w^h(\cdot, t)\delta_i' \text{ for } i = 0, 1, \ldots, n.$$

Then we can calculate $\bar{g}_u(t) = \left(T^h\right)^{-1} g_u^h(t)$ and $\bar{g}_w(t) = \left(T^h\right)^{-1} g_w^h(t)$ from

$$M\bar{g}_u(t) = -L_d\bar{u}(t),$$
$$M\bar{g}_w(t) = -L_d\bar{w}(t).$$

From Equation (5.3.6) we again define $\bar{d}_s$ by

$$d_{s,i}(t) = \sqrt{(1 + g_{u,i}(t))^2 + (g_{w,i}(t))^2}.$$

Further, from Equations (5.3.7) and (5.3.8) we again have

$$s_{\theta,i}(t) = \frac{g_{w,i}(t)}{d_{s,i}(t)} \text{ and } c_{\theta,i}(t) = \frac{1 + g_{u,i}(t)}{d_{s,i}(t)}$$

so that $\bar{\theta}$ is defined by

$$\sin\theta_i(t) = s_{\theta,i}(t) \text{ and } \cos\theta_i(t) = c_{\theta,i}(t)$$

from Equations (5.3.9) and (5.3.10).

In this case, $\bar{\theta} \in \mathbb{R}^{n+1}$ and $\bar{\phi} \in \mathbb{R}^{n+1}$, so we can define

$$\bar{V}(t) = \bar{\theta}(t) - \bar{\phi}(t) \text{ and}$$
$$\bar{S}(t) = \frac{1}{\gamma}\left(\bar{d}_s(t) - 1\right)$$

from Equations (5.3.11) and (5.3.12).

Finally, Equations (5.3.13) and (5.3.14) imply that

$$F_1^h \approx \left(T^h\bar{S}\right)\left(T^h\bar{c}_\theta\right) - \left(T^h\bar{V}\right)\left(T^h\bar{s}_\theta\right),$$
$$F_2^h \approx \left(T^h\bar{V}\right)\left(T^h\bar{c}_\theta\right) + \left(T^h\bar{S}\right)\left(T^h\bar{s}_\theta\right)$$

as before.

Note that here $\bar{u}(t) = \left(T_2^h\right)^{-1} u^h(t)$, $\bar{w}(t) = \left(T_2^h\right)^{-1} w^h(t)$, and $\bar{\phi}(t) = \left(T^h\right)^{-1} \phi^h(t)$.

Define the vectors $\bar{G}_1$ and $\bar{G}_2$ by

$$G_{1,i}(t) = \int_0^1 F_1^h(\cdot,t)\delta_i',$$
$$G_{2,i}(t) = \int_0^1 F_2^h(\cdot,t)\delta_i'$$

for $i = 1, 2, \ldots, n-1$, define the vectors $\bar{H}_u$ and $\bar{H}_w$ by

$$H_{u,i}(t) = \int_0^1 F_2^h(\cdot, t)\left(1 + g_u^h(t)\right)\delta_i,$$
$$H_{w,i}(t) = \int_0^1 F_1^h(\cdot, t) g_w^h(t)\delta_i$$

for $i = 0, 1, 2, \ldots, n$, and define $\bar{P}_1$ and $\bar{P}_2$ by

$$P_{1,i}(t) = \int_0^1 P_1(\cdot, t)\delta_i,$$
$$P_{2,i}(t) = \int_0^1 P_2(\cdot, t)\delta_i$$

for $i = 1, 2, \ldots, n-1$.

Then we obtain a linear system for $\bar{u}, \bar{w}$ and $\bar{\phi}$:

$$M_2\bar{u}'' = -\bar{G}_1 + \bar{P}_1, \tag{5.3.15}$$
$$M_2\bar{w}'' = -\bar{G}_2 + \bar{P}_2, \tag{5.3.16}$$
$$\frac{1}{\alpha}M\bar{\phi}'' = \bar{H}_u - \bar{H}_w - \frac{1}{\beta}K\bar{\phi}. \tag{5.3.17}$$

The central difference scheme is then derived exactly as for the cantilever case. To this end, let m be the number of time steps, and suppose we approximate the solution at time point t^*. Let $\delta t = \dfrac{t^*}{m}$. Denote $a_{u,i} = \alpha_d(x_i)$ for $i = 1, 2, \ldots, n-1$ and $b_{u,i} = \alpha_0(x_i)$ for $i = 1, 2, \ldots, n-1$, and similar notation for w and ϕ respectively. Then we obtain the following system,

$$\frac{1}{\delta t^2}M_2\left[\bar{u}_{k+1} - 2\bar{u}_k + \bar{u}_{k-1}\right] = -\bar{G}_1 + \bar{P}_1,$$
$$\frac{1}{\delta t^2}M_2\left[\bar{w}_{k+1} - 2\bar{w}_k + \bar{w}_{k-1}\right] = -\bar{G}_2 + \bar{P}_2,$$
$$\frac{1}{\delta t^2}\frac{1}{\alpha}M\left[\bar{\phi}_{k+1} - 2\bar{\phi}_k + \bar{\phi}_{k-1}\right] = \bar{H}_u - \bar{H}_w - \frac{1}{4\beta}K\left[\bar{\phi}_{k+1} + 2\bar{\phi}_k + \bar{\phi}_{k-1}\right],$$

where $\bar{u}_0 = \bar{b}_u$, $\bar{w}_0 = \bar{b}_w$ and $\bar{\phi}_0 = \bar{b}_\phi$ and $\dfrac{1}{2\delta t}\left[\bar{u}_1 - \bar{u}_{-1}\right] = \bar{a}_u$, $\dfrac{1}{2\delta t}\left[\bar{w}_1 - \bar{w}_{-1}\right] = \bar{a}_w$ and $\dfrac{1}{2\delta t}\left[\bar{\phi}_1 - \bar{\phi}_{-1}\right] = \bar{a}_\phi$.

5.4 Numerical results

5.4.1 Small vibrations of the pinned-pinned LLT rod

In this subsection, we briefly consider some numerical results for the free vibration of the LLT rod with pinned-pinned boundary conditions. Here, suppose $P_1 = P_2 = 0$ in Equations (1.4.1) and (1.4.2), suppose $S = 0$, and consider the boundary conditions for the pinned-pinned case:

$$u(0,t) = w(0,t) = u(1,t) = w(1,t) = 0 \text{ and } M(0,t) = M(1,t) = 0.$$

Note that for free vibration of the linear Timoshenko beam with pinned-pinned boundary conditions, it was shown in [VV06] that a nonconstant eigenfunction corresponding to the eigenvalue λ_k of the associated eigenvalue problem is given by

$$[w_k, \phi_k]^t = [\sin(k\phi x), \mathcal{C}_k \cos(k\pi x)]^t,$$

where

$$\begin{aligned} k^2\pi^2 - k\pi\mathcal{C}_k &= \lambda_k \\ \frac{k^2\pi^2\mathcal{C}_k}{\gamma} - \alpha k\pi + \alpha\mathcal{C}_k &= \lambda_k\mathcal{C}_k. \end{aligned}$$

It was shown in [VV06] that $\lambda_1 \approx 0.3119$ and $\mathcal{C}_1 \approx 3.042$. For the following numerical results, the first modal solution (i.e. where $k = 1$) was used to choose the initial conditions. Further, for the linear Timoshenko beam, there is no axial displacement u. Hence we consider the following initial conditions:

$$u(x,0) = u_0(x) = 0, \tag{5.4.1}$$

$$w(x,0) = w_0(x) = c\sin(\pi x), \tag{5.4.2}$$

$$\phi(x,0) = \phi_0(x) = c\mathcal{C}_1\cos(\pi x), \tag{5.4.3}$$

$$u_d(x) = w_d(x) = \phi_d(x) = 0. \tag{5.4.4}$$

Finally, choose $\alpha = 1200$, $\gamma = 0.25$ and $c = 0.001$. In [DLV22], pointwise convergence of the LLT-FEM algorithm for this problem was investigated by calculating the error ratios

$$\frac{w_{4n} - w_{2n}}{w_{2n} - w_n} \text{ and } \frac{\phi_{4n} - \phi_{2n}}{\phi_{2n} - \phi_n}$$

at the time point $t = \frac{\pi}{2}$ and at the points $x = 0.5$ and $x = 1$ for w and ϕ respectively, where the largest values were expected to occur.

In [DLV22] it was noted that pointwise convergence was observed from the fact that all ratios were approximately 0.25. Consider the following numerical values, calculated using the algorithm, at the time point $t = \frac{\pi}{2}$ and at $x = 0.5$ and $x = 1$ for w and ϕ respectively:

$$w_8 = -0.00092509 \text{ and } \phi_8 = -0.00281415$$
$$w_{16} = -0.00093103 \text{ and } \phi_{16} = -0.00283219$$
$$w_{32} = -0.00093251 \text{ and } \phi_{32} = -0.00283676.$$

Note that, indeed,

$$\frac{w_{32} - w_{16}}{w_{16} - w_8} = 0.24916 \text{ and } \frac{\phi_{32} - \phi_{16}}{\phi_{16} - \phi_8} = 0.25333.$$

5.4.2 Forced vibrations of the cantilever LLT rod

Next, we consider some results when using the LLT-FEM algorithm for the case of cantilever boundary conditions,

$$u(0,t) = w(0,t) = \phi(0,t) = 0 \text{ and } F_1(1,t) = F_2(1,t) = M(1,t) = 0.$$

We again suppose $S = 0$, and in this case we suppose that the rod is set in motion by a transverse load near the free endpoint. As a result, we use

$$P_1 = 0,$$
$$P_2 = cq(x)\sin t,$$

where c is constant and

$$q(x) = \begin{cases} x - 0.9 \text{ for } x > 0.9, \\ 0 \text{ for } x \leq 0.9. \end{cases}$$

It is assumed that the rod is initially at rest, with no deformation, and hence all initial conditions are zero. Choose $\alpha = 4800$, $\gamma = 0.25$ and $c = 0.001$.

In [DLV22] the $\mathcal{L}^2$-convergence of the LLT-FEM algorithm was investigated. There, the algorithm was used for the time interval $[0, 12\pi]$ with 3200 time steps, and spatially with 8, 16 and 32 elements. Errors were defined in terms of the difference between the approximate solutions u, w and ϕ when doubling the number of subintervals, and finally taking the $\mathcal{L}^2$-norm. For example, $\epsilon^w_{n,2n} = ||w_{2n} - w_n||$. Note that an approximation for the $\mathcal{L}^2$-norm has to be used, since the terms w_{2n} etc. are vector-valued. This was done by using the finite element matrix M on $\mathbb{R}^{2n}$ and using the approximation $\left|\left|\bar{f}(t)\right|\right|^2 = \bar{f}(t)^t M \bar{f}(t)$. It is also necessary to project the approximate solutions u_n, w_n and ϕ_n into $\mathbb{R}^{2n}$, which was done using linear interpolation.

The authors used the relative difference $\dfrac{\epsilon^w_{2n,4n}}{\epsilon^w_{n,2n}}$ to investigate the convergence of the LLT-FEM algorithm, and it was found that while no clear order of convergence is immediately apparent, the calculated ratios remain similar over the time interval $[0, 12\pi]$, which is reassuring for the algorithm's performance.

Finally, the LLT cantilever rod was compared to the linear Timoshenko cantilever beam, and plots for w and ϕ calculated using the LLT-FEM algorithm, at the three time points $6\pi, 9\pi, 12\pi$ were given, and compared to the results obtained when approximating the solution of the linear cantilever Timoshenko beam when using the mixed finite element method. This comparison is replicated here. The central difference scheme derived for the mixed finite element method was given in Section 4.2.2, and here the approximation of the solution to the linear model is plotted together with the results from applying the LLT-FEM algorithm, to compare the two models. The plots are given in Figure 5.1. The plots correspond to those in [DLV22], and it can be seen that the results between the two methods are in agreement.

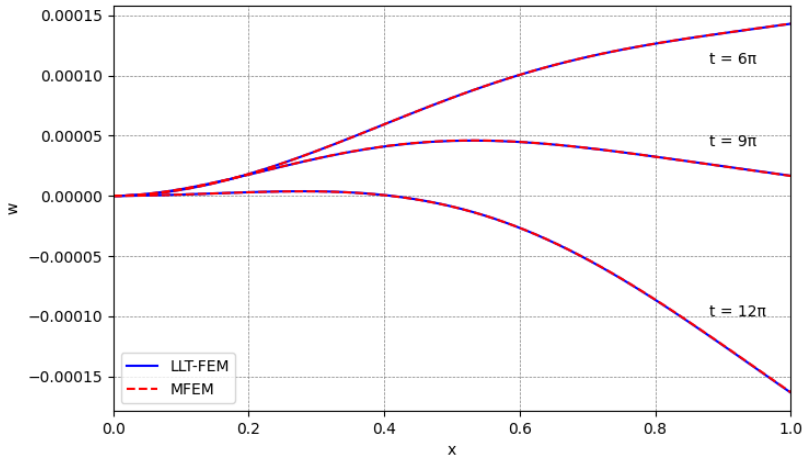

(a) Transverse displacement of the cantilever LLT rod.

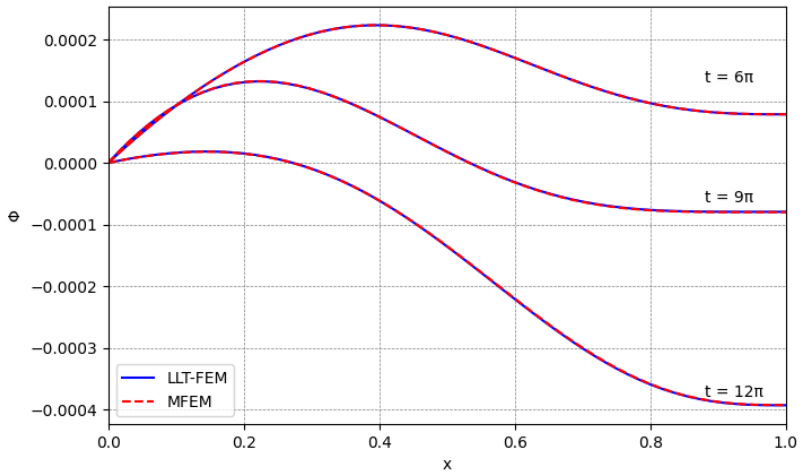

(b) Angle of rotation of the cantilever LLT rod.

Figure 5.1: Comparison of forced vibrations of the LLT cantilever rod with the linear Timoshenko beam using mixed finite element method, with $\alpha = 4800$, $\gamma = 0.25$ and $c = 0.001$.

As was mentioned in Remark 1.2.2, the value of α determines the length versus depth ratio of the beam. We investigate how a change in α changes the shape of the LLT rod. Suppose the value of α is doubled in the problem considered above, i.e. $\alpha = 9600$, so a more slender rod is considered. The resulting plots of applying the LLT-FEM algorithm are given in Figure 5.2, together with the results obtained for the linear model when using the mixed

finite element method. The resulting plots are quite different from those in Figure 5.1. For both w and ϕ, the values are much larger. For the cases $t = 6\pi$ and $t = 9\pi$, the plots of w slant upwards much more for a larger α. This indicates that more angular deformation takes place for a more slender rod, as would be expected. Further, for $t = 6\pi$ for example, the variation in values of ϕ is much larger. Thus we can see that changing the value of α significantly changes the shape of the LLT rod. The comparison with the mixed finite element approximation shows once more that the results coincide between the two methods.

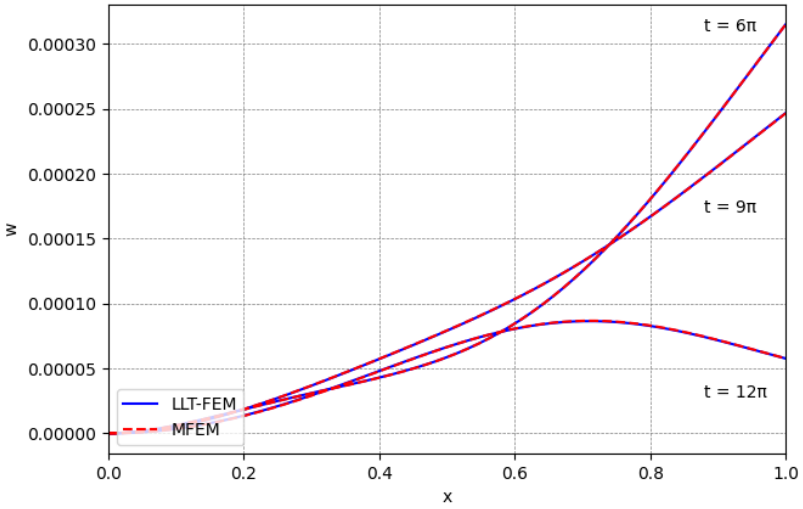

(a) Transverse displacement of the cantilever LLT rod.

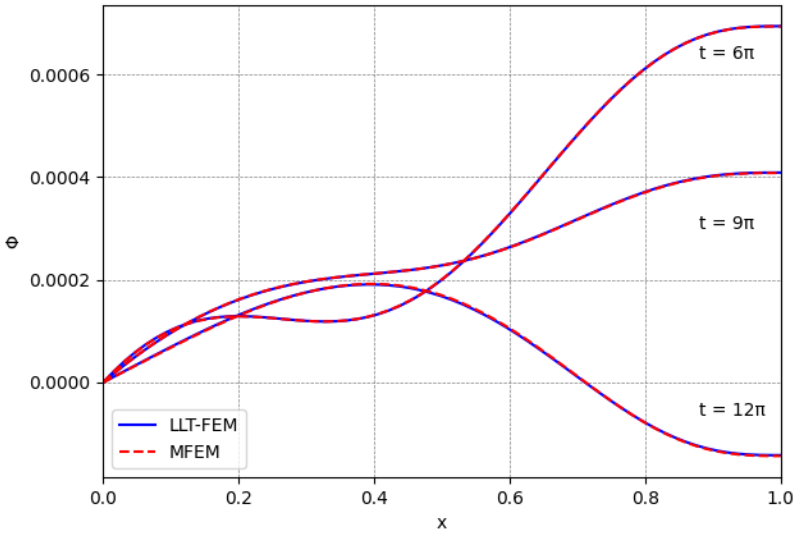

(b) Angle of rotation of the cantilever LLT rod.

Figure 5.2: Comparison of forced vibrations of the LLT cantilever rod with the linear Timoshenko beam using mixed finite element method, with $\alpha = 9600$, $\gamma = 0.25$ and $c = 0.001$.

5.4.3 Oscillations of the compressed LLT rod

In this section, we consider another example of the pinned-pinned LLT rod. In the previous sections, the assumption was that the distance between the two endpoints of the beam was equal to the length of the undeformed beam. This may not be the case in applications, where the beam could be under tension or compressed. In this section we consider the latter case, where the endpoint of the beam where $x = 1$ is initially displaced to the left by a small distance $d > 0$.

As such, the initial condition (5.4.1) becomes

$$u(x, 0) = -dx.$$

Additionally, it is assumed that d is small enough that the initial conditions (5.4.2)-(5.4.4) can still be used. We consider the case where $P_1 = P_2 = 0$.

As mentioned in [DLV22], the boundary condition

$$u(1,t) = -d \tag{5.4.5}$$

is sufficient to model the compressed beam. Note that as a result, slight adjustments need to be made to the variational forms in Sections 1.4.2 and to the algorithm in Section 5.3. The main changes are highlighted below.

Recall the classes of test functions $T_P[0,1]$ and $T_C[0,1]$ and the variational problem LLTV-P defined in Section 1.4.2. Note that since $d > 0$, the boundary condition (5.4.5) implies that u is no longer in $T_P[0,1]$, and we instead consider a space of trial functions. Define

$$T_E[0,1] = \left\{ y \in C^1[0,1] : y(0) = 0 \right\}.$$

Then we arrive at the following variational problem.

Problem LLTV-PC

Find $\langle u, w, \phi \rangle$ such that for each $t > 0$, $u(\cdot,t) \in T_E[0,1]$, $w(\cdot,t) \in T_P[0,1]$, $\phi(\cdot,t) \in C^1[0,1]$, $u(1,t) = -d$ and the equations in (1.4.17) hold for all $\langle v, z, \psi \rangle \in T_P[0,1] \times T_P[0,1] \times C^1[0,1]$.

In addition to S_0^h, S_1^h and S_2^h defined in Section 5.3, we also define $S_E^h = span\left\{\delta_1, \delta_2, \ldots, \delta_n\right\}$. Then we can write the problem as follows:
Find $u^h \in S_E^h$, $w^h \in S_2^h$ and $\phi^h \in S_0^h$ such that for each $t > 0$, $u^h(1) = -d$ and Equations (5.3.1) - (5.3.3) hold for all $v, z \in S_2^h$ and $\psi \in S_0^h$, where $F_1^h, F_2^h \in S_0^h$.

For this new problem, some additional notation is required. Denote

$$T_E^h \bar{x} = \sum_{i=1}^{n} x_i \delta_i \in S_1^h \text{ for any } \bar{x} \in \mathbb{R}^n$$

and

$$A_e = [A_{ij}] \text{ for } i = 0, 1, \ldots, n, j = 1, 2, \ldots, n,$$
$$A_f = [A_{ij}] \text{ for } i = 1, 2, \ldots, n-1, j = 1, 2, \ldots, n.$$

Remark 5.4.1. The definitions of $T_E[0,1]$, S_E^h and T_E^h are the same as those of $T_P[0,1]$, S_1^h and T_1^h defined above respectively, but are kept separate here to avoid confusion with the cantilever case.

Using integration by parts and properties of the basis functions, Equation (5.3.4) in this case is

$$\int_0^1 g_u^h(\cdot,t)\delta_i = u^h(1,t)\delta_i(1) - \int_0^1 u^h(\cdot,t)\delta_i' \text{ for } i = 0,1,\ldots,n.$$

Note that here $\bar{u}(t) = \left(T_E^h\right)^{-1} u^h(t)$.

Then we can calculate $\bar{g}_u(t) = \left(T^h\right)^{-1} g_u^h(t)$ from

$$M\bar{g}_u(t) = -L_e^*\bar{u}(t)$$

where $L_{ij}^* = L_{ij}$ but $L_{nn}^* = L_{nn} - 1$.

Note that since $\bar{u}_n(t) = -d$, we can rewrite this system as

$$M\bar{g}_u(t) = -L_d^*\tilde{u}(t) + d[L_e^*]_n$$

where L_d is defined as before, $\tilde{u}_i(t) = \bar{u}_i(t)$ for $i = 1,2,\ldots,n-1$ and $[L_e^*]_n$ denotes the nth column of L_e^*.

Similarly, the first equation of (5.3.15) becomes

$$M_f\bar{u}'' = -\bar{G}_1 + \bar{P}_1,$$

and as a result, the first equation of the central difference scheme is

$$\frac{1}{\delta t^2}M_f\left[\bar{u}_{k+1} - 2\bar{u}_k + \bar{u}_{k-1}\right] = -\bar{G}_1 + \bar{P}_1.$$

Since $\bar{u}_n(t_k) = -d$ for each k, this can be rewritten as

$$\frac{1}{\delta t^2}M_2\left[\tilde{u}_{k+1} - 2\tilde{u}_k + \tilde{u}_{k-1}\right] + \frac{1}{\delta t^2}[M_f]_n\left[d - 2d + d\right] = -\bar{G}_1 + \bar{P}_1,$$

where M_2 is defined as before, $\tilde{u}_i(t_k) = \bar{u}_i(t_k)$ for $i = 1,2,\ldots,n-1$ and $[M_f]_n$ denotes the nth column of M_f.

This of course just simplifies to

$$\frac{1}{\delta t^2}M_2\left[\tilde{u}_{k+1} - 2\tilde{u}_k + \tilde{u}_{k-1}\right] = -\bar{G}_1 + \bar{P}_1.$$

The rest of the algorithm remains exactly the same.

Now, it was shown in [VDL21] that for the adapted linear Timoshenko model with pinned-pinned boundary conditions and an axial load S, there is a critical load at which the corresponding nonlinear model yields a buckled state, and was calculated to be $S_{crit} = -\dfrac{\pi^2}{\pi^2 + \beta}$. Then a critical value, d_{crit} can be calculated from $d_{crit} = -\gamma S_{crit}$. In [DLV22] it was shown that for the case where $\alpha = 1200$, the critical value was $d_{crit} = 0.00796$.

Figure 5.3 illustrates the displacement at the midpoint of the compressed beam over a period of time, obtained by applying this altered algorithm, for various values of d. The results agree with those presented in [DLV22]. As noted by the authors, there seems to be a critical compression value, denoted d_0, for the LLT rod, and for values $d > d_0$, the rod exhibits buckled states, which depend on the value of d. Note that for $d > d_0$, the oscillations of the midpoint are no longer around $w = 0$, as was the case when $d < d_0$. Further, the numerical results indicate that the critical value d_0 here differs from the value d_{crit} calculated for the adapted linear model mentioned above.

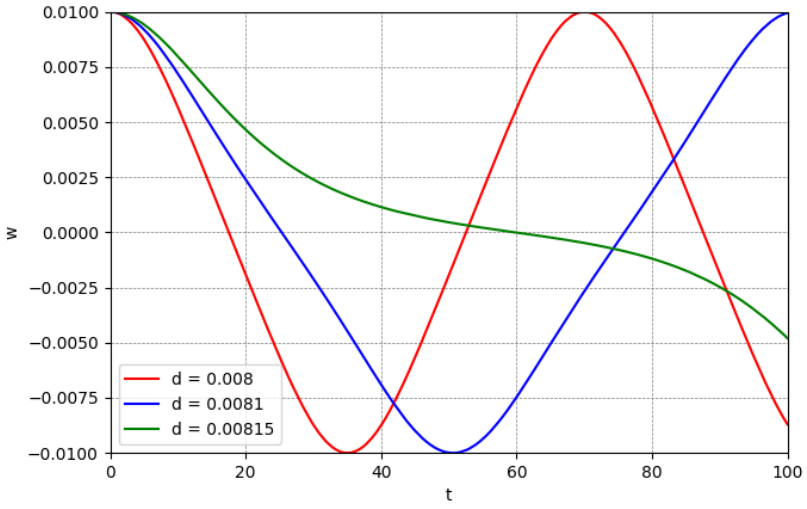

(a) Displacement w at the midpoint, with $\alpha = 1200$ and $d < d_0$.

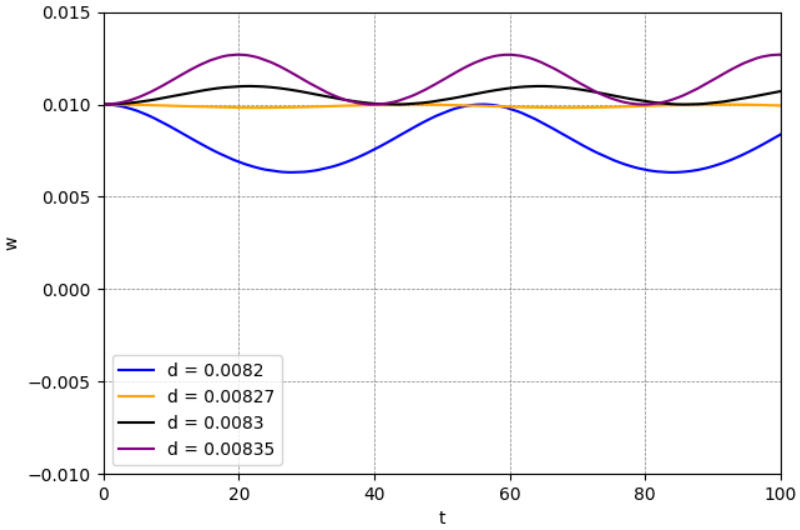

(b) Displacement w at the midpoint, with $\alpha = 1200$ and $d > d_0$.

Figure 5.3: Oscillations of the displacement w at the midpoint for the compressed LLT rod, with $\alpha = 1200$.

As mentioned above, the critical value d_{crit} for the adapted linear Timoshenko model is calculated using γ and β. Since $\beta = \gamma\alpha$, a change in α would affect the value of d_{crit}. In Section 5.4.2, it was reiterated that the value of α determines the length versus depth ratio of the beam, and it was investigated how an increase in α affected the displacement and angle of rotation of the cantilever LLT beam. It is interesting, then, to investigate how a change in the slenderness of the compressed beam affects its buckled state.

For this investigation, $\alpha = 2400$ is considered (i.e. α is doubled), and $\gamma = 0.25$ remains as before. Then $\beta = \gamma\alpha = 600$, and as a result $d_{crit} = -\gamma\left(-\frac{\pi^2}{\pi^2+\beta}\right) \approx 0.00405$ for the adapted linear model. Figure 5.4 illustrates the displacements of the midpoint of the compressed rod obtained using the algorithm described above, for various values of d around this critical value, to investigate the buckled states of the more slender beam. The shapes of the graphs are similar to those observed for $\alpha = 1200$ above, but of course for smaller values of d. Notice that, as was the case above, the oscillations of the midpoint are no longer around $w = 0$, and the critical value d_0 here is larger than that of the associated adapted

linear model. These numerical results confirm that for a more slender beam, the critical value at which buckled states occur is still close to that approximated for the adapted linear model, but is smaller than that of a thicker beam of the same length.

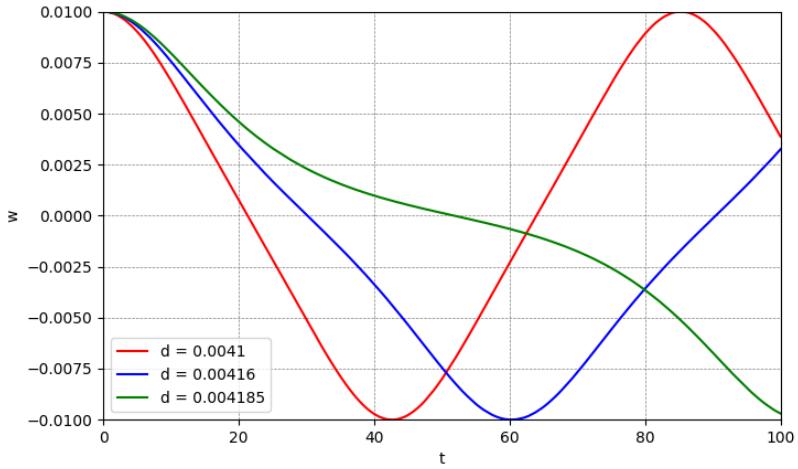

(a) Displacement w at the midpoint, with $\alpha = 2400$ and $d < d_0$.

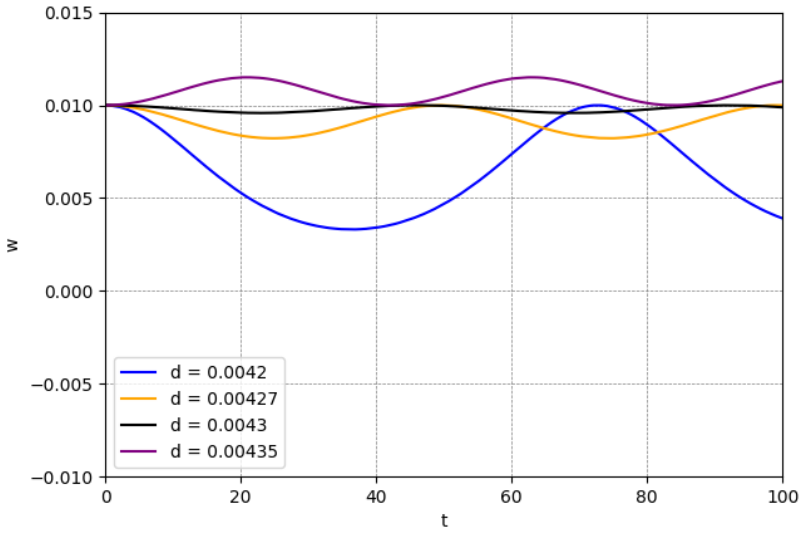

(b) Displacement w at the midpoint, with $\alpha = 2400$ and $d > d_0$.

Figure 5.4: Oscillations of the displacement w at the midpoint for the compressed LLT rod, with $\alpha = 2400$.

Chapter 6

A Local Linear Rayleigh Model

6.1 Introduction

The derivation of the locally linear Timoshenko beam model was presented in Chapter 5. It is interesting, then, to see if similar ideas can be used to derive a locally linear Rayleigh or Euler-Bernoulli model. In Section 1.3, the original linear Rayleigh beam model, of which the linear Euler-Bernoulli model is a special case, was derived from the Timoshenko beam model, under specific assumptions. In Section 6.2 below, a locally linear Rayleigh model is derived, and compared to the one given in [HT12]. The same ideas as in Section 5.2 were followed, as opposed to the approach presented in [HT12], which is to use the total energy of the system, and Hamilton's principle.

6.2 The Local Linear Rayleigh rod model

The derivation of the equations of motion is exactly the same as in Section 5.2.2.

Recall the resulting Equations (5.2.12) and (5.2.13):

$$\rho A \partial_t^2 \bar{r}_0 = \partial_x \bar{F} + \bar{P}, \tag{5.2.12}$$

$$\rho I \partial_t^2 \phi \bar{e}_3 = \partial_x \bar{r}_0 \times \bar{F} + \partial_x \bar{M}. \tag{5.2.13}$$

Note that for the Rayleigh and Euler-Bernoulli beam models, the assumption is that cross sections remain plane after deformation; that is, $\theta = \phi$.

For the constitutive equations, we again use

$$F_1 = S\cos\theta - V\sin\theta,$$

$$F_2 = S\sin\theta + V\cos\theta.$$

The following constitutive equation is similar to the one used in Section 1.3:

$$M = M_3 = EI\partial_x\theta^2.$$

Recall the definitions of $\{\bar{e}_1, \bar{e}_2, \bar{e}_3\}$, θ, ϕ and $\bar{e}_y$ and $\bar{e}_x$ from Section 5.2.2.

Additionally, we had

$$\bar{e}_T(x,t) = \cos\left(\theta(x,t)\right)\bar{e}_1 + \sin\left(\theta(x,t)\right)\bar{e}_2.$$

So let

$$\bar{e}_\theta(x,t) = -\sin\left(\theta(x,t)\right)\bar{e}_1 + \cos\left(\theta(x,t)\right)\bar{e}_2.$$

Then we have the following two lemmas.

Lemma 6.2.1. Consider $\bar{e}_T$ and $\bar{e}_\theta$ as defined above. We have the following results:

$$\partial_x \bar{e}_T = \partial_x\theta\bar{e}_\theta, \tag{6.2.1}$$

$$\partial_x \bar{e}_\theta = -\partial_x\theta\bar{e}_T, \tag{6.2.2}$$

$$\partial_t \bar{e}_T = \partial_t\theta\bar{e}_\theta, \text{ and} \tag{6.2.3}$$

$$\partial_t \bar{e}_\theta = -\partial_t\theta\bar{e}_T. \tag{6.2.4}$$

Proof. We prove the first equation. The other three equations' proofs follow similarly.

We have from the sum and chain rules for derivatives that

$$\begin{aligned}\partial_x \bar{e}_T &= \partial_x \left(\cos\left(\theta(x,t)\right)\bar{e}_1 + \sin\left(\theta(x,t)\right)\bar{e}_2\right)\\ &= -\sin\left(\theta(x,t)\right)\partial_x\theta(x,t)\bar{e}_1 + \cos\left(\theta(x,t)\right)\partial_x\theta(x,t)\bar{e}_2\\ &= \partial_x\theta(x,t)\left(-\sin\left(\theta(x,t)\right)\bar{e}_1 + \cos\left(\theta(x,t)\right)\bar{e}_2\right)\\ &= \partial_x\theta(x,t)\bar{e}_\theta \text{ for each } x,t.\end{aligned}$$

□

Lemma 6.2.2. Consider $\bar{e}_T$ and $\bar{e}_\theta$ as defined above. We have the following results:

$$\partial_x^3\bar{e}_T = \partial_x^3\theta\bar{e}_\theta - \partial_x^2\theta\partial_x\theta\bar{e}_T - \partial_x(\partial_x\theta)^2\bar{e}_T - (\partial_x\theta)^2\partial_x\bar{e}_T, \text{ and}$$

$$\partial_x\partial_t^2\bar{e}_T = \partial_x\partial_t^2\theta\bar{e}_\theta - \partial_t^2\theta\partial_x\theta\bar{e}_T - (\partial_t\theta)^2\partial_x\bar{e}_T - \partial_x(\partial_t\theta)^2\bar{e}_T.$$

Proof. We use Lemma 6.2.1 for both derivations.

For the first equation, note that

$$\begin{aligned}\partial_x^2\bar{e}_T &= \partial_x^2\theta\bar{e}_\theta + \partial_x\theta\partial_x\bar{e}_\theta\\ &= \partial_x^2\theta\bar{e}_\theta - (\partial_x\theta)^2\bar{e}_T.\end{aligned}$$

Then

$$\begin{aligned}\partial_x^3\bar{e}_T &= \partial_x^3\theta\bar{e}_\theta + \partial_x^2\theta\partial_x\bar{e}_\theta - \partial_x(\partial_x\theta)^2\bar{e}_T - (\partial_x\theta)^2\partial_x\bar{e}_T\\ &= \partial_x^3\theta\bar{e}_\theta - \partial_x^2\theta\partial_x\theta\bar{e}_T - \partial_x(\partial_x\theta)^2\bar{e}_T - (\partial_x\theta)^2\partial_x\bar{e}_T.\end{aligned}$$

For the second equation, we have that

$$\begin{aligned}\partial_x\partial_t^2\bar{e}_T &= (\partial_x\partial_t^2\theta)\bar{e}_\theta + (\partial_t^2\theta)\partial_x\bar{e}_\theta - (\partial_t\theta)^2\partial_x\bar{e}_T - \partial_x(\partial_t\theta)^2\bar{e}_T\\ &= \partial_x\partial_t^2\theta\bar{e}_\theta - \partial_t^2\theta\partial_x\theta\bar{e}_T - (\partial_t\theta)^2\partial_x\bar{e}_T - \partial_x(\partial_t\theta)^2\bar{e}_T.\end{aligned}$$

□

Finally, we also assume in this case that there is no load, i.e. $\bar{P} = \bar{0}$.

Derivation of the Rayleigh Model

First note that

$$\begin{aligned}\bar{F} &= F_1\bar{e}_1 + F_2\bar{e}_2 \\ &= S\bar{e}_T + V\bar{e}_\theta.\end{aligned}$$

For convenience, we denote

$$\bar{e}_T = \frac{\partial_x \bar{r}_0}{||\partial_x \bar{r}_0||} = \zeta \partial_x \bar{r}_0,$$

where $\zeta = ||\partial_x \bar{r}_0||^{-1}$.

Then, since $\bar{e}_T \times \bar{e}_\theta = \bar{e}_3$,

$$\begin{aligned}\partial_x \bar{r}_0 \times \bar{F} &= \frac{1}{\zeta}\bar{e}_T \times (S\bar{e}_T + V\bar{e}_\theta) \\ &= \frac{1}{\zeta}V\bar{e}_3.\end{aligned}$$

Hence

$$\rho I \partial_t^2 \phi \bar{e}_3 = \frac{1}{\zeta}V\bar{e}_3 + \partial_x M_3 \bar{e}_3 \text{ from Equation (5.2.13)}, \tag{6.2.5}$$

and thus

$$\begin{aligned}\rho I \partial_t^2 \theta &= \frac{1}{\zeta}V + \partial_x M \\ &= \frac{1}{\zeta}V + EI\partial_x^2\theta,\end{aligned} \tag{6.2.6}$$

since $\theta = \phi$ and $M = M_3 = EI\partial_x^2\theta$.

It follows from Equation (5.2.12), Lemma 6.2.1 and Equation (6.2.6) that

$$\begin{aligned}
\rho A\partial_t^2\bar{r}_0 &= \partial_x\bar{F} \\
&= \partial_x(S\bar{e}_T) + (\partial_x V)\bar{e}_\theta + V\partial_x\bar{e}_\theta \\
&= \partial_x(S\bar{e}_T) + (\partial_x V)\bar{e}_\theta - V\partial_x\theta\bar{e}_T \\
&= \partial_x(S\bar{e}_T) - \left(\left[\rho\zeta I\partial_t^2\theta - \zeta EI\partial_x^2\theta\right]\partial_x\theta\right)\bar{e}_T \\
&+ \left(\left[\rho\zeta I\partial_x\partial_t^2\theta - \zeta EI\partial_x^3\theta\right]\right)\bar{e}_\theta \\
&= \partial_x(S\bar{e}_T) + \left(-\rho\zeta I\partial_t^2\theta\partial_x\theta + \zeta EI\partial_x^2\theta\partial_x\theta\right)\bar{e}_T \\
&+ \left(\rho\zeta I\partial_x\partial_t^2\theta - \zeta EI\partial_x^3\theta\right)\bar{e}_\theta. \qquad (6.2.7)
\end{aligned}$$

Now, we simplify the expressions on the right-hand side of Equation (6.2.7) in the following steps.

It follows from Lemma 6.2.2 that

$$\begin{aligned}
\zeta EI\partial_x^2\theta\partial_x\theta\bar{e}_T - \zeta EI\partial_x^3\theta\bar{e}_\theta &= \zeta EI\partial_x^2\theta\partial_x\theta\bar{e}_T - \zeta EI\left(\partial_x^3\bar{e}_T + \partial_x^2\theta\partial_x\theta\bar{e}_T + \partial_x(\partial_x\theta)^2\bar{e}_T + (\partial_x\theta)^2\partial_x\bar{e}_T\right) \\
&= -\zeta EI\partial_x^3\bar{e}_T - \zeta EI\partial_x(\partial_x\theta)^2\bar{e}_T - \zeta EI(\partial_x\theta)^2\partial_x\bar{e}_T.
\end{aligned}$$

It furthermore follows from Lemma 6.2.2 that

$$\begin{aligned}
-\rho\zeta I\partial_t^2\theta\partial_x\theta\bar{e}_T + \rho\zeta I\partial_x\partial_t^2\theta\bar{e}_\theta &= -\rho\zeta I\partial_t^2\theta\partial_x\theta\bar{e}_T + \rho\zeta I\left(\partial_x\partial_t^2\bar{e}_T + (\partial_t^2\theta)\partial_x\theta\bar{e}_T\right. \\
&\left.+(\partial_t\theta)^2\partial_x\bar{e}_T + \partial_x(\partial_t\theta)^2\bar{e}_T\right) \\
&= \rho\zeta I\partial_x\partial_t^2\bar{e}_T + \rho\zeta I\partial_x(\partial_t\theta)^2\bar{e}_T + \rho\zeta I(\partial_t\theta)^2\partial_x\bar{e}_T.
\end{aligned}$$

Now let

$$\mu = -\zeta EI(\partial_x\theta)^2 + \rho\zeta I(\partial_t\theta)^2.$$

Then we have that

$$-\zeta EI\partial_x(\partial_x\theta)^2\bar{e}_T + \rho\zeta I\partial_x(\partial_t\theta)^2\bar{e}_T = (\partial_x\mu)\bar{e}_T$$

and

$$-\zeta EI(\partial_x\theta)^2\partial_x\bar{e}_T + \rho\zeta I(\partial_t\theta)^2\partial_x\bar{e}_T = \mu(\partial_x\bar{e}_T).$$

Finally, combining Equation (6.2.7) with the results above, we have

$$\begin{aligned}\rho A\partial_t^2\bar{r}_0 &= \partial_x(S\bar{e}_T) - \zeta EI\partial_x^3\bar{e}_T + \rho\zeta I\partial_x\partial_t^2\bar{e}_T + (\partial_x\mu)\bar{e}_T + \mu(\partial_x\bar{e}_T)\\ &= \zeta\partial_x(C\partial_x\bar{r}_0) - \zeta^2 EI\partial_x^4\bar{r}_0 + \rho\zeta^2 I\partial_t^2\partial_x^2\bar{r}_0\end{aligned}$$

where $C = S + \mu$.

Dimensionless form

For the dimensionless form, let

$$\tau = \frac{t}{T}, \xi = \frac{x}{\ell}, r_1^*(\xi,\tau) = \frac{r_1(x,t)}{\ell}, r_2^*(\xi,\tau) = \frac{r_2(x,t)}{\ell}, \text{ and } C^*(\xi,\tau) = C(x,t),$$

and denote $\bar{r}_0^* = r_1^*\bar{e}_1 + r_2^*\bar{e}_2$.

In this case a convenient choice for T is $T = \sqrt{\dfrac{\rho A\ell^4}{EI\zeta^2}}$. It then follows that

$$\partial_\tau^2\bar{r}_0^* = \frac{T^2}{\rho A\ell}\partial_\xi(C^*\partial_\xi\bar{r}_0^*) - \frac{\zeta^2 EIT^2}{\rho A\ell^4}\partial_\xi^4\bar{r}_0^* + \frac{\zeta^2 I}{\ell^2 A}\partial_t^2\partial_\xi^2\bar{r}_0^*.$$

In original notation, the equation of motion is then

$$\partial_t^2\bar{r}_0 = \delta\partial_x(C\partial_x\bar{r}_0) - \partial_x^4\bar{r}_0 + \gamma\partial_t^2\partial_x^2\bar{r}_0,$$

where $\gamma = \dfrac{\zeta^2 I}{\ell^2 A}$ and $\delta = \dfrac{\ell^3}{EI\zeta^2}$.

Remark 6.2.1. Note that if the rotary inertia term $\gamma\partial_t^2\partial_x^2\bar{r}_0$ is ignored, then the above equation is the equation of motion for the non-linear Euler-Bernoulli rod.

6.3 Non-linear Rayleigh model of Hegarty and Taylor

The derivation of the non-linear Rayleigh model in Section 6.2 was done using the same approach as for the LLT model in Chapter 5. The approach by Hegarty and Taylor [HT12] was to derive the total energy of the beam, and use Hamilton's principle. Using the notation used throughout the dissertation, their model is as follows.

The equation of motion is

$$\partial_t^2 \bar{r} = \partial_x \left(\tau \partial_x \bar{r}\right) - \partial_x^4 \bar{r} + \gamma \partial_t^2 \partial_x^2 \bar{r}, \tag{6.3.1}$$

and the boundary conditions are

$$\bar{r}(0,t) = (0,0),\ \partial_x \bar{r}(0,t) = (1,0) \text{ and} \tag{6.3.2}$$

$$\gamma \partial_t^2 \partial_x^2 \bar{r}(1,t) + \tau \partial_x \bar{r}(1,t) - \partial_x^3 \bar{r}(1,t) = -\alpha \partial_t \bar{r}(1,t),\ \partial_x^2 \bar{r}(1,t) = \beta \partial_t \partial_x \bar{r}(1,t). \tag{6.3.3}$$

The initial conditions are

$$\bar{r}(x,0) = \bar{r}_c(x) \text{ and } \partial_x \bar{r}(x,0) = \bar{r}_d(x) \tag{6.3.4}$$

for some functions $\bar{r}_c$ and $\bar{r}_d$.

The model appears to be almost the same as the one derived in Section 6.2. Note that what is denoted as r in [HT12] corresponds to the unit tangent vector $\bar{e}_T$, the normalised vector of what we defined as $\bar{r}_0$. Thus the dimensionless constants α, β and γ above do not necessarily correspond to the same values as defined in previous sections. Further, note that according to Equation (2.1) in [HT12], the value of T chosen to derive the dimensionless form is $T = \sqrt{\dfrac{\rho \ell^4}{EI}}$, which differs slightly from what we derived. Finally, note that in Hegarty and Taylor's model, the axial force, denoted by τ, appears to be independent of θ. This could not be achieved in our model, where the corresponding term was $\partial_x \left(C \partial_x \bar{r}\right)$, and $C = S + \mu$ clearly still depends on θ, since μ is a function of θ.

Based on their model, the authors derived a number of existence results. For completeness, and in light of existence theory being a fundamental part of this dissertation, their results are given below. The detailed proofs are in [HT12], but are beyond the scope of the dissertation. Note that $\bar{N}_0$ below denotes the initial condition for the normal vector at (x,t), which corresponds to our $\bar{e}_\theta$, and E_0 denotes the total energy of the beam.

Theorem 6.3.1. Let $\alpha, \beta \geq 0$, $\gamma > 0$, and $\bar{r}_c \in H^4((0,1);\mathbb{R}^2)$, $\bar{r}_d \in H^3((0,1);\mathbb{R}^2)$ satisfy

$$\bar{r}_c(0) = \bar{r}_d(0) = \partial_x \bar{r}_d(0) = (0,0),\ \partial_x \bar{r}_c = (1,0),$$

$$\partial_x^2 \bar{r}_c(1) = -\beta \partial_x \bar{r}_d(1), \ \ \left(\gamma \partial_x^2 \bar{r}_d(1) - \alpha\beta \bar{r}_d(1) + \beta \partial_x^3 \bar{r}_c(t)\right) \cdot \bar{N}_0(1) = 0, \text{ and}$$

$$\partial_x \bar{r}_c \cdot \partial_x \bar{r}_c = 1, \ \partial_x \bar{r}_c \cdot \partial_x \bar{r}_d = 0.$$

Then the non-linear Rayleigh model (6.3.1)-(6.3.4) has a unique global classical solution

$$\bar{r} \in C^2((0,\infty); H^2((0,1),\mathbb{R}^2)) \cap C^1((0,\infty); H^3((0,1);\mathbb{R}^2)) \cap C((0,\infty); H^4((0,1);\mathbb{R}^2)).$$

An existence result was also obtained for the non-linear Euler-Bernoulli model; that is, the model (6.3.1)-(6.3.4) with $\gamma = 0$.

Theorem 6.3.2. Let $\alpha > 0$, $\beta \geq 0$, and $\bar{r}_c \in H^4((0,1);\mathbb{R}^2)$, $\bar{r}_d \in H^2((0,1);\mathbb{R}^2)$ satisfy

$$\bar{r}_c(0) = \bar{r}_d(0) = \partial_x \bar{r}_d(0) = (0,0), \ \partial_x \bar{r}_c = (1,0),$$

$$\partial_x^2 \bar{r}_c(1) = -\beta \partial_x \bar{r}_d(1), \ \ \left(\alpha \bar{r}_d(1) - \partial_x^3 \bar{r}_c(1)\right) \cdot \bar{N}_0(1) = 0, \text{ and}$$

$$\partial_x \bar{r}_c \cdot \partial_x \bar{r}_c = 1, \ \partial_x \bar{r}_c \cdot \partial_x \bar{r}_d = 0.$$

For any $T_0 > 0$ there exists a positive constant K_0 such that if $E_0(0) < K_0$, then the non-linear Euler-Bernoulli model (6.3.1)-(6.3.4) with $\gamma = 0$ has a local classical solution

$$\bar{r} \in L^\infty((0,T_0); H^4((0,1);\mathbb{R}^2)) \cap W^{1,\infty}((0,T_0); H^2((0,1);\mathbb{R}^2)) \cap W^{2,\infty}((0,T_0); L^2((0,1);\mathbb{R}^1)).$$

Chapter 7

Conclusion

7.1 Overview

Mathematical models for the vibration of flexible systems are of great importance in applied mathematics and engineering. To approximate solutions to these systems numerically, the finite element method (FEM) is an accurate and user-friendly approach. In order to apply such numerical methods, existence of solutions, as well as convergence of the method, must be considered.

This dissertation is mainly a literature study on models (both linear and "locally linear") for the vibration of flexible structures. The literature study includes work on existence theory and convergence theory of finite element approximations. For the latter, model problems are written in variational form. The main existence results for general linear second order hyperbolic type problems from the articles of van Rensburg and Stapelberg (2019) and van Rensburg and van der Merwe (2002) are written in terms of bilinear forms, making them easy to apply to such problems. This theory goes hand in hand with the convergence theory of Stapelberg and van Rensburg (2017) and of Basson and van Rensburg (2013), which takes advantage of the already existing results obtained from the existence theory to derive convergence results. A part of this dissertation is the application of this theory to well-known,

simple mathematical models for real-world applications.

As mentioned, the FEM is particularly convenient for the types of problems studied in the above literature. An objective of this dissertation was thus to illustrate convergence of the method to problems for which the existence of solutions has already been established. A further focus was to study the locally linear model in the article by van Rensburg, du Toit and Labuschagne (2021) and a subsequent currently unpublished work by du Toit, Labuschagne and van der Merwe (2022), where a new model for two-dimensional motion of a rod, the Locally Linear Timoshenko (LLT) model, was developed, and the FEM was used to derive an algorithm to approximate solutions.

An initial aim of the research was to investigate linear models. In the first chapter of the dissertation, several second-order hyperbolic type problems are introduced, which are used throughout the dissertation to illustrate application of the theory and the FEM. The linear Timoshenko beam model was presented, and subsequently the Rayleigh and Euler-Bernoulli models, which can both be derived from the former model. Further, the LLT model (mentioned above) was introduced, as well as several of its special cases, one of which was the original linear Timoshenko model. Finally, the multi-dimensional wave equation was presented. For both the theory and application of the FEM, variational forms for these problems are convenient, and were derived in this chapter.

In the following chapter, the existence theory from the articles by van der Merwe and van Rensburg (2002), and by van Rensburg and Stapelberg (2019), mentioned above, was studied and compared. The theory from these articles focused on deriving existence results for the general linear second-order hyperbolic type problem written in terms of bilinear forms. In the former article, two of the bilinear forms are symmetric; in the latter, only one is assumed to be symmetric. The chapter highlights the main results, differences and similarities between the two articles. Finally, the main existence theorem was applied to the linear Timoshenko model and the multi-dimensional wave equation, to demonstrate use of the theory.

The introduction of the existence theory is followed by a chapter on the convergence theory for the same type of problem, with general damping, in the Stapelberg and van Rensburg

(2017) article, which makes use of the results already obtained in the existence theory. The theory from the article was presented and proved, and where appropriate, comparisons were made to another article by Basson and van Rensburg (2013), where the same model problem was considered, but with weak damping.

Chapter 4 of the dissertation is dedicated to the implementation and convergence analysis of the finite element method to model problems. In particular, a finite element algorithm for the Timoshenko model and the two-dimensional wave equation on a rectangle, for which existence was proved in a previous chapter, were derived.

For the Timoshenko model, both pinned-pinned and cantilever boundary conditions were considered. In some applications, as was the case for this model, the standard FEM is not appropriate, and may lead to poor numerical results. The mixed FEM proves to be an effective alternative, and was therefore used in the numerical approximations for the Timoshenko model. For the wave equation, Dirichlet boundary conditions were used, and the standard FEM was applied with rectangle and then triangle elements. It was observed that as the number of elements and time steps in the algorithm are increased, the approximations converged to the exact solution. It was also noted that the relative errors were smaller for the case of rectangle elements, and hence rectangular elements appear to be sufficient for the approximation.

The LLT rod model takes up its own chapter. The derivations of the model and its finite element algorithm for pinned-pinned and cantilever boundary conditions are presented. Selected results from the currently unpublished article of du Toit, Labuschagne and van der Merwe (2022) were reproduced, namely small vibrations of the pinned-pinned LLT rod, the cantilever rod with a transverse load near the free endpoint, and the compressed LLT rod. The numerical results indicate pointwise convergence for the pinned-pinned rod. Further, comparison of the results obtained for the cantilever rod using the LLT finite element algorithm with those obtained using the mixed FEM showed that these two methods were in agreement. Investigation of the compressed rod showed that there is a critical value after which the rod exhibits buckled states. For the latter two cases, a brief investigation was

done on the effects of the slenderness of the rod on the numerical results.

Finally, a chapter is dedicated to a brief investigation into using the same ideas applied to obtain the LLT model, to obtain "locally linear" Rayleigh and Euler-Bernoulli rod models. The models are compared to those in [HT12], where existence results for these types of models are proved.

7.2 Accomplishments

This dissertation provides a detailed comparison between the articles on existence theory by van der Merwe and van Rensburg (2002), and by van Rensburg and Stapelberg (2019), for the general linear second-order hyperbolic type problems with weak and general damping respectively. The most noteworthy differences were in the preliminary assumption made on the boundedness of one of the bilinear forms, the proof that the linear operator defined was dense and closed in the Hilbert space, and the proof that the operator is an infinitesimal generator of a C_0 semigroup of contractions.

The results of the existence theory can be used to obtain convergence results. The article of Stapelberg and van Rensburg (2017) was studied and proofs given in detail. An interesting observation was that a proposition used to prove an important lemma in the article was found to be unnecessary, and a slightly milder result than the one obtained from the proposition was sufficient to prove the lemma. Differences between this article and the article by Basson and Van Rensburg (2013) were also included.

This dissertation also provides simple illustrative examples of applications of the existence and convergence theory from the literature, but also implementation and convergence of the FEM.

Further, some numerical results using a proposed FEM algorithm for the approximation of solutions of the LLT rod were replicated and confirmed. Being able to confirm these results is promising for the validity of the proposed algorithm, especially the results where

the LLT-FEM algorithm for small vibrations and the mixed FEM algorithm for the linear Timoshenko model are in agreement.

Finally, the ideas of the LLT model were used to derive a possible locally linear Euler-Bernoulli type model, which is new and not widely studied in the literature.

7.3 Future Work

The LLT rod model shows promising results for obtaining models for two-dimensional displacement using linear constitutive equations that are simple to use. Future investigations could include further investigation into extending this approach to obtain a locally linear Euler-Bernoulli model; in particular, if similar existence results to those in the article by Hegarty and Taylor (2012) can be achieved using the approaches considered in this dissertation. Further, an investigation could be taken into obtaining a finite element algorithm to approximate the solution of such a model.

Appendix A

Sobolev Spaces

This section provides some basic theory on weak derivatives and Sobolev spaces.

The one-dimensional case

Let $I = (a, b)$ be an open interval in $\mathbb{R}$. Denote $\bar{I} = [a, b]$. The space $L^2(a, b)$ is the space of all functions f such that f^2 is Lebesgue integrable on (a, b).

Definition (Support of a function)
The closure of the set $\{x \in I : f(x) \neq 0\}$ is called the support of the function f on I.

Notation

1. $C^m(I)$: The class of functions with continuous derivatives up to order m in I.
2. $C_0(I)$: The class of functions in $C(I)$ with support contained in I.
3. $C^\infty(I)$: The class of functions in $C^m(I)$ for all m.
4. $C_0^\infty(I)$: Functions in $C^\infty(I) \cap C_0(I)$.

Definition (Weak Derivative)
Let m be any natural number. Suppose $u \in L^2(I)$ and there exists a $v \in L^2(I)$ such that

$$(u, \phi^{(m)}) = (-1)^m (v, \phi) \text{ for each } \phi \in C_0^\infty(I).$$

Then v is called the m-th order weak derivative of u, and is denoted by $D^m u$.

Theorem A.0.1. The m-th order weak derivative $D^m u$ of u is uniquely determined.

Notation The set of functions with weak derivatives up to order m is denoted by $W^m(I)$.

Theorem A.0.2. $C^m(\bar{I}) \subset W^m(I)$ and if $u \in C^m(\bar{I})$, then $D^m u = u^{(m)}$.

Theorem A.0.3. $W^m(I)$ is a vector space.

Theorem A.0.4. The following are true.

1. If $u \in W^m(I)$ and $i, j \in \mathbb{N}$ such that $i + j \leq m$, then $D^i(D^j u) = D^{i+j} u$.
2. If $D^k u \in W^m(I)$, then $u \in W^{k+m}(I)$.

Definition. For functions u and v in $W^m(I)$, define

$$(u, v)_m = (u, v) + (Du, Dv) + \cdots + (D^m u, D^m v).$$

Theorem A.0.5. $(u, v)_m$ is an inner product for $W^m(I)$.

Definition. $||u||_m = (u, u)_m^{\frac{1}{2}}$ is a norm for $W^m(I)$.

Definition. The Sobolev Space $W^m(I)$ is the vector space $W^m(I)$ with inner product $(u, v)_m$.

Theorem A.0.6. The space $W^m(I)$ is complete.

Definition (The space $H^m(I)$)
$H^m(I)$ is the closure of $C^m(I)$ in $W^m(I)$ with respect to the form of $W^m(I)$.

Theorem A.0.7. $H^m(I)$ is a closed subspace of $W^m(I)$.

Theorem A.0.8. If $u \in W^m(I)$, then there exists a sequence (u_n) in $C^m(\bar{I})$ such that $||u - u_n||_m \to 0$ as $n \to \infty$.

Theorem A.0.9. $H^m(I) = W^m(I)$.

Remark A.0.1. The result of Theorem A.0.9 is not always true in higher dimensions.

The higher-dimensional case

Let Ω be an open subset of $\mathbb{R}^n$. Let $\bar{\Omega}$ denote the closure of Ω. The space $\mathcal{L}^2(\Omega)$ is the space of all functions f such that f^2 is Lebesgue integrable on Ω.

Definition (Support of a function)
The closure of the set $\{x \in \Omega : f(x) \neq 0\}$ is called the support of the function f on Ω.

Notation

1. $C^m(\Omega)$: The class of functions with continuous derivatives up to order m in $\bar{\Omega}$.
2. $C_0(\Omega)$: The class of functions in $C(\Omega)$ with support contained in Ω.
3. $C^\infty(\Omega)$: The class of functions in $C^m(\Omega)$ for all m.
4. $C_0^\infty(\Omega)$: Functions in $C^\infty(\Omega) \cap C_0(\Omega)$.

Notation Let n be any natural number.

$$\partial^\alpha = \partial_1^{\alpha_1}\partial_2^{\alpha_2}\dots\partial_n^{\alpha_n} \text{ and}$$
$$|\alpha| = \alpha_1 + \alpha_2 + \cdots + \alpha_n$$

Definition (Weak Derivative)
Suppose $u \in \mathcal{L}^2(\Omega)$ and there exists a $v \in \mathcal{L}^2(\Omega)$ such that

$$(u, \partial^\alpha \phi) = (-1)^{|\alpha|}(v, \phi) \text{ for each } \phi \in C_0^\infty(\Omega).$$

Then v is called the weak derivative $D^\alpha u$ of u.

Notation

The set of functions with weak derivatives of order $|\alpha| \leq m$ is denoted by $W^m(\Omega)$.

Theorem A.0.10. The set $W^m(\Omega)$ is a vector space.

Theorem A.0.11. The following are true.

1. If $u \in W^m(\Omega)$ and α_i and α_j are multi-indices such that $|\alpha_i| + |\alpha_j| \leq m$, then $D^{\alpha_i}(D^{\alpha_j}u) = D^{\alpha_i+\alpha_j}u$.

2. If $D^\alpha u \in W^m(\Omega)$ where $|\alpha| \leq k$, then $u \in W^{k+m}(\Omega)$.

Definition. For functions u and v in $W^m(\Omega)$, define $(u,v)_m = \sum_{|\alpha|\leq m}(D^\alpha u, D^\alpha v)$.

Theorem A.0.12. $(u,v)_m$ is an inner product for $W^m(\Omega)$.

Definition. $||u||_m = (u,u)_m^{\frac{1}{2}}$ is a norm for $W^m(\Omega)$.

Definition. The Sobolev Space $W^m(\Omega)$ is the vector space $W^m(\Omega)$ with inner product $(u,v)_m$.

Theorem A.0.13. The space $W^m(\Omega)$ is complete.

Theorem A.0.8 above states that a function $u \in W^m(I)$ can be approximated by functions in $C^m(\bar{I})$. In higher dimensions, restrictions on the set Ω are required. An example, Theorem 3 in Section 5.3.3 of [Eva97], is given below.

Definition. $\partial\Omega$ is C^k if for each point $x^0 \in \partial\Omega$ there exist $r > 0$ and a C^k function $\gamma : \mathbb{R}^{n-1} \to \mathbb{R}$ such that

$$\Omega \cap B(x^0, r) = \left\{x \in B(x^0, r) : x_n > \gamma(x_1, x_2, \ldots, x_{n-1})\right\}.$$

Theorem A.0.14. Suppose Ω is bounded and $\partial\Omega$ is C^1. If $u \in W^m(\Omega)$, then there exists a sequence (u_n) in $C^m(\bar{\Omega})$ such that $||u - u_n||_m \to 0$ as $n \to \infty$.

Bibliography

[AKS96] KT Andrews, KL Kuttler, and M Shillor. Second order evolution equations with dynamic boundary conditions. *Journal of mathematical analysis and applications*, 197(3):781–795, 1996.

[Arn81] DN Arnold. Discretization by finite elements of a model parameter dependent problem. *Numerische Mathematik*, 37(3):405–421, 1981.

[Bak76] GA Baker. Error estimates for finite element methods for second order hyperbolic equations. *SIAM journal on numerical analysis*, 13(4):564–576, 1976.

[BSV17] M Basson, B Stapelberg, and NFJ Van Rensburg. Error estimates for semi-discrete and fully discrete Galerkin finite element approximations of the general linear second-order hyperbolic equation. *Numerical Functional Analysis and Optimization*, 38(4):466–485, 2017.

[BV13] M Basson and NFJ Van Rensburg. Galerkin finite element approximation of general linear second order hyperbolic equations. *Numerical Functional Analysis and Optimization*, 34(9):976–1000, 2013.

[CH15] MH Cheng and TH Heaton. Simulating building motions using ratios of the building's natural frequencies and a Timoshenko beam model. *Earthquake Spectra*, 31(1):403–420, 2015.

[CJ99] MA Crisfield and G Jelenić. Objectivity of strain measures in the geometrically exact three-dimensional beam theory and its finite-element implementation. *Pro-*

ceedings of the Royal Society of London. Series A: Mathematical, Physical and Engineering Sciences, 455(1983):1125–1147, 1999.

[Cos09] E Cosserat. *Théorie des corps déformables*. Librairie Scientifique A. Hermann et Fils, 1909.

[DD20] B Deka and J Dutta. Finite element methods for non-fourier thermal wave model of bio heat transfer with an interface. *Journal of Applied Mathematics and Computing*, 62(1):701–724, 2020.

[DLV22] S Du Toit, M Labuschagne, and AJ Van der Merwe. Large displacements and rotations for a local linear elastic rod. Manuscript submitted for publication, 2022.

[DRS21] F Dadgar-Rad and S Sahraee. Large deformation analysis of fully incompressible hyperelastic curved beams. *Applied Mathematical Modelling*, 93:89–100, 2021.

[Dup73] T Dupont. L^2-estimates for Galerkin methods for second order hyperbolic equations. *SIAM journal on numerical analysis*, 10(5):880–889, 1973.

[ET14] Mahdi Ebrahimian and Maria I Todorovska. Wave propagation in a Timoshenko beam building model. *Journal of Engineering Mechanics*, 140(5), 2014.

[Eva97] LC Evans. *Partial differential equations*, volume 19. American Mathematical Soc., 1997.

[FL97] RF Fung and FY Lee. Dynamic analysis of the flexible rod of quick-return mechanism with time-dependent coefficients by the finite element method. *Journal of sound and vibration*, 202(2):187–201, 1997.

[FXX99] M Feng, XP Xie, and H Xiong. Semi-discrete and fully discrete partial projection finite element methods for the vibrating Timoshenko beam. *Journal of Computational Mathematics*, pages 353–368, 1999.

[Hod06] DH Hodges. *Nonlinear composite beam theory*. American Institute of Aeronautics and Astronautics, 2006.

[HT12] G Hegarty and S Taylor. Classical solutions of nonlinear beam equations: existence and stabilization. *SIAM Journal on Control and Optimization*, 50(2):703–719, 2012.

[II92] M Iura and T Iwakuma. Dynamic analysis of the planar Timoshenko beam with finite displacement. *Computers & structures*, 45(1):173–179, 1992.

[Inm94] DJ Inman. *Engineering vibration*. Prentice-Hall Inc., Englewood Cliffs, New Jersey, 1994.

[LA12] H Lang and M Arnold. Numerical aspects in the dynamic simulation of geometrically exact rods. *Applied Numerical Mathematics*, 62(10):1411–1427, 2012.

[LM72] JL Lions and E Magenes. *Nonhomogeneous Boundary Value Problems and Applications*, volume 1. Springer Verlag, 1972.

[LVV09] A Labuschagne, NFJ Van Rensburg, and AJ Van der Merwe. Comparison of linear beam theories. *Mathematical and Computer Modelling*, 49(1-2):20–30, 2009.

[MPW19] C Meier, A Popp, and WA Wall. Geometrically exact finite element formulations for slender beams: Kirchhoff–Love theory versus Simo–Reissner theory. *Archives of Computational Methods in Engineering*, 26(1):163–243, 2019.

[NSH17] TL Nguyen, C Sansour, and M Hjiaj. Long-term stable time integration scheme for dynamic analysis of planar geometrically exact Timoshenko beams. *Journal of Sound and Vibration*, 396:144–171, 2017.

[OR76] JT Oden and JN Reddy. *An introduction to the mathematical theory of finite elements*. John Wiley and Sons, 1976.

[Paz83] A Pazy. *Semigroups of linear operators and applications to partial differential equations*. New York: Springer, 1983.

[PR05] Y Pinchover and J Rubinstein. *An introduction to partial differential equations*, volume 10. Cambridge University Press, 2005.

[PRT14] P Pei, M A Rammaha, and D Toundykov. Global well-posedness and stability of semilinear Mindlin–Timoshenko system. *Journal of Mathematical Analysis and Applications*, 418(2):535–568, 2014.

[PTL19] G Piccardo, F Tubino, and A Luongo. Equivalent Timoshenko linear beam model for the static and dynamic analysis of tower buildings. *Applied Mathematical Modelling*, 71:77–95, 2019.

[Sem94] B Semper. Semi-discrete and fully discrete Galerkin methods for the vibrating Timoshenko beam. *Computer methods in applied mechanics and engineering*, 117(3-4):353–360, 1994.

[Sho77] RE Showalter. *Hilbert Space Methods for Partial Differential Equations*. Pitman, London, 1977.

[SNH15] C Sansour, TL Nguyen, and M Hjiaj. An energy-momentum method for in-plane geometrically exact Euler–Bernoulli beam dynamics. *International Journal for Numerical Methods in Engineering*, 102(2):99–134, 2015.

[SPS+22] A Sahraei, P Pezeshky, S Sasibut, F Rong, and M Mohareb. Finite element formulation for the dynamic analysis of shear deformable thin-walled beams. *Thin-Walled Structures*, 173, 2022.

[SR79] MH Sapir and EL Reiss. Dynamic buckling of a nonlinear Timoshenko beam. *SIAM Journal on Applied Mathematics*, 37(2):290–301, 1979.

[TGA17] E Taciroglu, SF Ghahari, and F Abazarsa. Efficient model updating of a multi-story frame and its foundation stiffness from earthquake records using a Timoshenko beam model. *Soil dynamics and earthquake engineering*, 92:25–35, 2017.

[Tim37] H Timoshenko. *Vibration Problems in Engineering*. D van Nostrand Company, Inc., New York, second edition, 1937.

[TLK74] B Tabarrok, CM Leech, and YI Kim. On the dynamics of an axially moving beam. *Journal of the Franklin Institute*, 297(3):201–220, 1974.

[VDD15] TD Vu, D Durville, and P Davies. Finite element simulation of the mechanical behavior of synthetic braided ropes and validation on a tensile test. *International Journal of Solids and Structures*, 58:106–116, 2015.

[VDL21] NFJ Van Rensburg, S Du Toit, and M Labuschagne. Local linear Timoshenko rod. *Acta Mechanica*, 232(10):4057–4079, 2021.

[VS19] NFJ Van Rensburg and B Stapelberg. Existence and uniqueness of solutions of a general linear second-order hyperbolic problem. *IMA Journal of Applied Mathematics*, 84(1):1–22, 2019.

[VV02] NFJ Van Rensburg and AJ Van der Merwe. Analysis of the solvability of linear vibration models. *Applicable Analysis*, 81(5):1143–1159, 2002.

[VV06] NFJ Van Rensburg and AJ Van der Merwe. Natural frequencies and modes of a Timoshenko beam. *Wave motion*, 44(1):58–69, 2006.

[VVS21] AJ Van der Merwe, NF Janse Van Rensburg, and RH Sieberhagen. Comparing the dual phase lag, Cattaneo-Vernotte and Fourier heat conduction models using modal analysis. *Applied Mathematics and Computation*, 396, 2021.

[VZV09] NFJ Van Rensburg, L Zietsman, and AJ Van der Merwe. Solvability of a Reissner–Mindlin–Timoshenko plate–beam vibration model. *IMA journal of applied mathematics*, 74(1):149–162, 2009.

[WFH01] A-P Wang, R-F Fung, and S-C Huang. Dynamic analysis of a tall building with a tuned-mass-damper device subjected to earthquake excitations. *Journal of Sound and Vibration*, 244(1):123–136, 2001.

[WT99] TX Wu and DJ Thompson. A double Timoshenko beam model for vertical vibration analysis of railway track at high frequencies. *Journal of Sound and Vibration*, 224(2):329–348, 1999.

[ZVV04] L Zietsman, NFJ Van Rensburg, and AJ Van der Merwe. A Timoshenko beam with tip body and boundary damping. *Wave motion*, 39(3):199–211, 2004.